AD_____
(Leave blank)

Award Number : **W81XWH-08-1-0605**

TITLE: **The Role of Polycomb Group Gene BMI1 in the Development of Prostate Cancer**

PRINCIPAL INVESTIGATOR : **Mohammad Saleem Bhat**

CONTRACTING ORGANIZATION: **University of Minnesota-Twin Cities, MINNEAPOLIS, MN 55455-2070**

REPORT DATE: **March 2014**

TYPE OF REPORT: **Final**

PREPARED FOR: **U.S. Army Medical Research and Materiel Command Fort Detrick, Maryland 21702-5012**

REPORT DOCUMENTATION PAGE

Form Approved
OMB No. 0704-0188

1. REPORT DATE *(DD-MM-YYYY)*	2. REPORT TYPE	3. DATES COVERED *(From - To)*
March 2014	Final	1Sep2008 to 6Dec2013

4. TITLE AND SUBTITLE
The Role of Polycomb Group Gene BMI1 in the Development of Prostate Cancer

5a. CONTRACT NUMBER

5b. GRANT NUMBER
W81XWH-08-1-0605

5c. PROGRAM ELEMENT NUMBER

6. AUTHOR(S)
Mohammad Saleem Bhat

email:msbhat@hi.umn.edu

5d. PROJECT NUMBER

5e. TASK NUMBER

5f. WORK UNIT NUMBER

7. PERFORMING ORGANIZATION NAME(S) AND ADDRESS(ES)
University of Minnesota

Minneapolis, MN 55455

8. PERFORMING ORGANIZATION REPORT NUMBER

9. SPONSORING / MONITORING AGENCY NAME(S) AND ADDRESS(ES)
U.S.Army Medical Research and Materiel Command
Fort Detrick, Maryland,
MD, 21702-5012

10. SPONSOR/MONITOR'S ACRONYM(S)

11. SPONSOR/MONITOR'S REPORT NUMBER(S)

12. DISTRIBUTION / AVAILABILITY STATEMENT
Approved for public release; Distribution Unlimited

13. SUPPLEMENTARY NOTES

14. ABSTRACT: We proposed to investigate the role of BMI1 (a member of polycomb gene family) in human prostate cancer (CaP) development. Here, we present the work accomplished during the final phase of the project. During the 1st phase of study we established the relevance of BMI1 in the growth and proliferation of normal and malignant prostate tumor CaP cells. In the second phase (2nd annual report), we investigated the mechanistic basis of the role of BMI1 in human CaP and established the proof of principle for BMI1 as a relevant target for CaP therapy. As provided in the 2nd annual report, we showed the data generated from studies where we employed relevant cell-based models, gene modulation techniques (such as micro-array and PCR array) and animal models. These studies showed that BMI1 sustains the proliferation of chemoresistant CaP cells (during and after chemotherapy) by regulating the expression and activity of cyclin D1 (Wnt target) and Bcl-2 (Sonic Hedgehog-SHH target). The novel finding in presented in the 2nd annual report was that regulation of Bcl-2 expression by BMI1 is independent of SHH activity in CaP cells. We showed that BMI1 regulates BCl2 by inducing the transcriptional activity of TCF4-transcriptional factor. Using cell-culture models and human prostatic tissues we showed that BMI1 regulates the binding of TCF4 on the promoter region of *BCL2* gene. In the final report, we show that Cyclopamine (SHH inhibitor) which is known to reduce Bcl2, fails to inhibit the growth of chemoresistant CaP cells. However, targeting of BMI1 sensitizes such chemoresistant CaP cells to Cyclopamine (SHH inhibitor) therapy. We suggested that targeting of BMI1 is an ideal strategy to sensitize hard-to-treat CaP cells for chemotherapies. We show that targeting of BMI1 by gene-silencing improved the outcome of Docetaxel (targets cell division) and Sulindac (Wnt-signaling inhibitor) therapies in animal models bearing prostatic tumors. We suggest that BMI1 could be exploited as a potential molecular target for therapeutics to treat chemoresistant tumors.

15. SUBJECT TERMS
BMI1, Wnt Signaling, Bcl-2, TCF, Prostate Cancer

16. SECURITY CLASSIFICATION OF:			17. LIMITATION OF ABSTRACT	18. NUMBER OF PAGES	19a. NAME OF RESPONSIBLE PERSON
a. REPORT	b. ABSTRACT	c. THIS PAGE			USAMRMC
U	U	U	UU	61	19b. TELEPHONE NUMBER *(include area code)*

Table of Contents

Introduction:

Prostate cancer (CaP) is the most common visceral cancer diagnosed in men; it is the second leading cause of cancer related deaths in males in the United States and the Western world (1). Prostate cancer (CaP) patients (30-50%) will have a local or distant recurrence of disease after surgery or radiation therapy (2-4). Although castration is a common treatment option for metastatic CaP, it does not significantly prolong the survival of patients and majority of these patients progress to castration-resistant prostate cancer (CRPC). A treatment option for CRPC is cytotoxic chemotherapy; however, chemotherapy improves overall survival in such patients by only a median of 2.9 months (4). Despite chemotherapy, CRPC patients typically show rapid progression and develop chemoresistant disease (4-5). Therefore emergence of chemoresistance is considered a major hurdle in the management of CaP. The dismal outcome of the management of chemoresistant CRPC disease could also be associated to the lack of knowledge about the molecular mechanism involved in the development of chemoresistant disease.

There is increasing evidence that polycomb group (PcG) proteins, first discovered in *Drosophila* as epigenetic gene silencers of homoeotic genes, play a crucial role in cancer development and disease recurrence (6). BMI1, a member of PcG family of repressor proteins, is a well-known marker used in stem cell biology (6-7). There is an enormous body of evidence suggesting that increased expression of BMI1 could facilitate chemoresistance in solid tumors (6-7). Recent studies show that BMI1 is positively correlated with poor prognosis in cancer patients (8-11). We recently reviewed the significance of BMI1 in the emergence of chemoresistance in various types of cancers (6). Glinsky *et al* identified BMI1 as one the signature molecules in a broad spectrum of therapy-resistant cancers included CaP (12). Except a few regulatory functions of BMI1 in cell cycle (suppressing p16INK4a and p14ARF), not much is known about the mechanism of action of BMI1. In this current study, we determined the relevance of BMI1 in the chemoresistance of CaP disease and delineate its mechanism of action both *in vitro* and *in vivo*. In addition, we establish the utility of BMI1 as a molecular target for therapeutic agents to overcome chemoresistance.

Body

Under this section we provide information about the experimental and materials and methods used to accomplish our objectives as stated in the proposal.

Experimental Design for Specific Aim #1.

We conducted the experiments to define the effect of overexpression and silencing of BMI1 gene in CaP cells. For this purpose, we (a) knockdown the BMI1 gene by transfection of siRNA and (b) overexpressed the BMI1 gene by transfecting BMI1 construct (pbabe-BMI1 plasmid provided by

Professor Chi Van Dang, Professor of Cell Biology, School of Medicine, The Johns Hopkins University, Baltimore, MD) in PC3 (androgen-independent), LNCaP (androgen-dependent), 22R□1 (androgen-sensitive) and normal prostate epithelial cells (PrEC) cells. We then studied the growth and viability of transfected cells *in vitro* by employing the MTT assay. To investigate the effect of BMI1 gene on the rate of proliferation of CaP cells, we employed ^{3}[H]thymidine uptake assay. This assays measures the amount of ^{3}[H]thymidine taken up by dividing cells (for DNA synthesis) thus gives a measure of the rate of division or proliferation of cells. BMI1 silenced and BMI1 overexpressing CaP cells were cultured in presence of ^{3}[H]thymidine and ^{3}[H] thymidine uptake was measured by Liquid scintillation counter. These cells were also measured for DNA content. Since BMI1 was observed to increase the proliferative potential of CaP cells and to establish that BMI1 indeed was a driving force for proliferating cells, we investigated whether BMI1 has to potential to drive proliferation of normal prostate epithelial cells. For this purpose, BMI1 was overexpressed in normal prostate epithelial cells (PrEC). We chose PrEC cells because under normal culture conditions, PrEC cells are known to replicate between 3-4 cycles and after 4 cycles, these cells enter into a mode of senescence. The break of senescence in normal epithelial cells is a hall mark of progression towards proliferation. As a control to study, another set of PrEC cells were transfected alone vector (pbabe). Further a microarray was performed with BMI1 silenced LNCaP cells to understand the mechanism of action of BMI1 in CaP cells. Experiments conducted under this aim provided information whether genes involved in proliferation are regulated by BMI1 gene. These data were validated by western blot analysis. We analyzed the expression level of Cyclin D1, p16 and Bcl-2 protein in CaP cells. Next we investigated whether the overexpression generates the data contrary to what was observed in BMI1 silenced cells. For this purpose BMI1 was overexpressed in LNCaP, PC-3 and DU145 cells by transfecting pbabe-BMI1 plasmid. Cell lysates prepared from these cells were analyzed for Cyclin D1, Bcl-2 and p16 proteins by employing western blot analysis. To understand the mechanism through which BMI1 regulates Cyclin D1, we carried out experiments on critical pathways which are already know to be associated with Cyclin D1 expression. This includes Wnt/β-catenin signaling pathway. We asked whether BMI1 has any association with Wnt/□-catenin signaling (which is itself reported to control Cyclin D1). Interestingly, we found that BMI1 overexpression causes an increase in the transcriptional activation of *TCF*-responsive element (a bio-marker of Wnt signaling) in CaP cells. Since Bcl-2 was observed to be modulated by BMI1, we investigated if BMI1 has any association with sonic hedgehog (SHH) pathway that is very well know to regulate Bcl-2. For this purpose we determined the expression level of Bcl-2 in BMI1-overexpressing and BMI1-silenced CaP cells in presence of Cyclopamine, a SHH pathway inhibitor. We also tested if re-introduction of BMI1 would restore the Bcl-2 levels in CaP cells pre-treated with

cyclopamine (SHH inhibitor). Further, we investigated an association of tcf and Bcl-2 in CaP cells. We investigated the mechanism through which BMI1 drives the Tcf/Bcl-2 signaling in CaP cells.

Experimental Design for Specific Aims #2 and 3.

Animal studies showed a significant lower tumor growth in PC-3-empty vector and PC-3-BMI1-supressing cell-originated tumors than PC-3-BMI1-overexpressing cell originated tumors in athymic mice. We showed that knocked down of BMI1 sensitized the chemoresistant prostatic tumors for the Docetaxel and sulindac therapies.

Material and Methods:

Cell Lines and plasmids: Primary prostate epithelial cell (PrEC) was procured from Cambrex BioScience (Walkersville, MD). Normal prostate cell line **(**RWPE1), CaP cell lines (LNCaP, PC3 and Du145), and colon cancer cell line HT29 were obtained from ATCC (Manassas, VA). pGeneClip-BMI1-shRNA plasmid was procured from SA-Biosciences (Fredrick, MD). pTK-TCF-Luc (TopFlash & FopFlash) was procured from Millipore (Temecula, CA).

Tumor tissues: Frozen prostatic tissues (surgically obtained from CaP patients) and tissues in paraffin blocks, and tissue microarrays were procured from NCI-sponsored Cooperative Human Tissue Network (CHTN, Mid-West Division, University of Ohio, Columbus).

Chemicals and reagents: Docetaxel, casodex, cyclopamine and cisplatin were purchased from LKT Laboratories (St. Paul, MN). Puoromycin, G418 and BrdU labeling reagent were purchased from Invitrogen (Carlsbad, CA). The anti-BMI1 antibody, ChIP-grade anti-TCF1 and anti-TCF4 antibody was obtained from Millipore. Anti-BCL2 and anti-BrdU antibodies were purchased from Cell Signaling (Danvers, MA).

Cell growth assay. Cell growth was determined by MTT (3-[4, 5-dimethylthiazol-2-yl□2, 5-diphenyl tetrazoliumbromide; Sigma, Saint Louise, MO, USA) assay as described earlier.[27-28] Briefly, transfected cells were grown in complete medium. Each condition was repeated in 10 wells. After incubation for specified time at 37 °C in a humidified incubator, MTT (5 mg/ml in phosphate buffered saline, PBS) was added to each well. After 2 h of incubation with MTT, the plates were centrifuged at 500 g for 5 min. After careful removal of the solution, 0.1 ml of DMSO was added to each well and plates were shaken. The absorbance was recorded on a microplate reader at the wavelength of 540 nm. The cell growth was assessed as percent cell growth where vehicle-treated cells were taken as 100% viable.

3[H]-thymidine incorporation assay: 3[H]-thymidine incorporation assay was performed as described earlier.[27] Briefly, Cells grown in 24-well plates in the presence of 3[H]thymidine (0.5 μCi/ml). Cells were then washed twice with cold PBS and then were incubated with trichloroacetic acid solution on ice for 30 min. Next, acid-insoluble fraction was dissolved in 1 ml of NaOH (1 M).

Incorporated 3[H]thymidine were quantified using a scintillation counter.

Colony formation assay: A total of 0.5% agar was prepared in appropriate culture media containing 20% fetal calf serum (bottom layer). Cells (1×10^5 cell/ 100 mm plate) in 20% fetal calf serum and 0.7% agarose (top layer) were plated and incubated at 37°C. The medium was removed and replaced with fresh medium in every 2 days. After 14 days of incubation, the cells were stained with 0.05% crystal violet/methanol for 2 h and colonies were counted in two colony grids using a microscope.

Immunohistochemistry. Briefly, paraffin embedded sections (to be evaluated for BMI1, BrdU and BCL2) were treated with Retrievagen A solution (pH 6) for antigen retrieval (BD Biosciences, San Diego, CA). Sections were incubated with primary antibody for overnight at 4ºC. Slides were then washed and incubated for 2 h at room temperature with appropriate HRP-conjugated secondary antibody. Finally, slides were developed in 3, 3'-diaminobenzidene (DAB kit, Invitrogen) and counter stained with hematoxylin. The stained slides were dehydrated and mounted in permount solution.

Western blot Analysis. Briefly, cell lysates were prepared by incubation of cells for 30 min in ice-cold lysis buffer [(0.05 mmol/L Tris-HCl, 0.15 mmol/L NaCl, 1 mole/L EGTA, 1 mol/L EDTA, 20 mmol/L NaF, 100 mmol/L Na_3VO4, 0.5% NP-40, 1% Triton X-100, 1 mol/L phenyl methylsulfonyl flouride (pH 7.4)] with protease inhibitor cocktail (Roche, Indianapolis, IN). The lysate was collected; insoluble materials were removed by centrifugation at 4°C for 15 minutes at 15,000g, and stored at -80 °C. BCA protein estimation kit was used to estimate the protein concentration in the lysates (Pierce, Rockford, IL), as per the vendor's protocol. Next, 40 µg protein was resolved in 10% SDS-PAGE gels, transferred onto PVDF membranes (Millipore) and incubated in blocking buffer (5% nonfat dry milk/1% Tween 20; in 20mmol/L TBS, pH 7.6) for 2 h. The blots were incubated with appropriate primary antibody, washed and incubated with HRP-conjugated secondary antibody (Sigma). The blots were detected with chemiluminescence (ECL kit, Amersham Biosciences, Piscataway, NJ). Equal loading of protein was confirmed by stripping the blots and re-probing with □-actin (Sigma).

Luciferase reporter activity. In these studies, cells were co-transfected with the pTK-TCF, (200 ng/well) and pGeneClip-BMI1-shRNA or pbabe-BMI1. Renilla luciferase (pRL-TK) was used as an internal control and reporter activity was measured as described earlier.[27-28] For controls, the similar amount of empty vectors (pGL3, pbabe and pGeneClip) was transfected in cells.

Quantification of apoptosis. Apoptosis was evaluated using the Annexin V-FITC Apoptosis detection kit from MBL International Corporation (Watertown, MA). Briefly, docetaxel resistant and BMI1-silenced docetaxel resistant cells were harvested with 0.025% trypsin + 5 mM EDTA in PBS (containing 2.5% FBS). Then the cells were washed with PBS and incubated for 5 min at room temperature with Annexin V-FITC plus propidium iodide (PI) as per vendor's protocol. Cells were

analyzed on a Becton Dickinson FACS Calibur flow cytometer (BD Biosciences), placing the FITC signal in FL1 and the PI signal in FL2. Intact cells were gated in the FSC/SSC plot to exclude small debris. Cells in the lower right quadrant of the FL1/FL2 dot plot (labeled with Annexin V-FITC only) are considered to be in early apoptosis, and cells in the upper right quadrant (labeled with Annexin V-FITC and PI) are in late apoptosis/necrosis.

Generation of stable cell lines: PC3 cells were transfected with either pbabe-BMI1 (BMI1-overexpressing) or pGeneClip-BMI1-shRNA (BMI1-silenced) using Lipofectamine and selected in presence of puromycin (1 μg/ml) and G418 (400 μg/ml), respectively.

(i). *Stable BMI1-overexpressing CaP Cells:* For this purpose PC-3 cells were stably transfected with pbabe-BMI1. The transfections were performed by Lipofectamine method. BMI1 overexpressing PC-3 clones were selected in presence of puromycin. The selection of BMI1-overexpressing PC-3 cells under puromycin continued for 4 weeks. Cells were tested for BMI1 overexpression. Among 24 clones generated, we selected 3 clones those exhibited the highest degree of BMI1 expression level.

(ii). *Stable BMI1-silenced CaP Cells*: For this purpose PC-3 cells were stably transfected with vector-based shRNA plasmid, pGeneCLIP-BMI1-shRNA. The shRNA plasmids are designed using an experimentally validated algorithm. These constructs specifically knock down the expression of specific genes by RNA interference and allow for enrichment or selection of transfected cells. Each vector expresses a short hairpin RNA, or shRNA, under control of the U1 promoter and neomycin gene. Neomycin resistance permits selection of stably transfected cells. The ability to select or track and enrich shRNA-expressing cells brings RNA interference to cell lines with lower transfection efficiencies. Unlike siRNA, plasmid-based shRNA also provide a renewable source of RNA interference reagent. The transfections were performed by Lipofectamine method. PC-3 cells were selected in presence of neomycin analogue G418 (300 μg/ml). The selection of BMI1-overexpressing PC-3 cells under G418 continued for 4 weeks. Cells were tested for BMI1 expression. Among 20 clones generated, we selected 3 clones those exhibited the least or no BMI1 expression level.

Senescence-associated β-Galactosidase analysis: Senescence-associated β-galactosidase (SA-β-gal) cytochemistry was performed by using X-gal (5-bromo-4-chloro-3-indolyl-β-d-galactopyranoside) substrate kit (Cell Signaling) as per vendor's protocol.

Chemosensitivity assay: Transfected cells (BMI1-overexpressing and BMI1-suppressed) at 12 h post-transfection time period were treated with casodex (10 μM), docetaxel (10 nM) and cisplatin (10 μM) for additional 24 h. Growth of cells was determined by measuring rate of proliferation and viability by employing using 3[H]thymidine incorporation and MTT [3-(4,5-dimethylthiazol-2-yl)-2,5-

diphenyltetrazolium bromide] assay as described (13-15)

Generation of chemoresistant CaP cells: One million cells were seeded in 100 mm tissue culture dish with advanced-RPMI (Invitrogen) media containing 5% FBS and 1% penicillin /streptomycin for 24 h. At 24 h, the cells were exposed to 10 nM docetaxel for 48 h. The selection of concentration was based on the IC_{50} value. The drug containing medium was replaced after two days and the surviving (adherent) cells were cultured in a fresh drug-free complete medium. The cycle was repeated total 10 times. Following each treatment, cells were allowed to fully recover before next treatment. Next, the adherent cells were collected and exposed to higher doses of docetaxel (15, 20, to 25 nM) for 6 weeks (two weeks for each concentration). Finally, the surviving cells were maintained in RPMI/5% FBS containing 10 nM docetaxel. Untreated PC3 cells aged alongside the treated cells (to avoid aging effect) were considered as control.

CaP-specific membrane hybridization and quantitative RT-PCR array: The membrane (printed with probes for CaP-specific genes) was hybridized with cRNA (synthesized from RNA of cells) and detected by chemiluminescence as per vendor's protocol (SA-Biosciences Super Array, Frederick, MD). Further, RNA from cells was also used for performing qRT-PCR array of CaP specific genes. The data analysis was performed by using array analyzer software (SA-Biosciences Super Array, Frederick, MD).

Quantitative chromatin immunoprecipitation (ChIP) assay: ChIP analysis for TCF1 and TCF4 occupancy on promoter region of BCL2 gene was performed as described (14). samples were cross-linked with 1% formaldehyde. Anti-AR antibodies were used with protein A-Sepharose (Sigma) to adsorb immune-specific complexes. Preimmune serum was used as a control. Purified DNA was analyzed by real-time PCR (ABI Prism 7500) using appropriate primers. Product was measured by SYBR green fluorescence and the amount of product was calculated by determining relative expression to a standard curve generated from a titration of input chromatin. Following primers were used to amplify segments that overlap with the appropriate regions: BCL2 (-3.91Kb), Forward, *5'CTGTGGGAGCAAAGGAAGAC3'*; Reverse, *5'AGAAGGAAACGGATCCCCTA3'*: BCL2 (P2-promoter, TATA site), Forward, *5'CAAGTGTTCCGCG`TGATTG3';* Reverse *5'CCCGGTTA TCGTACCCTGTT3':* BCL2 (-0.8Kb), Forward, *5'GTCCAAGAATGCAAAGCACA3';* Reverse-*5'CCCCCAGAGAAAGAAG AGGA3';* SP5 (promoter) - Forward 5'-*GGGTCTCCAGGCGGC AAG-3*`; Reverse, *5`-AGCGAAAGCAAATCC TTTGAA-3'*.

***Tumor studies*:** Athymic (nu/nu) male nude mice (6 weeks old; HarlanTek, Madsion, WI), were implanted with PC3 cells (1×10^6) in 50 µl RPMI + 50 µl Matrigel (BD Biosciences, Bedford, MA) subcutaneously into the right flanks of each mouse. At 7th day post-implantation, the study was divided into three protocols.

Overexpression protocol. Group-1 (n=10) of mice implanted with empty-vector transfected stable cells and treated with vehicle alone served as control. Group-II (n=10) included mice implanted with vector transfected cells and treated with an intraperitoneal (*i.p*.) administration of docetaxel (10 mg/kg in 100 μl of saline; thrice/week). Group-III (n=10) included mice implanted with BMI1-overexpressing cells and received *i.p.* administration of 100 μl of saline. Group-IV (n=10) included mice bearing BMI1-overexpressing tumors and received docetaxel (thrice/week).

Stable transfection- BMI1-shRNA-mediated Silencing protocol. Group-1 (n=10) of mice implanted with empty-vector (pGenCLIP) transfected stable cells and treated with vehicle served as control. Group-II (n=10) included mice implanted with vector transfected cells and treated with docetaxel (10 mg/kg). Group-III (n =10) included mice implanted with BMI1-silenced tumor cells and received *i.p.* administration of saline. Group-IV (n = 10) included mice implanted with BMI1-silenced tumor cells and received docetaxel treatment.

SiRNA-treatment mediated BMI1-silencing protocol : *Group I* of mice served as control group and recieved 0.1. ml of corn oil and scrambled siRNA in 0.1ml of liposomes through intraperitoneal (i.p.) route. *Group II* of mice received Sulindac (50 mg/kg in 0.1 ml of corn oil *i.p*.) and scrambled siRNA in 0.1 ml of liposomes (3-times/wk, i.p). *Group III* mice were treated with BMI1-siRNA (0.8mg/kg ; 3-times/week in 0.1 ml liposomes) and Sulindac (50 mg/kg; 3-times/week).

Tumor measurement: Body weights were recorded seven days/week throughout the study. Tumor growth was recorded as described (13-15). Tumors from three animals from control and treated groups were excised at the 35th day post administration when 100% of control animals reached the preset end point of tumor volume of 1,000 mm^3 (for stable transfection protocols) and 500 mm^3 (for BMI1-siRNA treatment protocol). Rest of the animals in other groups remained under protocol for a maximum time of 10 weeks. Before 2 h of sacrifice, each animal received an *i.p.* administration of BrdU labeling reagent (10 ml/ kg) to label proliferating cells within tumors (13). All procedures conducted were in accordance with the IACUC guidelines.

***Statistical analyses*:** Student's *t test* for independent analysis was applied to evaluate differences between the treated and untreated cells with respect to the expression of various proteins. A Kaplan-Meier survival analysis with the corresponding Log-Rank and Linear Regression analysis was used to measure the rate of mean tumor volume growth as a function of time. A p-value of < 0.05 was considered to be statistically significant.

Key Research Accomplishments:

Under the final phase of the study, we accomplished goals as proposed under tasks 2 and 3 (provided in the Statement of Work-SOW). These are described as following:

Task 2 : To evaluate the effect of BMI1 overexpression and silencing on SHH and Wnt/β-catenin signaling pathways and to define the underlying mechanism of SHH-BMI1-β-catenin interaction at transcriptional and translational level in human CaP cells. :

Status: Completed; Data presented in this report.

Task 3 : **Studies in athymic nude mouse xenograft model will be conducted (a) to analyze the consequences of BMI1 overexpression and silencing on tumorigenicity of human CaP cells, and (b) to evaluate the effect of BMI1 siRNA in combination with chemotherapies *in vivo*.**

Status : Completed; Data presented in this report.

Results :

BMI1 protein levels in prostatic tissues increases with progressive stages of disease in human CaP patients*:* As an attempt towards identifying the expression status of BMI1 protein in human prostatic tissues, we measured its expression levels by performing immunoblot analysis of snap-frozen prostatic tissues from normal, dysplasia and CaP patients (stage II-IV) procured from NCI-sponsored Cooperative Human Tissue Network (CHTN, Mid-West Division, University of Ohio, Columbus). BMI1 protein was observed to be progressively increased from normal prostate to prostatic dysplasia to malignant prostate in humans (Fig. 1A).

We next determined the expression of BMI1 protein in 72 pair-matched specimens of normal and CaP representing all tumor stages by employing immunohitochemical analysis. The intensity of immunoperoxidase staining for BMI1 was scored as 0 (negative), 1 (weak), 2 (moderate) and 3 (strong). Immunostains showed granular cytoplasmic staining in both non-neoplastic and neoplastic epithelium. In general, the staining was stronger in neoplastic epithelial cells than in non-neoplastic epithelial cells (Fig. 1Bi). We next compared the staining pattern of BMI1 protein of stages II-IV CaP specimens. As shown in box-plot, a progressive increase of BMI1 was observed as the disease progressed from low-grade to high grade tumor in humans CaP patients (Fig. 1Bii). The box plots of the data for BMI1 protein expression in epithelial cells exhibited a wide inter-specimen variation in cancer specimens, compared with normal tissues and revealed a significant difference in the level of

protein between normal and CaP tissues ($p<0.05$, Fig. 1Bii). The average score for the staining intensity of BMI1 in normal tissues was 1.3 ± 0.07 (n=72), and was significantly lower than high-grade stage II (1.9 ± 0.09; n=36), stage III (2.4 ± 0.08; n=28) and stage IV (2.92 ± 0.08; n=6) cancer specimens (Fig.1Bii; $p < 0.05$). Taken together, these data show that expression of BMI1 increases with increasing stage of CaP.

BMI1 expression is independent of androgen: We next investigated if the observed increase in BMI1 levels during the progression of CaP disease in humans has a correlation with presence or absence of androgen. Androgen analogue (R1881; 1 nM) treated LNCaP, LAPC4, 22Rν1 and C4-2b cells did not show any significant change in the levels of BMI1 protein (Fig. 1C) suggesting that BMI1 expression is independent of influence of androgen.

BMI1 regulates the proliferation of prostatic tumor cells: We investigated whether BMI1 regulates the growth of prostatic tumor cells. We employed a two-way approach where BMI1 was (i) either suppressed by transfecting a vector-based shRNA (pGenCLIP-BMI1-shRNA) or (ii) overexpressed by a ectopic transfection with BMI1 expressing plasmid (pBabe-BMI1) in prostatic tumor cells (LNCaP, Du145 and PC3) (Suppl. Fig. 1). The effect of differential expression of BMI1 (overexpression or suppression) on the growth potential of CaP cells was determined by measuring cell viability and the rate of proliferation of cells. LNCaP cells duplicate within 48-72 h while as Du145 and PC3 cells duplication takes 24 h under culture conditions. BMI1-suppressed CaP cells (LNCaP, DU145 and PC3) did grow between 50-65% even after 72 h post-transfection (Fig. 1Di). However, BMI1-overexpressing CaP cells achieved 65-90% confluence only at 36h post-transfection suggesting the significance of BMI1 in the growth of tumor prostatic cells (Fig. 1Dii).

We next asked if the pro-growth role of BMI1 is due to its effect on the proliferative potential of tumor cells. For this purpose, we employed 3[H]thymidine uptake assay that measures the rate of uptake of thymidine by dividing/proliferating cells. As evident from the rate of 3[H]thymidine uptake by proliferating cells, suppression of BMI1 was observed to cause a decrease in rate of proliferation of tumor cells (Fig. 1Ei). Conversely, forced overexpression of BMI1 caused a significant increase in the rate of proliferation ($p<0.05$, Fig. 1Eii). Since, we used vector-based shRNA that provides an advantage to investigate the effect of BMI1 suppression over a long period in cells; we also assessed proliferative potential of tumor cells by employing soft-agar colony formation assay. BMI1-suppressed tumor cells exhibited significantly reduced number of colonies formed ($p<0.05$, Fig. IFi). On the contrary, forced overexpression of BMI1 induced clonogenic potential of tumor cells as was evident from the number of colonies formed by these cells (Fig. 1Fii). These data suggested that BMI1 confers proliferative attributes to the CaP cells.

BMI1 increases the replicative life of normal prostate epithelial cells (PrEC)*:* To further confirm that BMI1 indeed drives the proliferation of epithelial cells, we selected normal primary epithelial cells (PrEC). It is well known that normal prostate cells enter into senescence and do not grow or replicate after 4-5 passages under culture conditions. It is noteworthy that forced expression of BMI1 in normal cells (transfected with pbabe-BMI1) abolished senescence and caused an increase in the replicative cycles (Fig. 2A). This was evident from the number of passages (8 passages) that we were able to subculture BMI1-overexpressing normal cells. Due to transient nature of transfection, the effect of overexpression lasted up to 7th passage, and cells entered into senescence at 8th passage. To further confirm if the increase in replicative potential (conferred by BMI1 overexpression) was due to abolishment of senescence in normal cells, we measured senescence-associated β-galactosidase (SA-β-gal) activity, a general marker of senescence, at various passage/replication levels in PrEC cells. By employing a cytochemical reaction that is indicative SA-β-gal activity, normal cells exhibited positive staining for SA-β-gal at the 4th passage/subculture. Notably, BMI1 overexpressing normal cells did not show positive staining for SA-β-gal at the 4th passage. BMI1-overexpressing normal cells showed for SA-β-gal activity at the 7th passage (Fig. 2B). These data further strengthen our hypothesis that BMI1 has the potential to drive both normal and neoplastic cells towards proliferation though its activity is increased in neoplastic cells.

Molecular mechanism of action of BMI1 in tumor cells: We investigated the mechanism through which BMI1 controls the proliferation of CaP cells. For this purpose we performed focused membrane and quantitative-PCR based array analysis of well-characterized genes known to be involved in the proliferation of CaP cells. Since LNCaP cells exhibit the expression of majority of the human genes, we performed the primary analysis in these cells. A cut-out point of 2-fold was selected for analysis. To observe if the effect of BMI1 suppression (as observed in LNCaP cells) was similar to all CaP cells, the data were further validated in DU145 and PC-3 cells. BMI1-suppressed LNCaP cells exhibited a significant change in the expression level of several proliferation-associated genes (Fig. 1C & Suppl. Table-1). The prominent genes downregulated by suppression of BMI1 in cells were Cyclin D1, BCL2, IL and NFκB (Fig. 1C & Suppl. Table-1). An increased expression of p16, p15 and TIMP3 in BMI1-suppressed tumor cells was observed (Fig. 1C & Suppl. Table-1 & Figure 2A). To validate whether changes induced by BMI1 suppression on gene transcripts translated to protein level, we performed immunoblot analysis for selected gene products in LNCaP, DU145 and PC3 cells. BMI1-silenced tumor cells exhibited decreased levels of Cyclin D1 and BCL2, and increased p16 (Fig 2D). These data were further validated in BMI1 overexpressing cells which were observed to display increased BCL2 and CyclinD1 in cells (Fig. 2E). The data suggested a possible association between the BMI1, BCL2 and Cyclin D1 in CaP cells.

BMI1 in survival, growth and chemoresistance of tumor cells: Since BMI1 was observed to regulate the expression of proliferation-associated genes, we sought to determine if this phenomenon is responsible for chemoresistance of CaP cells. By employing 3[H]thymidine uptake and cell viability assays, we next determined the growth potential of BMI1-overexpressing and –suppressing CaP cells treated with clinically used chemotherapeutic drugs (bicalutamide or casodex, docetaxel and cisplatin). The working concentrations of the drugs were determined by the time course and dose titration for the chemotherapeutic agents (Suppl. Fig. 2C-D). We avoided casodex treatment in androgen-independent PC3 cells. The 3[H]thymidine incorporation analysis of cells showed that BMI1-overexpressing tumor cells significantly were non-responsive to chemotherapeutic agents suggesting that BMI1-rich tumor cells harbor the potential of escaping the chemotherapy (Fig. 3B & D). On the contrary, BMI1-suppressed prostate tumor cells were significantly responsive to chemotherapeutic treatments and exhibited reduced rate of proliferation suggesting that abolishing BMI1 render tumor cells sensitive to the chemotherapy ($p < 0.05$, Fig. 3A & C). The observed differences between the BMI-overexpressing and BMI1-suppressed tumor cells in responsiveness towards chemotherapy were also reflected in cell viability (Suppl. Figs. 3 & 4). Cell viability data was concomitant to the 3[H]thymidine incorporation data (Suppl. Figs. 3 &4). These data established the significance of BMI1 protein in cell growth and suggest that presence of BMI1 in tumor cells play a critical role in deciding the therapeutic outcome.

BMI1 is critical for regrowth of tumors post-chemotherapy: We conducted a proof of principle study where adherent PC3 cells which survived docetaxel treatment were repopulated and allowed to regrow. These regrown CaP cells were termed as chemoresistant as these did not responded to subsequent docetaxel treatments and exhibited increased expression levels of BMI1, BCL2 and Cyclin D1, and rate of proliferation (Fig. 2Ei-ii**).** We next asked if targeting BMI1 render the BMI1-rich chemoresistant tumor cells amenable to therapy. Chemoresistant CaP cells were subjected to BMI1-suppression by shRNA. 3[H]thymidine uptake and FACS analysis for Annexin V/PI staining of cells showed that targeting BMI1 significantly inhibited the proliferation of chemoresistant CaP cells, increased the apoptosis and caused a remarkable decrease in the levels of BCL2/Cyclin D1 (Fig. 2F-H) suggesting a possible association between BMI1 and the survival of tumor cells post-chemotherapy.

Molecular mechanism through which BMI1 regulate BCL2 in tumor cells: Cyclin D1 and BCL2 are both down-stream targets of Wnt and Sonic hedgehog (Shh) signaling (16-17). Therefore, we determined if BMI1 has (i) any direct or indirect association with Wnt and Shh-signaling in proliferating tumor cells, and (ii) regulates BCL2 under Wnt or Shh guidance. We first determined the status of Wnt-signaling in BMI1-suppressed and BMI1-overexpressing CaP cells. By utilizing transcriptional

reporter activity of TCF element (a biomarker for Wnt activation), we observed that BMI1-overexpressed cells harbor increased TCF-transcriptional activity concomitant with the increased BCL2 and Cyclin D1 expression (Fig. 4A). Notably, BMI1-silenced tumor cells exhibited decreased TCF-transcriptional activation (Fig. 4B). Since our data showing a regulatory role of BMI1 on TCF-transcriptional activity in tumor cells is novel, we asked if this phenomenon is only limited to CaP cells. To validate our observations, we selected colon cancer cell line HT29 which is known to exhibit increased Wnt signaling and TCF-transcriptional activity (18). We first determined BMI1 levels in HT29 cells and then generated BMI1-silenced and BMI1-overexpresed HT29 cells by transfecting plasmids for BMI1-silencing and -overexpression, respectively. Significant modulations of TCF-transcriptional activity concomitant with BCL2 and Cyclin D1 were observed in HT29 cells after BMI1-silencing or -overexpression (Fig. 4C-E). These data established the role of BMI1 on TCF-transcriptional activity in other tumor cells.

Since BCL2 is also a downstream target of Shh, we next determined if BMI1 (i) partially regulated BCL2, or (ii) regulation of BCL2 is solely under the control of Shh as reported (18). For this reason, CaP cells were treated with cyclopamine (5 μM), an inhibitor of Shh signaling. As expected control (vehicle treated) CaP cells exhibited a reduction in BCL2 expression after cyclopamine treatment, however BMI1-overexpressing tumor cells did not show an apparent decrease in BCL2 (Fig. 4Fi). Furthermore, when BMI1 was suppressed in BMI1-rich tumor cells, they responded well to cyclopamine and exhibited reduced BCL2 levels (Fig. 4Fii). To validate if BMI1 was involved in regulation of BCL2 independent of Shh, we next reintroduced BMI1 in (a) cyclopamine treated, and (b) BMI1-deficeint CaP cells. Reintroduction of BMI1 in cyclopamine treated and BMI1-suppressed cells caused a gain in BCL2 promoter activity and expression level suggesting that BCL2 expression is not solely under the control of Shh-signaling but is in part regulated by BMI1 (Fig. 4G).

Since both TCF and BCL2 were observed to be under the guidance of BMI1, we next investigated whether there is a direct association of TCF and BCL2 gene in tumor cells. We measured BCL2 activity under condition when TCF was suppressed in cells. For this purpose, LNCaP, PC3 and HT29 cells were co-transfected with TCF-shRNA and BCL2-luc reporter plasmid and were analyzed for BCL2-promoter activity after 36 h. TCF-suppressed CaP and HT29 cells exhibited decreased BCL2-promoter activity (Fig. 4H). This report suggests that BCL2 acts as a downstream target of TCF-mediated signaling pathway.

TCF4 transcriptional factor binds to promoter region of BCL2 gene in tumor cells: To further identify the underlying mechanism, we investigated whether BCL2 gene has possible TCF binding sites on its promoter. By employing TESS analysis, we observed that BCL2-promoter region exhibits multiple sites where TCF possess the affinity to bind. We next sought the validation of TESS data

(which is a mathematical data) by biochemical analysis. We tested TCF1 and TCF4 occupancy on multiple sites on the promoter region of BCL2 gene by employing ChIP assay in CaP and HT29 cells. The TCF unresponsive SP5 promoter was used as a negative control (data not shown). TCF1 was observed to have insignificant occupancy on the examined sites of BCL2-promoter in both CaP and colon cells (data not shown). Among the three region analyzed, TCF4 was observed to occupy only TATA region of BCL2-promoter (P2 promoter). We found very little or no occupancy by TCF4 on -3.41Kb and -8.41kb of BCL2 promoter (data not shown). Notably, BMI1-overexpression was observed to increase the TCF4 occupancy on the TATA region of BCL2-promoter in the PC3 and HT29 cells (Fig. 5A-B). An opposite result was observed with that of BMI1-suppressed CaP and HT29 cells (Fig. 5A-B).

TCF4 binds to promoter region of BCL2 gene in human prostatic tissues: We next investigated if the *in vitro* observation of TCF4 occupancy on BCL2-promoter binding has translational relevance. From the outcome of immunoblot analysis data (Fig. 5C), we selected human normal and malignant prostatic tissues (which exhibited increased BMI1) and determined TCF4-occupancy on BCL2-promoter. As compared to the normal prostatic tissues, TCF4 exhibited increased occupancy at TATA region of *BCL2* in human prostate tumor tissues (Fig.5D).

BMI1 confers chemoresistance to human prostatic tumors in xenograft mouse models: Since BMI1 was observed to be involved in the proliferation and chemoresistance of CaP cells to various antitumor agents under *in vitro* conditions, we next determined whether these observations could be translated under *in vivo*. For this purpose, we measured the differential growth rate of tumors-derived from BMI1-overexpressing protocol.

BMI1-overexpression protocol: At one week post-implantation, the average volume of control and BMI1-overexpressing tumors in mice increased as a function of time (Fig. 5E). BMI1-overexpressing tumors were observed to grow at faster rate and larger in size than control tumors (Fig. 5E). Mice implanted with control-tumors reached a preset end-point tumor volume of 1000 mm3 at 49th day of post-implantation (Fig. 5E). However, mice implanted with BMI1-overexpressing tumors reached the preset end-point tumor volume at 35th day of post-implantation (Fig. 5E). At 49th and 35th days, mice implanted with control and BMI1-overexpressing tumors exhibited average tumor volumes of 1076 and 1023 mm^3, respectively (Fig. 5E).

Docetaxel treatment decreased the growth of tumors in control mice (Group-II). Interestingly, docetaxel treatment failed (for 10-weeks) to produce an effect on the growth of tumors expressing high BMI1 protein. At 49th day, the average tumor volume in control mice (Group-II) treated with docetaxel was 850 mm3 (Fig. 5E). However, BMI1-overexpressing tumors though treated with docetaxel reached an average tumor volume of 997 mm^3 as early as 35^{th} day (Fig. 5E). Next, we

evaluated whether treatment of docetaxel to animals caused a delay in the growth of tumors harboring increased BMI1 levels. As evident from the number of mice reaching the preset end-point tumor volume (1000 mm^3), the observed differences between the control and BMI1-overexpresed group of animals for the outcome of docetaxel therapy was statistically significant ($p<0.05$; Fig. 5F).

Targeting of BMI1 sensitized human prostatic tumors to Docetaxel and Sulindac therapies in xenograft mouse models:

Our studies showed that BMI1-overexpressing tumors exhibit hard-to treat character, which is generally termed as chemoresistance. We next asked if targeting of BMI1 could sensitize the CaP tumors for clinically used chemotherapies. For this reason we employed two approaches. Under first approach, we rendered CaP cells BMI1-suppressed by a stable transfection technique. Under the 2nd approach, we used a continuous gene therapy technique to suppress the BMI1 expression in tumors. Mouse under protocols such as BMI1-suppression protocol and gene therapy protocol were exposed to chemotherapies.

Rationale for selection of chemotherapeutic agents: The selection for chemotherapies was performed on the basis of their relevance to clinical use and the signaling pathways identified as targets of BMI1 in the current study. For the BMI1-suppression protocol, we selected Docetaxel as a chemotherapeutic agent because it is widely used in clinics to treat metastatic CaP in men. Approved by the US Food and Drug Administration (FDA) in 2004 for clinical use, docetaxel remain a mainstay of therapy for CRPC patients. However, resistance to docetaxel is a significant clinical problem given that 50% men suffering from CRPC exhibit poor or no responsiveness to therapy. The problem is further thus compounded from the clinical observations that patients who initially respond to therapy ultimately develop resistance to docetaxel. Therefore improving treatment outcomes for patients with docetaxel resistance is a high priority because of the limited number of treatment options historically available to this group of patients.

For the gene-therapy protocol, we selected Sulindac, a well-known inhibitor of Wnt/β-catenin signaling. Our mechanistic data showed that BMI1 control Bcl2 expression in chemoresistant CaP cells by a regulating activity of TCF4-transcriptional factor. We also observed that BMI1 regulates the binding of TCF4-transcriptional factor on the promoter region of *BCL2 gene* in CaP cells. TCF-4 transcriptional factor is the final molecule that relays Wnt signaling, and acts as the final executor of this important signaling pathway in tumor cells. Therefore, we speculated that targeting of Bcl2 expression at two critical upstream stages viz., (i) BMI1 (which is the master controller) and (ii) TCF-4 (which relays signal from BMI1 and Wnt), will be an ideal approach to inhibit growth of CaP cells, particularly chemoresistant phenotype.

BMI1-suppression by stable transfection and Docetaxel therapy: BMI1-supressed cell-derived tumors were observed to grow at slower rate than control tumors (Fig. 6A). This was evident from the significant difference in the rate of growth and tumor volumes between control and BMI1-supressed group of animals (Fig. 6A). Mice implanted with control tumors reached a preset end-point tumor volume of 1000 mm^3 at 49^{th} day of post-implantation (Fig. 6A). It is noteworthy that the average volume of tumors in mice bearing BMI1-silenced tumors did not reach the end-point even at 70^{th} day post-implantation (Fig. 6A). At 49^{th} day, control group of animals treated with docetaxel exhibited an average tumor volume of 850 mm^3. However at this point, BMI1-silenced group of animals treated with docetaxel exhibited an average tumor volume of 230 mm^3 suggesting that BMI1-silencing sensitizes tumor cells to docetaxel therapy (Fig. 6A). Next, we evaluated whether docetaxel caused a delay in the growth of BMI1-suppressed tumors. The observed differences between control and BMI-silenced group of animals were statistically significant ($p<0.05$, Fig. 6B).

BMI1-suppression by siRNA administration and Sulindac therapy: Our observations in BMI1-suppression protocol showed that targeting of BMI1 significantly decrease the growth of prostatic tumor implanted in mice (Figure 6A-B). This established the proof of principle that BMI1 targeting is an ideal approach for CaP treatment. However, BMI1 suppression by transfection is not possible in patients at clinics. Therefore, we hypothesized that targeting of BMI1 by gene therapy "with the use of siRNA-oligos" is practically possible. If successful, it would have high translational relevance.

Study Design: To test our hypothesis, we performed a 5-week treatment protocol study in athymic male mice and set 500 mm^3 tumor volumes as a preset-endpoint. Mice were implanted with PC-3 cells (1×10^6) cells and allowed to grow tumor for 1-Week. 100% of mice exhibited visible tumors after 1 week of implantation. At this stage mice were randomly divided into three (3) groups. Group 1 of mice receiving intraperitoneal (i.p.) administration of vehicle (corn oil + liposomes) alone (0.1.ml/3 time a week) served as control. The vehicle (liposomes) is a commercially available and tested vehicle designed to deliver oligos *in vivo*. The control mice exhibited increase in tumor growth as a function of time and majority of mice reached the preset-end-point at 5 week post-treatment. The second (2^{nd}) group of mice was treated mice with Sulindac (50 mg/kg in 0.1 ml corn oil; 3-times a week). This group also received scrambled siRNA in liposomes (0.1. ml; 3-times/week). The third (3^{rd}) group of mice received Sulindac (50mg/kg; 3-times a week) and BMI1-siRNA in liposomes (3-times/week).

Outcome: As compared to control mice, Sulindac treatment substantially decreased the growth of tumors in mice (Fig. 6C). At 5^{th} week when average tumor volume in control group was 773± 78 mm^3, (mean +SE) the Sulindac-treated group (2^{nd} group) exhibited an average tumor volume of 446 ± 24 mm^3 (mean +SE) (Fig. 6C). It is noteworthy that mice receiving combination treatment (3^{rd} group)

exhibited increased inhibition (almost 80% inhibition) in growth of tumors and at 5th week-post treatment, exhibited an average tumor volume of 100 ± 16 mm^3 (mean +SE) (Fig. 6C).

We next measured the average weights of the tumors excised from the mice of all group. It is noteworthy to mention that all mice received equal number of cells at the time of implantation, and treatments were started began when all mice were randomly distributed in groups after one of implantation (when all mice exhibited visible tumors). Therefore, it could be now ascertained that tumors grew as a function of time and tumor weights exhibited by different were indeed influenced by treatments. At the termination of study, the average tumor weight were in (a) 525 ± 35 mg (mean ± SE) in control group, (b) 236 ± 13 mg (mean ± SE) in Sulindac-treated group and (c) 98 ± 11 mg (mean ± SE) in combination group (BMI1-siRNA + Sulindac) (Fig. 6D).

BMI1 controls proliferation and BCL2 expression of tumor cells in vivo: We determined significance of BMI1 in the proliferation of cells within tumors exposed to docetaxel therapy. Proliferating tumor cells are known to uptake BrdU (thymidine analog) and its detection in tumor cells by immunostaining of tumors provides an indirect measure of *in vivo* proliferation. Notably, BrdU staining of tumor sections (harvested at 35th day) showed that docetaxel treatment decreased the number of proliferating cells in BMI1-silenced tumors and failed to inhibit proliferation of BMI1-overexpressing tumor cells (Fig. 7A). BMI1-silenced tumors exhibited decreased BCL2 levels than BMI1-overexpressing tumors (Fig. 7B). These data show that BMI1 confers chemoresistance to prostatic tumors, and abolishing BMI1 sensitizes chemoresistant tumors to chemotherapy, therefore establishes its significance as a therapeutic target.

Reportable Outcome: Based on our results, three major observations were found to be reportable. Two of these observations were submitted for their publication in scientific journals. A part of our observations has now been published in scientific journal “PLOS-One” (PLoS One. 2013 May 6;8(5):e60664. doi: 10.1371/journal.pone.0060664. Print 2013.PMID:23671559).

On the basis of our studies, following major observations were made:

1. BMI1 protein levels progressively increase with the advancement of CaP disease in humans. In addition, BMI1 protein is increased in disease which is resistant to therapy. The significance of this outcome is that tissue biopsies in future could be analyze for BMI1 protein to assess if the disease would be aggressive and treatable or not. BMI1 would act as a future biomarker. This would save time of clinicians to manage the CaP disease in men. This is an important reportable outcome.
2. The significance of this study is that chemoresistant prostatic tumors could be treated now by

targeting BMI1. This study open up the opportunities to develop new drugs and therapies those specifically could target BMI, thus could be used to overcome therapy resistance of hard-to treat tumors. This is an important outcome of this study.

Conclusion

Recent studies showed that dysregulation of BMI1 alters cell proliferation, senescence and self-renewal of several human cancers (6,10). BMI1 is reported to play a crucial role during epithelial mesenchymal transition during tumor development (6,20). However, the role of BMI1 in human CaP progression and chemoresistance is not well studied (21). It is speculated that inability of tumor cells to undergo apoptosis in response to chemotherapy results in a selective advantage for such tumor cells to become more aggressive compared to chemoresponsive cells during progression of CaP (6). Several studies demonstrate that BMI1 rescues tumor cells from apoptosis and could be a critical factor involved in the emergence of chemoresistance, however no concrete mechanism of action is yet known (8-10). Chemoresistant CRPC is hard-to-treat disease and identifying a critical molecule that confers the chemoresistant characteristic to such tumors would be an important advancement in the field of cancer therapy. In the current study, we provide mechanism-based evidence to show that BMI1 plays a critical role in deciding the therapeutic outcome and the fate of tumor cells undergoing chemotherapy. This study is significant because we demonstrated that BMI1 equally confers chemoresistance to hormone-sensitive CaP and CRPC cells. This is further strengthened by the data that BMI1 expression does not get influenced by androgen. Our data is significant because it explains the possibility of BMI1 as a part of the mechanism that drives indolent disease to aggressive phenotype which is often androgen-independent. This observation carries high significance because CRPC tumors in men proliferate under low androgen conditions (5). Based on our data we suggest that targeting BMI1 should be a part of strategy when therapeutic plans are devised to combat chemoresistant type of cancer.

One of the important observations of this study is that BCL2 and Cyclin D1 (found to be regulated by BMI1) have a commonality to also be functional members of Wnt and Shh pathways. Activity of BCL2 and Cyclin D1 are reported to be high in chemoresistant tumors (13,22-24). Keeping in view the critical role of BCL2 in chemoresistance, targeting the protein directly (anti-BCL2 immunotherapy) or blocking the pathways (such as Shh) which regulates its expression, is being suggested as an ideal strategy to overcome chemoresistance of tumor cells (21, 25-26). Shh inhibitor (Cyclopamine) known to downregulate BCL2 in some tumors is currently being investigated as a therapeutic agent for basal cell carcinoma, medulloblastoma, rhabdomyosarcoma, and glioblastoma (27). However the mechanism that causes the resurgence of tumor cells after BCL2-targeted therapy is not known. Our study is significant because we show that BCL2 is not completely lost in tumor cells after

chemotherapy and alternate pathways (such as BMI1/TCF4 molecular pathway) regulate BCL2 in chemoresistant tumor cells. This is based on our data showing that (i) BMI1 regulates BCL2 independent of Shh-signaling in chemoresistant tumor cells and (ii) elevated levels of BMI1 and BCL2 in cells those survived chemotherapy. We suggest that this mechanism could be an explanation for the survival of chemoresistant cells post-chemotherapy. Although the previous report showed that BMI1 itself is a target of Shh-signaling, our data show that BMI1 acts independent of Shh (28). It is possible that chemoresistant cells expressing BMI1 are a highly selected sub-population that remains hard to treat and play an important role in indolence of disease in human CaP patients.

BMI1 activity is manifested in the form of repression of target genes such as p16 and the mode of action could be through epigenetic silencing, modulation in the methylation states of genes.4 However, in this study we observed that BMI1 upregulates *BCL2* gene. Keeping in view the repressive nature of BMI1, there was a need to understand the mode of action (other than repression) through which BMI1 induces BCL2 expression and activity. We provided evidence that BCL2 activation in chemoresistant cells under the guidance of BMI1 is mediated by TCF4 in tumor cells. This was validated in prostate and colon cancer cells *in vitro*; and in human prostatic tissues. We identified the binding regions of TCF4 transcriptional factor on the promoter of *BCL2*. By conducting several ChIP assays, we observed that binding efficiency of TCF4 to the *BCL2*-promoter is dependent on the BMI1 levels. Although the complete information about the regulation of TCF4 by BMI1 is not completely understood, current data suggest that TCF4 indeed is in part under the control of BMI1. The significance of our data is that it (*i*) identifies BMI1-induced TCF4 as a molecular module that drives Wnt-signaling within chemoresistant tumor cells, and (*ii*) *BCl2* as a target of BMI1/TCF4 molecular module. Based on our data, we speculate that molecular module could be operational during emergence of chemoresistance in CaP cells and also responsible for the survival and proliferation of chemoresistant tumor cells after chemotherapy.

Docetaxel has been tested under several clinical trials alone and in combination with other agents to treat CaP. Docetaxel therapy was observed to result in a PSA drop of more than 50% in CaP patients, an observation made in several trials such as the SWOG trial (29). However, docetaxel alone, and in combination do not completely abrogate the tumor or bring down PSA levels to the normal in human CaP patients (29). Although effective in CaP patients to an extent, some CaP conditions do not respond to docetaxel therapy and such patients do not exhibit changes in PSA level after therapy (30). In this context, this study is highly significant as we show that targeting BMI1 in chemoresistant CRPC cells sensitizes tumor cells to docetaxel therapy both *in vitro* and *in vivo*. This study identified BMI1 as an ideal molecule to be targeted to overcome the chemoresistance of CaP cells and corroborates to earlier report showing the utility of BMI1 as a target to overcome

chemoresistance in ovarian cancer cells (9). Under *in vivo* conditions, the significance between BMI1-positive, BMI-silenced and BMI1-overexpressed tumor cells vis-à-vis docetaxel therapy was significant. The success of docetaxel therapy against prostatic tumors in a xenograft mouse model was observed to be highly dependent on the level of BMI1. We suggest that preventing the development of chemoresistance in CaP patients will be beneficial for a large group of patients and interventions directed against BMI1 may provide opportunities to enhance the efficacy of chemotherapy. In this direction we have opened another front by identifying small molecule inhibitors of BMI1. We suggest that these should be explored against chemoresistant tumors. The advanced work with small molecule inhibitors of BMI1 against chemoresistant tumors is underway in our laboratory.

References

1. Siegel R, Naishadham D, Jemal A. Cancer statistics, 2013. CA Cancer J Clin. 2013;63(1):11-30. PubMed PMID: 23335087.
2. Mahon KL, Henshall SM, Sutherland RL, Horvath LG. Pathways of chemotherapy resistance in castration-resistant prostate cancer. Endocr Relat Cancer. 2011; 18: R103-23.
3. Zhang L, Jiao M, Li L, Wu D, Wu K, Li X, et al. Tumorspheres derived from prostate cancer cells possess chemoresistant and cancer stem cell properties. J Cancer Res Clin Oncol. 2012; 138: 675-86.
4. Kotb AF, Elabbady AA. Prognostic factors for the development of biochemical recurrence after radical prostatectomy. Prostate Cancer. 2011; 2011: 485189.
5. Parray A, Siddique HR, Nanda S, Konety BR, Saleem M. Castration-resistant prostate cancer: potential targets and therapies. Biologics. 2012;6:267-76.
6. Siddique HR, Saleem M. Role of BMI1, a Stem Cell Factor in Cancer Recurrence and Chemoresistance: Preclinical and Clinical Evidences. Stem Cells. 2012; 30:372-8.
7. Kang MK, Kim RH, Kim SJ, Yip FK, Shin KH, Dimri GP, et al. Elevated BMI1 expression is associated with dysplastic cell transformation during oral carcinogenesis and is required for cancer cell replication and survival. Br J Cancer. 2007; 96: 126-33.
8. Jacobs JJ, Scheijen B, Voncken JW, Kieboom K, Berns A, van Lohuizen M. BMI1 collaborates with c-Myc in tumorigenesis by inhibiting c-Myc-induced apoptosis via INK4a/ARF. Genes Dev. 1999; 13: 2678-90.
9. Cui H, Hu B, Li T, Ma J, Alam G, Gunning WT, et al. BMI1 is essential for the tumorigenicity of neuroblastoma cells. Am J Pathol. 2007, 170: 1370-1378.
10. Wang E, Bhattacharyya S, Szabolcs A, Rodriguez-Aguayo C, Jennings NB, Lopez-Berestein G, et al. Enhancing chemotherapy response with BMI1 silencing in ovarian cancer. PLoS One

2011; 6: e17918.

11. Huber GF, Albinger-Hegyi A, Soltermann A, Roessle M, Graf N, Haerle SK et al. Expression patterns of BMI1 and p16 significantly correlate with overall, disease-specific, and recurrence-free survival in oropharyngeal squamous cell carcinoma. Cancer. 2011 117: 4659-70.
12. Glinsky GV, Berezovska O, Glinskii AB. Microarray analysis identifies a death-from-cancer signature predicting therapy failure in patients with multiple types of cancer. J Clin Invest. 2005; 115:1503-21.
13. Siddique HR, Liao DJ, Mishra SK, Schuster T, Wang L, Matter B et al. Epicatechin-rich cocoa polyphenol inhibits kras-activated pancreatic ductal carcinoma cell growth in vitro and in a mouse model. Int J Cancer. 2011; doi: 10.1002/ijc.27409.
14. Siddique HR, Mishra SK, Karnes RJ, Saleem M. Lupeol, a novel androgen receptor inhibitor: implications in prostate cancer therapy. Clin Cancer Res. 2011; 17: 5379-91.
15. Saleem M, Adhami VM, Zhong W, Longley BJ, Lin CY, Dickson RB et al. A novel biomarker for staging human prostate adenocarcinoma: overexpression of matriptase with concomitant loss of its inhibitor, hepatocyte growth factor activator inhibitor-1. Cancer Epidemiol Biomarkers Prev. 2006; 15: 217-27.
16. Hegde GV, Munger CM, Emanuel K, Joshi AD, Greiner TC, Weisenburger DD, Vose JM, et al. Targeting of sonic hedgehog-GLI signaling: a potential strategy to improve therapy for mantle cell lymphoma. Mol Cancer Ther 2008 7:1450-60.
17. Rohrs S, Kutzner N, Vlad A, Grunwald T, Ziegler S, Müller O. Chronological expression of Wnt target genes Ccnd1, Myc, Cdkn1a, Tfrc, Plf1 and Ramp3. Cell Biol Int. 2009; 33: 501-8.
18. Kanwar SS, Yu Y, Nautiyal J, Patel BB, Majumdar AP. The Wnt/beta-catenin pathway regulates growth and maintenance of colonospheres. Mol Cancer. 2010; 9:212.
19. Bigelow RL, Chari NS, Unden AB, Spurgers KB, Lee S, Roop DR, et al. Transcriptional regulation of BCL2 mediated by the sonic hedgehog signaling pathway through Gli-1. J Biol Chem. 2004; 279: 1197-205.
20. Song LB, Li J, Liao WT, Feng Y, Yu CP, Hu LJ et al. The polycomb group protein BMI1 represses the tumor suppressor PTEN and induces epithelial-mesenchymal transition in human nasopharyngeal epithelial cells. J Clin Invest. 2009; 119: 3626-36.
21. Crea F, Duhagon Serrat MA, Hurt EM, Thomas SB, Danesi R, Farrar WL. BMI1 silencing enhances docetaxel activity and impairs antioxidant response in prostate cancer. Int J Cancer 2011; 128: 1946-1954.
22. Casimiro M, Rodriguez O, Pootrakul L, Aventian M, Lushina N, Cromelin C et al. ErbB-2 induces the cyclin D1 gene in prostate epithelial cells in vitro and in vivo. Cancer Res. 2007;

67: 4364-72.

23. Kang MH, Reynolds CP. BCL2 inhibitors: targeting mitochondrial apoptotic pathways in cancer therapy. Clin Cancer Res. 2009; 15: 1126-32.
24. Brunelle JK, Letai A. Control of mitochondrial apoptosis by the BCL2 family. *J Cell Sci.* 2009; 122(Pt 4): 437-41.
25. Mackler NJ, Pienta KJ. Drug insight: use of docetaxel in prostate and urothelial cancers. Nat Clin Pract Urol 2005; 2: 92-100.
26. Straten P, Andersen MH. The anti-apoptotic members of the Bcl-2 family are attractive tumor-associated antigens. Oncotarget. 2010; 1: 239-45.
27. Mahindroo N, Punchihewa C, Fujii N. Hedgehog-Gli signaling pathway inhibitors as anticancer agents. J Med Chem. 2009; 52: 3829-45.
28. Liu S, Dontu G, Mantle ID, Patel S, Ahn NS, Jackson KW et al. Hedgehog signaling and BMI1 regulate self-renewal of normal and malignant human mammary stem cells. Cancer Res 2006; 66: 6063-6071.
29. Petrylak DP. New paradigms for advanced prostate cancer. Rev Urol. 2007; 9 Suppl 2:S3-S12.
30. Ross RW, Beer TM, Jacobus S, Bubley GJ, Taplin ME, Ryan CW, Huang J, et al. Prostate Cancer Clinical Trials Consortium. A phase 2 study of carboplatin plus docetaxel in men with metastatic hormone-refractory prostate cancer who are refractory to docetaxel. Cancer. 2008; 112: 521-6.

Legends to Figures

Figure 1. BMI1 Protein levels are increased during the progression of CaP from low to high-grade in human patients and plays an important role in cell proliferation, independent of androgen. (**A)** Figure represents the level of BMI1 protein in human normal, dysplasia and tumor prostatic tissues as assessed by immunoblot analysis. Equal loading of protein was confirmed by reprobing immunoblot for □-actin. (**Bi**) Photomicrographs represent immunostaining of BMI1 in CaP specimens and non-neoplastic regions of prostatic specimens of CaP patients. ➡ Arrows indicate staining for BMI1. Magnification X40. (**Bii**) Box plots for BMI1 protein based on score pertain to immunostaining pattern in normal and CaP specimens. *, $P < 0.05$; black bar in gray box, median values. **(C)** Figure represents the level of BMI1 protein in androgen (R1881) treated and non-treated CaP cells as assessed by immunoblot analysis. Equal loading of protein was confirmed by reprobing immunoblot for β-actin. (**Di-ii**) The histogram represents the rate of cell proliferation and % cell growth of CaP cells at 36h post-transfection as measured by MTT assay. (**Ei-ii**) Histogram showing rate of [3H]thymidine uptake in BMI1-silenced and -overexpressed CaP cells. (**Fi-ii**) Histogram

showing number of colonies formed by BMI1-silenced and –overexpressed CaP cells. Each bar in each histogram (Fig. D-F) represents mean ± S.E., * indicates $p<0.05$. All experiments were repeated three times with similar results.

Figure 2. BMI1 play a critical role in the proliferation of normal and tumor cells and regulates the expression of genes associated with the proliferation of prostatic tumor cells. (A) Photomicrographs represent the effect of BMI1-overexpression on the replication/ proliferation of normal prostate epithelial cells (PrEC). PrEC cells were transfected with pbabe-BMI1 plasmid and equal amount of empty vector (control). Confluent dishes containing BMI1-overexpressing cells and vector-transfected PrEC cells were split or seeded after every 36h. Left Panel: Cell splitting or seeding continued for 5 passages or replication cycles in control PrEC cells and did not duplicate after 5 passages and entered into senescence phase. Right Panel: Cell splitting or seeding continued for 8 passages or replication cycles in pbabe-BMI1 transfected PrEC cells. Inset regions (400X) showing cells with senescent morphology features of live cells such as globular shape. **(B)** Photomicrographs represent the effect of BMI1-overexpression on the senescence-associated □-galactosidase activity in normal prostate epithelial cells (PrEC). PrEC cells were transfected with pbabe-BMI1 plasmid and equal amount of empty vector (control). Confluent dishes containing BMI1-overexpressing cells and vector-transfected PrEC cells were split or seeded after every 36h. Upper Panel: Cell splitting or seeding continued for 4th passages or replication cycles in control PrEC cells and entered into senescence phase. Lower Panels: Cell splitting or seeding continued for 7 passages or replication cycles in pbabe-BMI1 transfected PrEC cells. ➡ Arrows indicate staining for β-galactosidase. **(C)** Scattered Plot for PCR array. The dots indicate the folds-Change of gene regulation. Fold change (2^- Delta Delta Ct) is the normalized gene expression (2^-Delta Ct) in the BMI1 suppressed sample divided the normalized gene expression (2^(- Delta Ct)) in the Control Sample. For details please see the Supplementary scatter plot excel data sheet and Clustrogram (Suppl. Fig. 2). **(D & E)** Figure represents the effect of (**A**) BMI1-silenced and (**B**) BMI1-overexpression on the expression level of Cyclin D1, BCL2 and p16 proteins in CaP cells as assessed by immunoblot analysis. For immunoblot data analyses, equal loading was confirmed by reprobing immunoblots for □-actin.

Figure 3. BMI1 confers chemoresistance against chemotherapeutic agents by inhibiting cell death of prostatic tumor cells. (A-D) The histogram represents the rate of proliferation of cells as measured by 3[H]thymidine uptake assay in (A-B) LNCaP and (C-D) PC3 cells harboring varied BMI1 levels treated with different chemotherapeutic agents. Vehicle treated cells were considered as control. (**Ei**) Figure represents the level of BMI1, Cyclin D1 and BCL2 protein in chemoresistant PC3 cells as assessed by immunoblot analysis. (**Eii**) Histogram showing the rate of

[3H]thymidine uptake in chemoresistant CaP cells. (**Fi**) Figure represents the level of BMI1, Cyclin D1 and BCL2 protein in BMI1-silenced chemoresistant PC3 cells as assessed by immunoblot analysis. (**Fii**) Histogram shows the rate of proliferation as assessed by [3H]thymidine uptake assay in BMI1-silenced chemoresistant CaP cells. Control cells were transfected with empty vector alone. For immunoblot data analyses (Fig. Ei and Fi), equal loading was confirmed by reprobing immunoblots for □-actin. Each bar in the histogram (Fig. A-D, Eii and Fii), represents mean ± SE of three independent experiments, * represents $P < 0.05$. (**G-H**) Quantitative estimation of apoptosis in BMI1-silencing chemoresistant cells as assessed by flow cytometry. Both docetaxel resistant and BMI1-silenced docetaxel resistant cells were labeled with Annexin-V and PI. Intact cells were gated in the FSC/SSC plot to exclude small debris. Cells in the lower right quadrant of the FL1/FL2 dot plot (labeled with Annexin V-FITC only) are considered to be in early apoptosis, and cells in the upper right quadrant (labeled with Annexin V-FITC and PI) are in late apoptosis/necrosis. The images shown here are representative of three independent experiments with similar results.

Figure 4: BMI1 modulates BCL2 activity in Tumor cells. (**A-B**) Histogram represents the effect of BMI1-overexpression (A) and –silencing (B) on the transcriptional activation of TCF responsive element in CaP cells as assessed by Luciferase based reporter assay. Relative luciferase activity was calculated with the values from vector alone group. **(C-D)** Histogram represents the effect of BMI1-overexpression (**C**) and -silencing (**D**) on the transcriptional activation of TCF responsive element in HT29 cells as assessed by Luciferase based reporter assay. (**E**) Figure represents the effect of BMI1-silencing and -overexpression on the level of BCL2 and Cyclin D1 proteins in HT29 cells as assessed by immunoblot analysis. **(F)** Figures represent the effect of cyclopamine treatment on the level of BCL2 protein in (Fi) BMI1-overexpressing and (Fii) -suppressing LNCaP cells. At 24h post-transfection, cells were treated with cyclopamine in fresh media. Control cells were treated with DMSO (vehicle alone). After 12h incubation of cells with cyclopamine or vehicle alone cells were harvested and immunoblot analysis were performed. (**G**) Histogram represents the effect of cyclopamine treatment on the transcriptional activity of BCL2 promoter in LNCaP cells under BMI1-overexpression and –suppression. (**H**) Histogram represents the effect of TCF-silencing on the transcriptional activity of BCL2 promoter in CaP and HT29 cells as assessed by Luciferase based reporter assay. Relative luciferase activity (G & H) was calculated with the values from vector alone group. For immunoblot data analyses (Fig. E and F), equal loading was confirmed by reprobing immunoblots for β-actin. Each bar in the histogram (Fig. A, B, C, D, G and H), represents mean ± SE of three independent experiments, * represents $P < 0.05$.

Figure 5. BMI1 regulates BCL2 by occupying its promoter in tumor cells and tissues and confers chemoresistance *in* a xenograft mouse model. (A-B) Effect of BMI1 expression on TCF4-

occupancy on promoter site of BCL2 in PC3 (A) and HT29 (B) cells as assessed by ChIP assay as described in materials and methods. (**C**) Figure represents the level of BMI1 protein in normal and malignant human prostate tissues as assessed by immunoblot analyses. (**D**) Histogram shows the TCF4-occupancy on promoter site of BCl2 in human normal and malignant prostate tissues as assessed by ChIP assay. For immunoblot data analyses, equal loading was confirmed by reprobing immunoblots for β-actin. Each bar in the histogram, represents mean ± SE of three independent experiments, * represents $P < 0.05$. **(E)** The graphical representation of data showing the effect of docetaxel therapy on the growth of BMI1-overexpressing (BO) PC3-derived tumor cells implanted in mice. The growth was measured in terms of average volume of tumors as a function of time. Data is represented as mean ± SE, * indicates $p< 0.05$ from the control group. (**F**) The graphical representation of the data showing the number of mice remain with tumor volumes <1000 mm^3 after either BMI1-overexpression for indicated weeks. The details are described under Materials and Methods.

Figure 6. Targeting of BMI1 by gene therapy sensitizes tumors to chemotherapy *in* xenograft mouse models. (A) The graphical representation of data showing the effect of targeting of BMI1 in tumor cells and responsiveness to docetaxel therapy in mice implanted with PC3-derived tumor cells. The growth was measured in terms of average volume of tumors as a function of time. Data is represented as mean ± SE, * indicates $p< 0.05$ from the control group. (**B**) The graphical representation of the data showing the number of mice remain with tumor volumes <1000 mm^3 after BMI1-silencing for indicated weeks. **(C)** The graphical representation of data showing the effect of targeting of BMI1 by siRNA delivered in liposomes (3-times/ week) in tumor cells and responsiveness to Sulindac therapy in mice implanted with PC3-derived tumor cells. The growth was measured in terms of average volume of tumors as a function of time. Data is represented as mean ± SE, * indicates $p< 0.05$ from the control group. (**D**) The bar graph shows the average tumor weights (harvested from mice at the termination of study). The details are described under Materials and Methods.

Figure 7. Relevance of BMI1 in (A) proliferation and (B) BCL2 expression of tumor cells *in vivo.* Photomicrographs (20x, magnification) showing (**A**) *in vivo* cell proliferation as assessed by BrdU assay and (**B**) BCL2-expression in tumors as assessed by immunostaining. The arrows in the micrographs represent regions exhibiting immunoreactivity. The immunostaining data was confirmed in all specimens from each group (n =10).

Legends to Supplementary figures:

Figure 1. (A) Figure represents the effect of BMI1-silencing and -overexpression on the level of BMI1 protein in CaP cells as assessed by immunoblot analyses. Equal loading was confirmed by reprobing

immunoblots for β-actin.

Figure 2. (A) Figure represents clustrogram of gene expression as assessed by PCR array. Clustrogam is the representation of three independent experiments. (B-D) Time-course and dose titration curves for the chemotherapeutic agents Casodex (B), Cisplatin (C) and Docetaxel (D) as assessed by MTT assay. Vehicle treated cells were considered as control. Data represents mean ± SE of three independent experiments.

Figure 3: (A-B) The histogram represents the rate of proliferation of cells as measured by MTT assay in BMI1 overexpressing (A) LNCaP and (B) PC3 cells treated with different chemotherapeutic agents. Vehicle treated cells were considered as control. Each bar in the histogram, represents mean ± SE of three independent experiments, * represents $P < 0.05$.

Figure 4: (A-B) The histogram represents the rate of proliferation of cells as measured by MTT assay in BMI1-silenced (A) LNCaP and (B) PC3 cells treated with different chemotherapeutic agents. Vehicle treated cells were considered as control. Each bar in the histogram, represents mean ± SE of three independent experiments, * represents $P < 0.05$.

<u>Acknowledgements of funding in manuscripts</u>:

The funding (W81XWH-08-1-0605) from CDMRP-DOD has been acknowledged in the paper published. Published papers are attached as Appendices I-II.

1: Paper published in Scientific Journal.“ **Stem Cells**, 30: 372-78; 2012” (**Appendix I**).

2. Paper Published in Scientific Journal ***PLOS-ONE***. 2013 May 6;8(5):e60664. PMID: 23671559 (**Appendix II**).

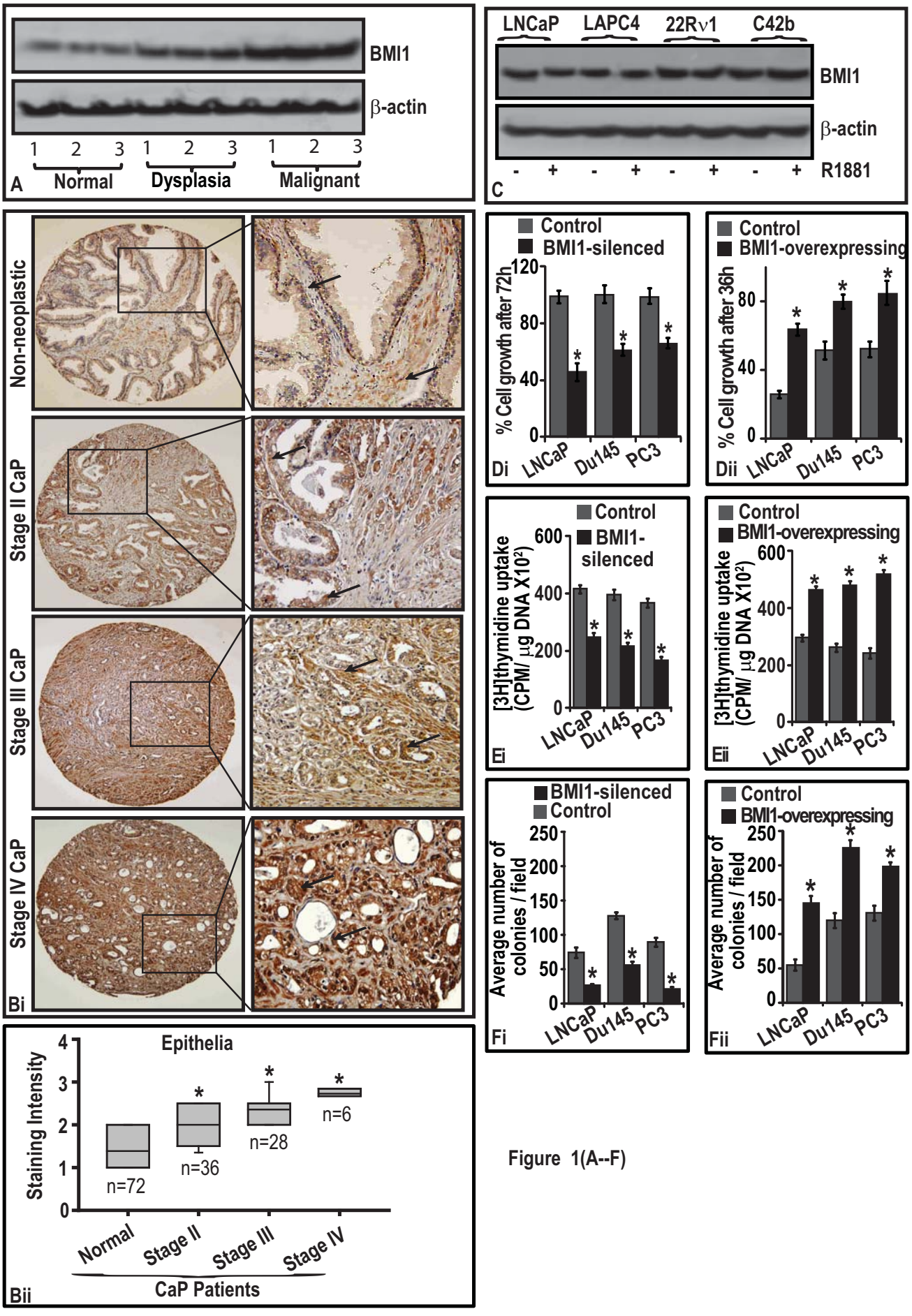
BMI1
β-actin
1 2 3 1 2 3 1 2 3
A
Normal
Dysplasia
Malignant
LNCaP
LAPC4
22Rv1
C42b
BMI1
β-actin
- + - + - + - + R1881
C
Non-neoplastic
Stage II CaP
Stage III CaP
Stage IV CaP
Bi
Control
BMI1-silenced
% Cell growth after 72h
120
80
40
0
LNCaP
Du145
PC3
Di
Control
BMI1-overexpressing
% Cell growth after 36h
80
40
0
LNCaP
Du145
PC3
Dii
Control
BMI1-silenced
[3H]thymidine uptake (CPM/ μg DNA X10²)
600
400
200
0
LNCaP
Du145
PC3
Ei
Control
BMI1-overexpressing
[3H]thymidine uptake (CPM/ μg DNA X10²)
600
400
200
0
LNCaP
Du145
PC3
Eii
BMI1-silenced
Control
Average number of colonies / field
250
200
150
100
50
0
LNCaP
Du145
PC3
Fi
Control
BMI1-overexpressing
Average number of colonies / field
250
200
150
100
50
0
LNCaP
Du145
PC3
Fii
Epithelia
Staining Intensity
4
3
2
1
0
n=72
n=36
n=28
n=6
Normal
Stage II
Stage III
Stage IV
CaP Patients
Bii

Figure 1(A--F)

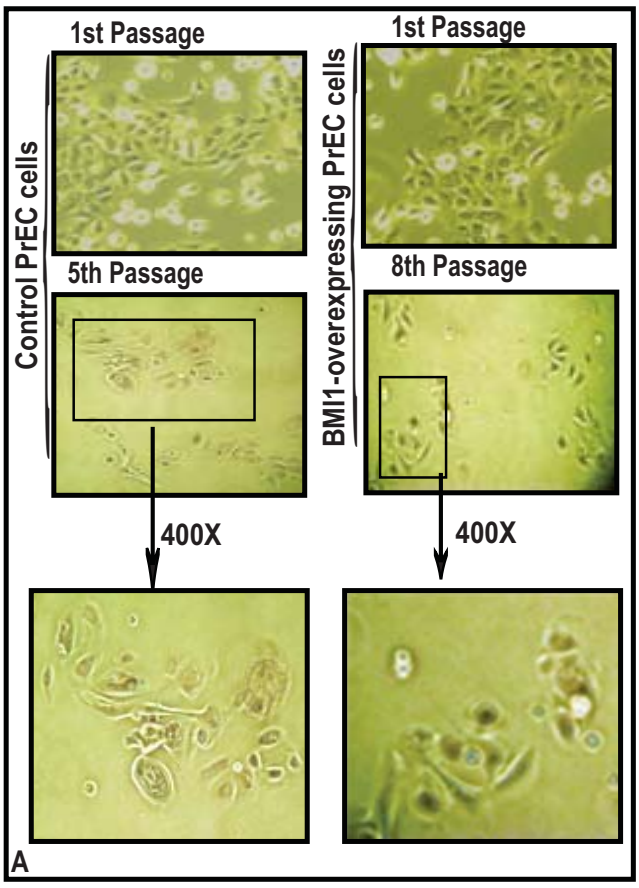
1st Passage
1st Passage
Control PrEC cells
BMI1-overexpressing PrEC cells
5th Passage
8th Passage
400X
400X
A

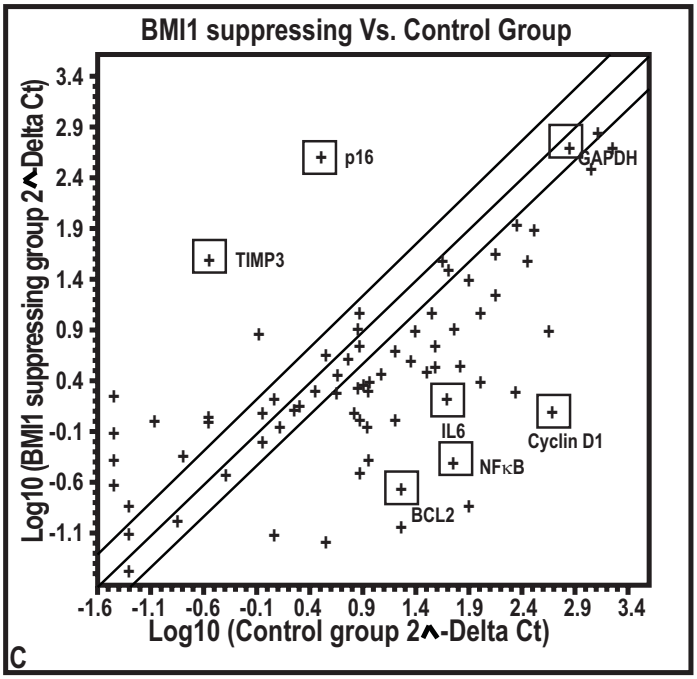
BMI1 suppressing Vs. Control Group
Log10 (BMI1 suppressing group 2^-Delta Ct)
Log10 (Control group 2^-Delta Ct)
3.4
2.9
2.4
1.9
1.4
0.9
0.4
-0.1
-0.6
-1.1
-1.6
-1.1
-0.6
-0.1
0.4
0.9
1.4
1.9
2.4
2.9
3.4
p16
GAPDH
TIMP3
IL6
Cyclin D1
NFκB
BCL2
C

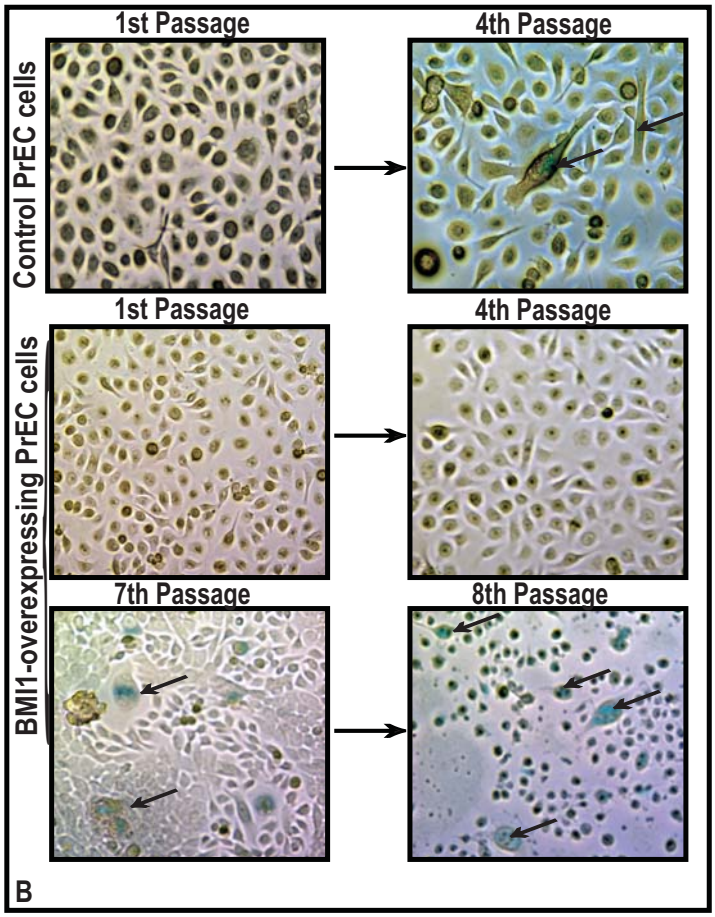
1st Passage
4th Passage
Control PrEC cells
1st Passage
4th Passage
BMI1-overexpressing PrEC cells
7th Passage
8th Passage
B

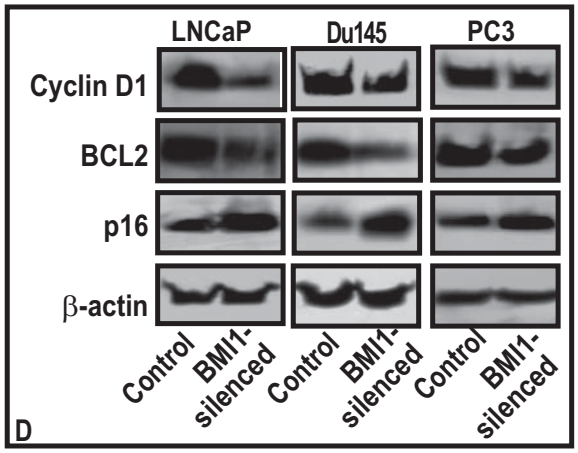
LNCaP
Du145
PC3
Cyclin D1
BCL2
p16
β-actin
Control
BMI1-silenced
Control
BMI1-silenced
Control
BMI1-silenced
D

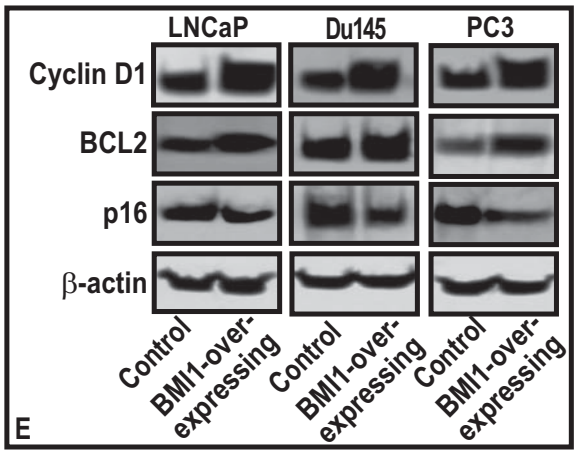
LNCaP
Du145
PC3
Cyclin D1
BCL2
p16
β-actin
Control
BMI1-over-expressing
Control
BMI1-over-expressing
Control
BMI1-over-expressing
E

Figure 2 (A-H)

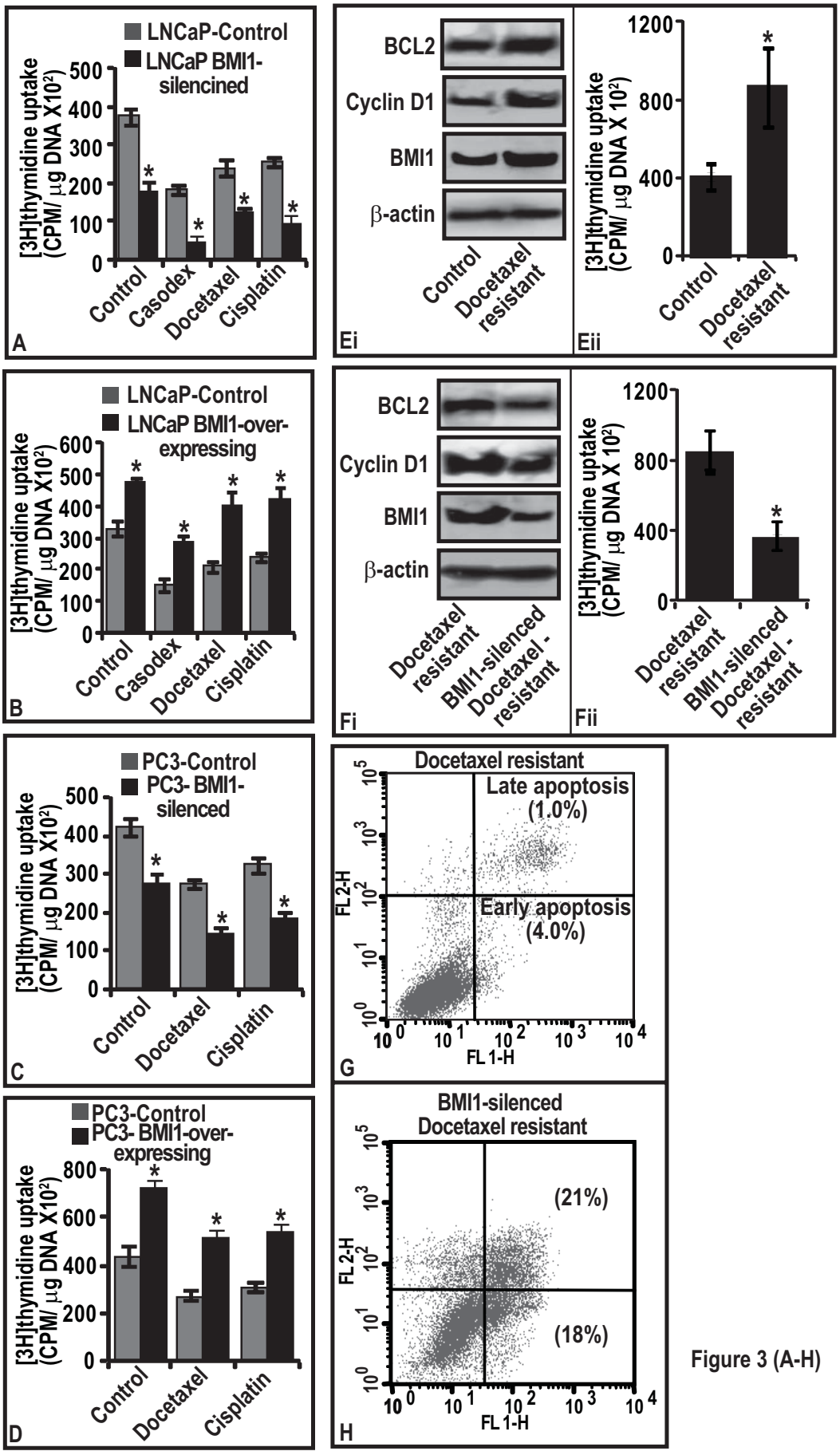
LNCaP-Control
LNCaP BMI1-silencined
[3H]thymidine uptake (CPM/ μg DNA X10²)
Control
Casodex
Docetaxel
Cisplatin
A
BCL2
Cyclin D1
BMI1
β-actin
Control
Docetaxel resistant
Ei
[3H]thymidine uptake (CPM/ μg DNA X 10²)
Control
Docetaxel resistant
Eii
LNCaP-Control
LNCaP BMI1-over-expressing
B
Docetaxel resistant
BMI1-silenced Docetaxel - resistant
Fi
Fii
PC3-Control
PC3- BMI1-silenced
C
PC3-Control
PC3- BMI1-over-expressing
D
Docetaxel resistant
Late apoptosis (1.0%)
Early apoptosis (4.0%)
FL2-H
FL 1-H
G
BMI1-silenced Docetaxel resistant
(21%)
(18%)
H

Figure 3 (A-H)

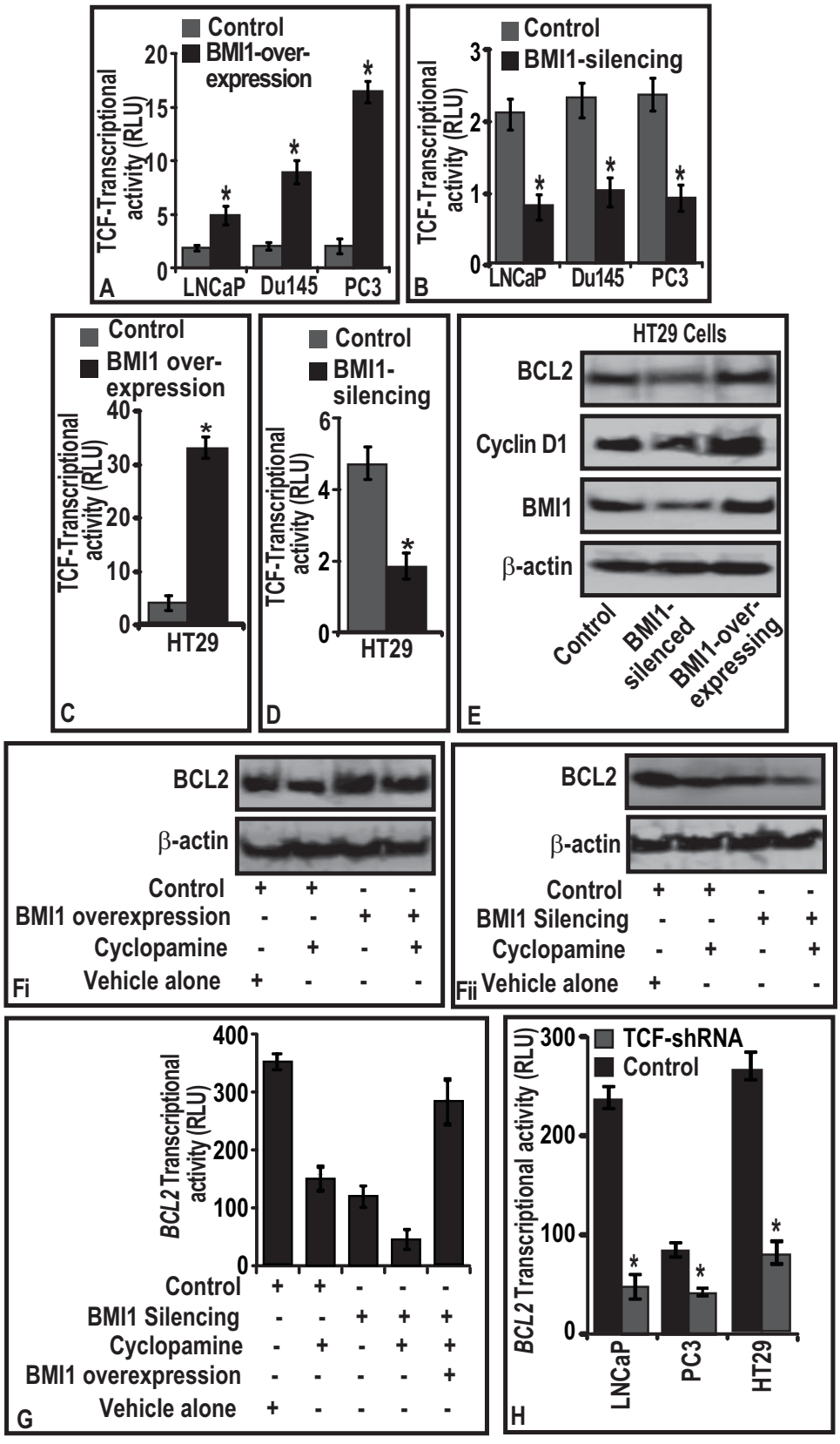
Control
BMI1-over-expression
TCF-Transcriptional activity (RLU)
20
15
10
5
0
LNCaP
Du145
PC3
A
Control
BMI1-silencing
3
2
1
0
B
Control
BMI1 over-expression
40
30
20
10
HT29
C
Control
BMI1-silencing
6
4
2
HT29
D
HT29 Cells
BCL2
Cyclin D1
BMI1
β-actin
Control
BMI1-silenced
BMI1-over-expressing
E
BCL2
β-actin
Control + + - -
BMI1 overexpression - - + +
Cyclopamine - + - +
Vehicle alone + - - -
Fi
BCL2
β-actin
Control + + - -
BMI1 Silencing - - + +
Cyclopamine - + - +
Vehicle alone + - - -
Fii
BCL2 Transcriptional activity (RLU)
400
300
200
100
0
Control + + - - -
BMI1 Silencing - - + + +
Cyclopamine - + - + +
BMI1 overexpression - - - - +
Vehicle alone + - - - -
G
TCF-shRNA
Control
300
200
100
0
LNCaP
PC3
HT29
H

Figure 4 (A-H)

(Figure 5)

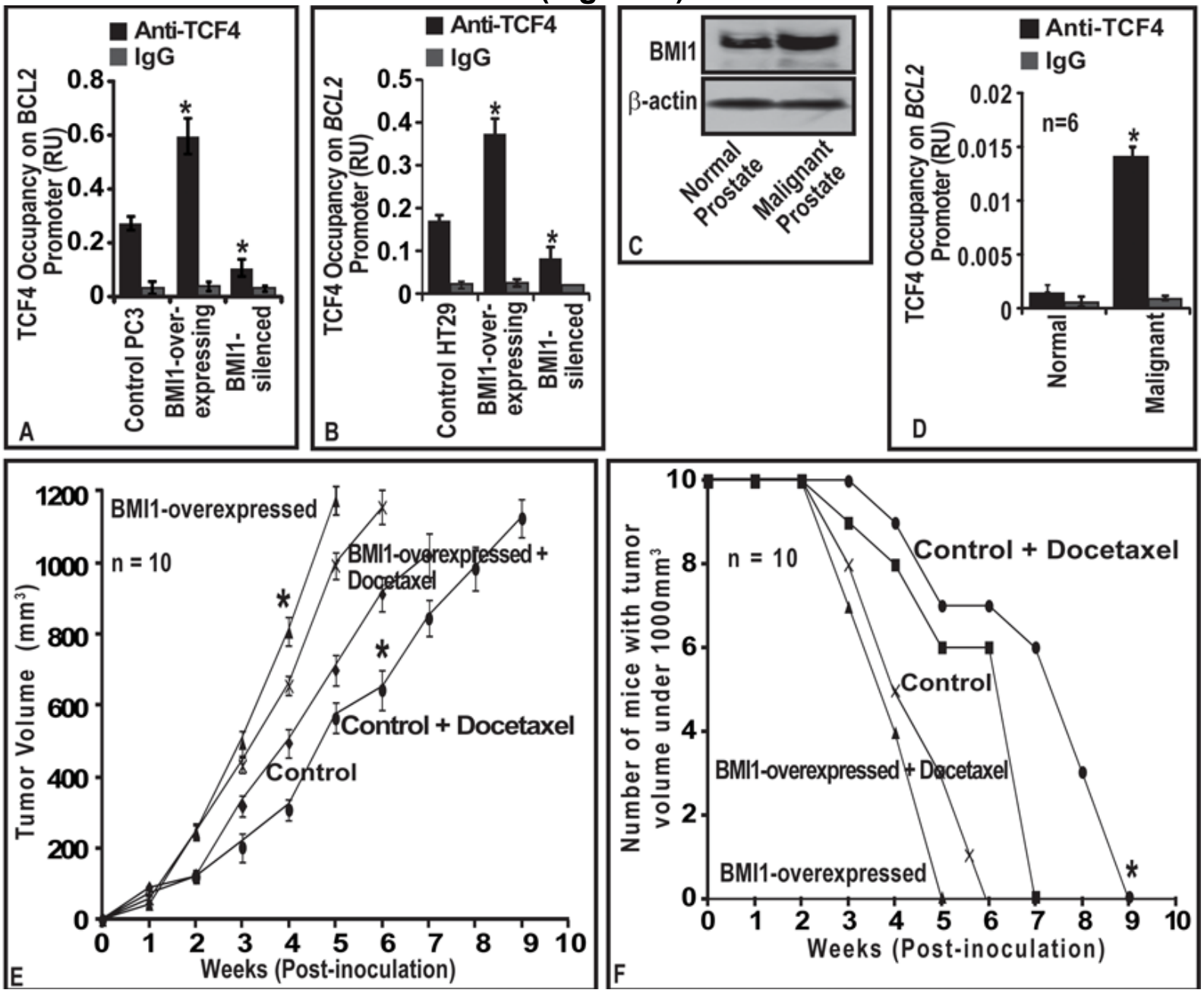
Anti-TCF4
IgG
TCF4 Occupancy on BCL2 Promoter (RU)
0.8
0.6
0.4
0.2
0
*
*
Control PC3
BMI1-over-expressing
BMI1-silenced
A
Anti-TCF4
IgG
TCF4 Occupancy on BCL2 Promoter (RU)
0.5
0.4
0.3
0.2
0.1
0
*
*
Control HT29
BMI1-over-expressing
BMI1-silenced
B
BMI1
β-actin
Normal Prostate
Malignant Prostate
C
Anti-TCF4
IgG
TCF4 Occupancy on BCL2 Promoter (RU)
0.02
0.015
0.01
0.005
0
n=6
*
Normal
Malignant
D
BMI1-overexpressed
n = 10
BMI1-overexpressed + Docetaxel
Control + Docetaxel
Control
Tumor Volume (mm3)
1200
1000
800
600
400
200
0
*
*
0 1 2 3 4 5 6 7 8 9 10
Weeks (Post-inoculation)
E
n = 10
Control + Docetaxel
Control
BMI1-overexpressed + Docetaxel
BMI1-overexpressed
Number of mice with tumor volume under 1000mm3
10
8
6
4
2
0
*
0 1 2 3 4 5 6 7 8 9 10
Weeks (Post-inoculation)
F

(Figure 6)

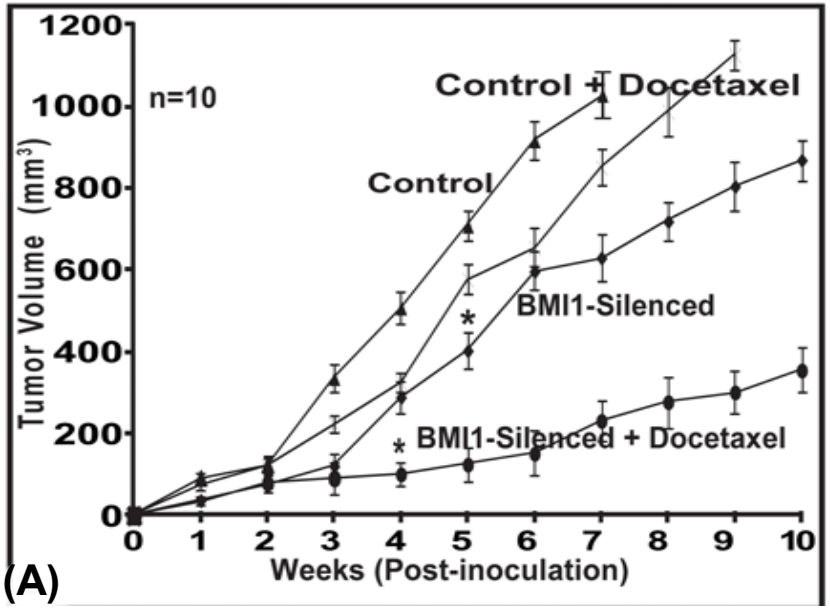
n=10
Control + Docetaxel
Control
BMI1-Silenced
BMI1-Silenced + Docetaxel
Tumor Volume (mm³)
Weeks (Post-inoculation)
(A)

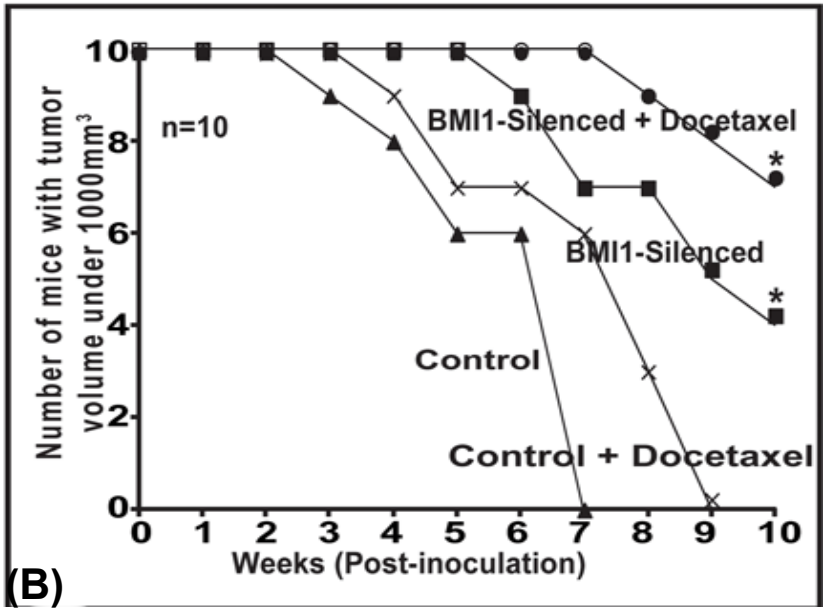
n=10
BMI1-Silenced + Docetaxel
BMI1-Silenced
Control
Control + Docetaxel
Number of mice with tumor volume under 1000mm³
Weeks (Post-inoculation)
(B)

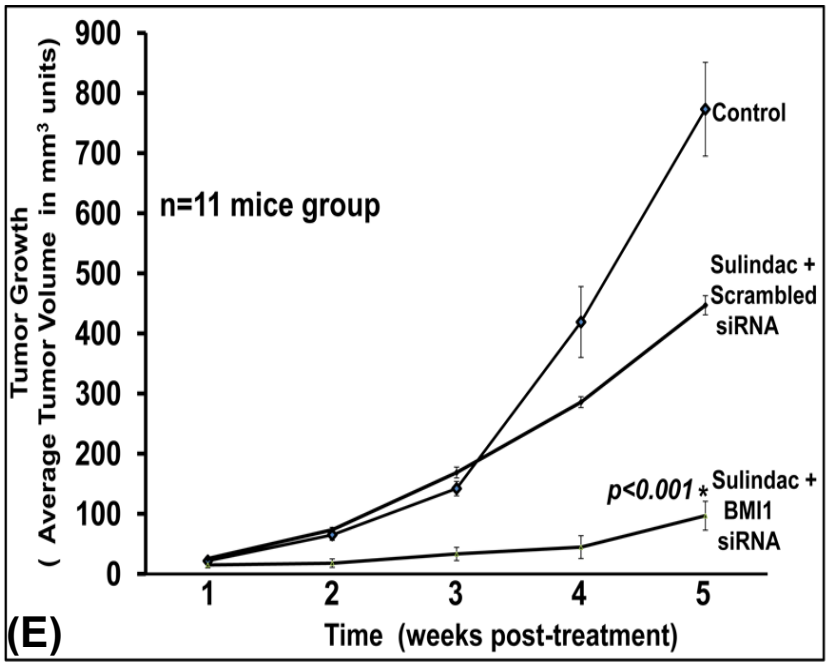
n=11 mice group
Control
Sulindac + Scrambled siRNA
Sulindac + BMI1 siRNA
p<0.001
Tumor Growth (Average Tumor Volume in mm³ units)
Time (weeks post-treatment)
(E)

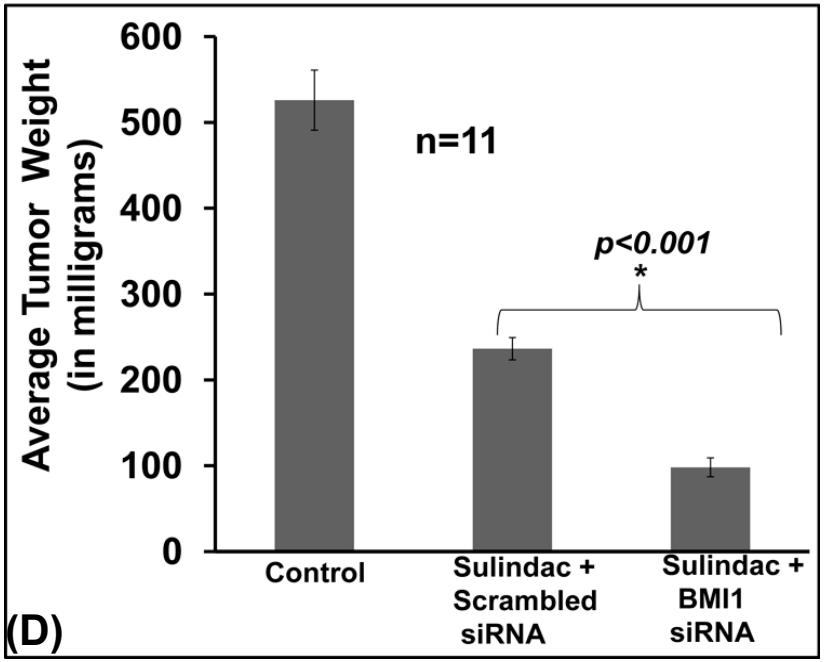
n=11
p<0.001
Average Tumor Weight (in milligrams)
Control
Sulindac + Scrambled siRNA
Sulindac + BMI1 siRNA
(D)

Figure 7

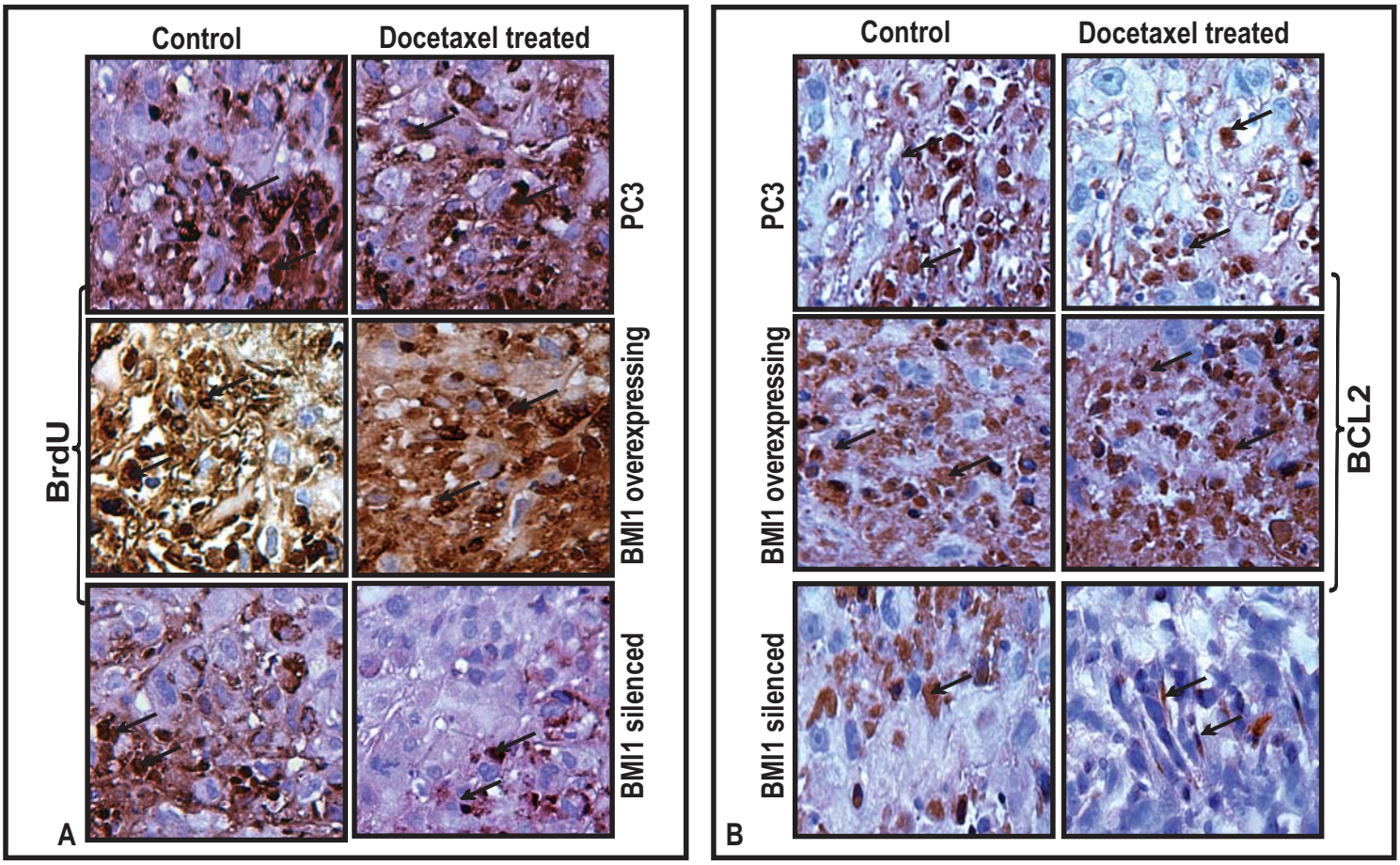
Control
Docetaxel treated
PC3
BMI1 overexpressing
BMI1 silenced
BrdU
A
Control
Docetaxel treated
PC3
BMI1 overexpressing
BMI1 silenced
BCL2
B

Supplementary Figure 1

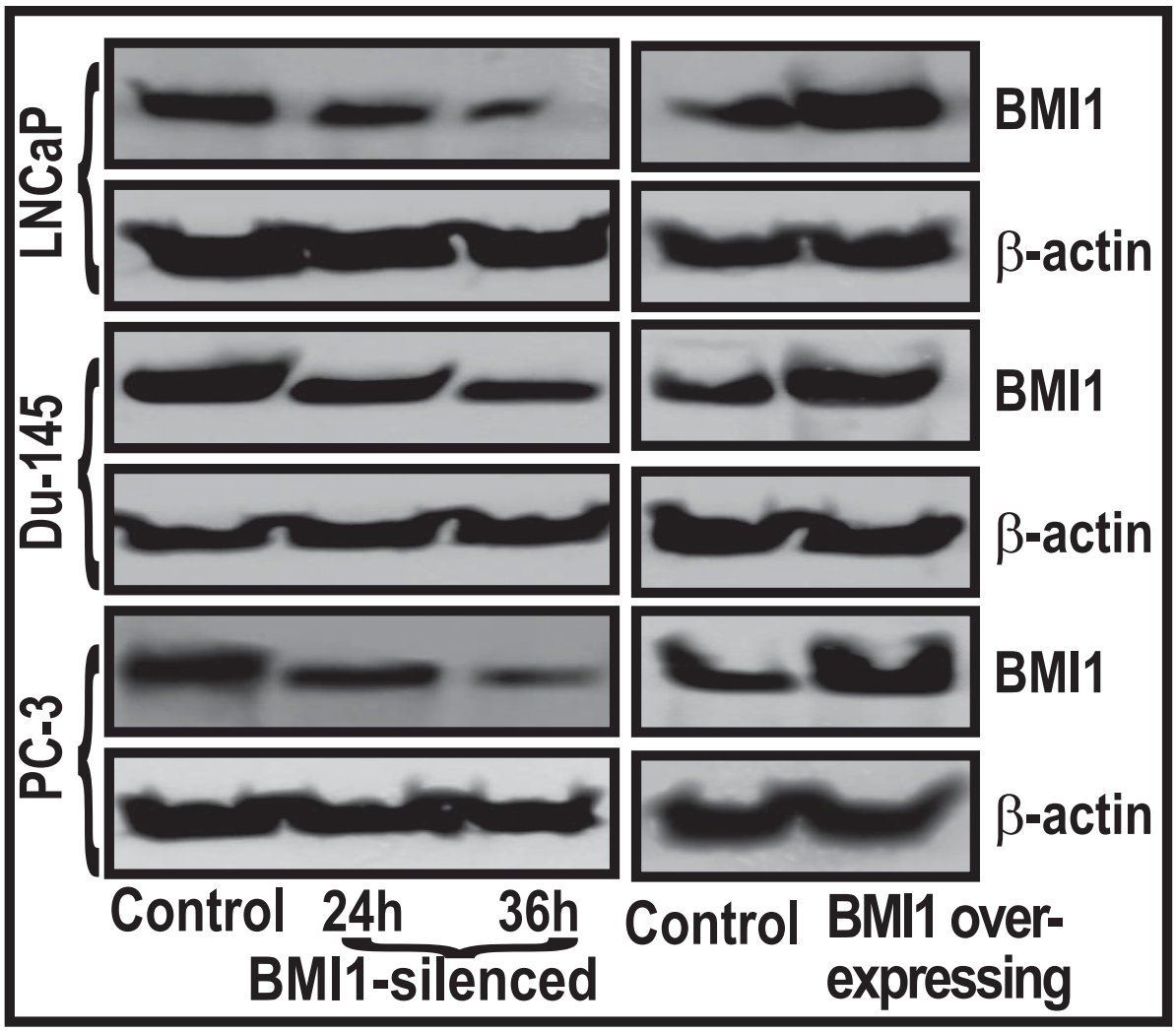

Figure 1

Supplementary Figure 2

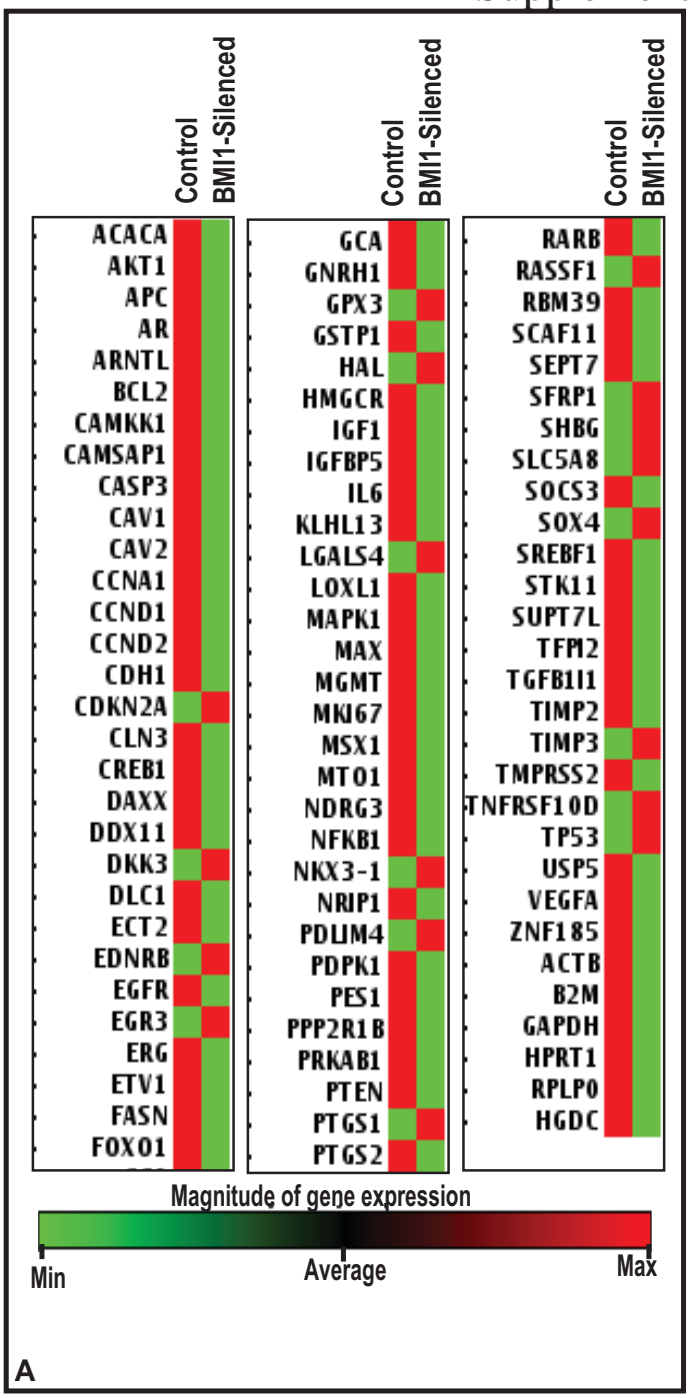

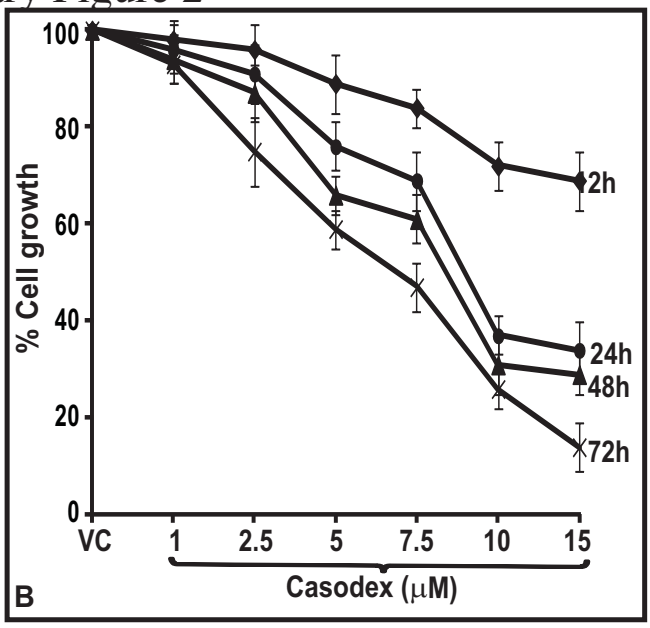

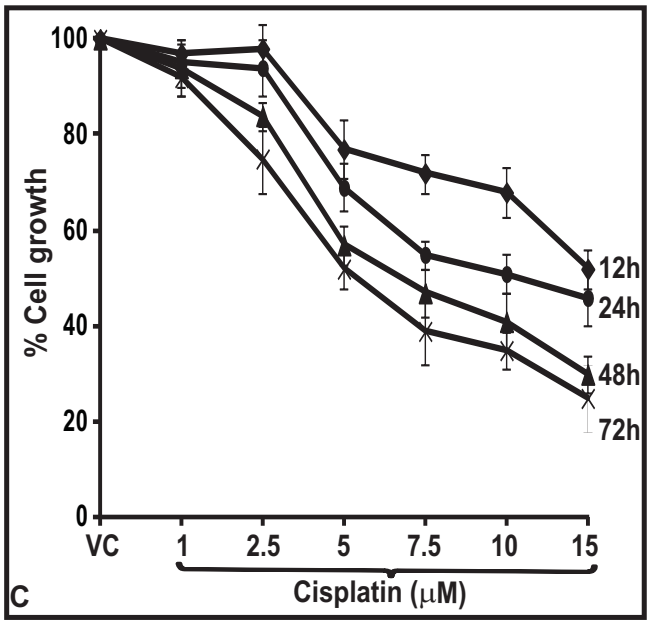

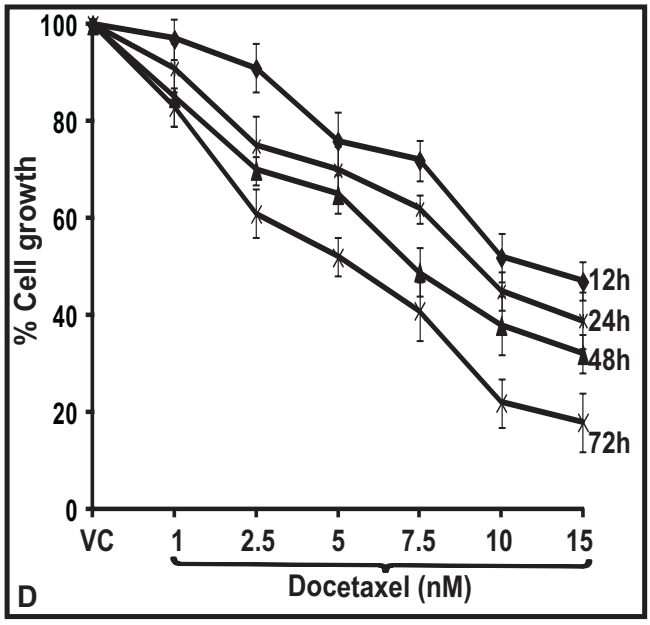

Figure 2(A-D)

Supplementary Figures 3 & 4

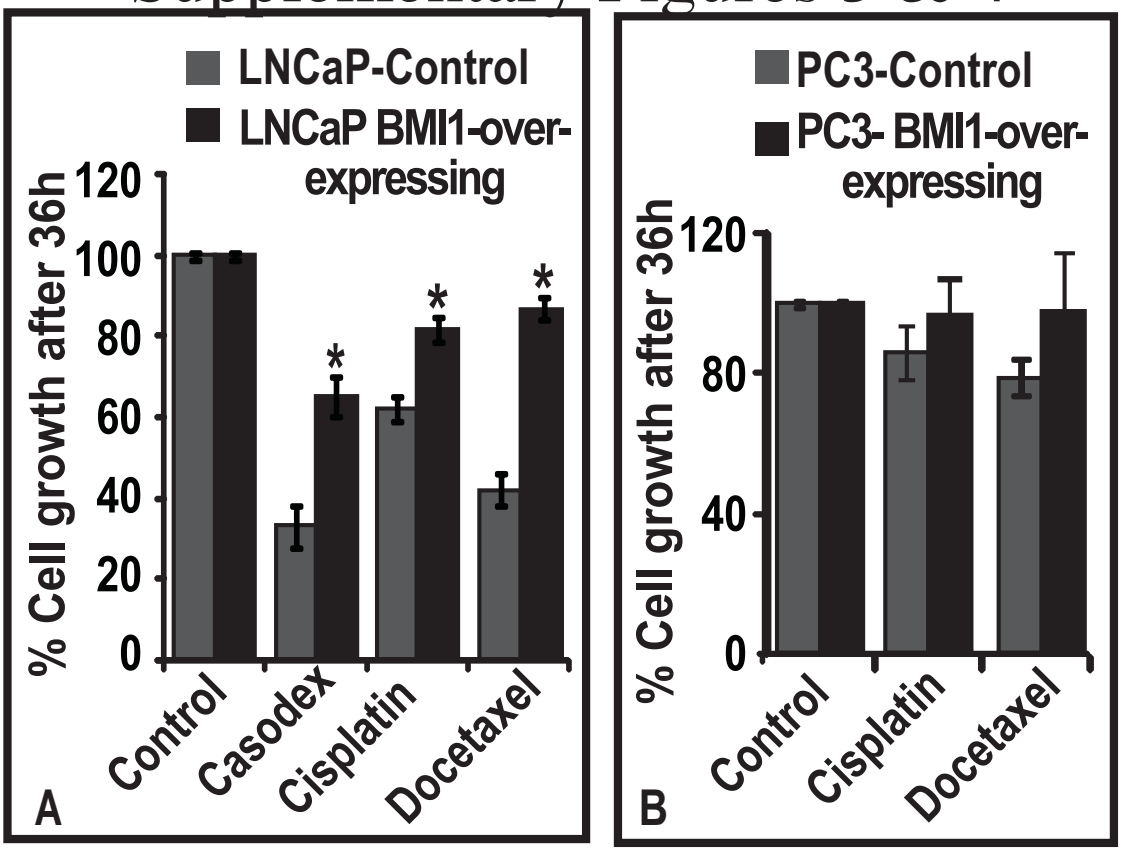

Figure 3A-B

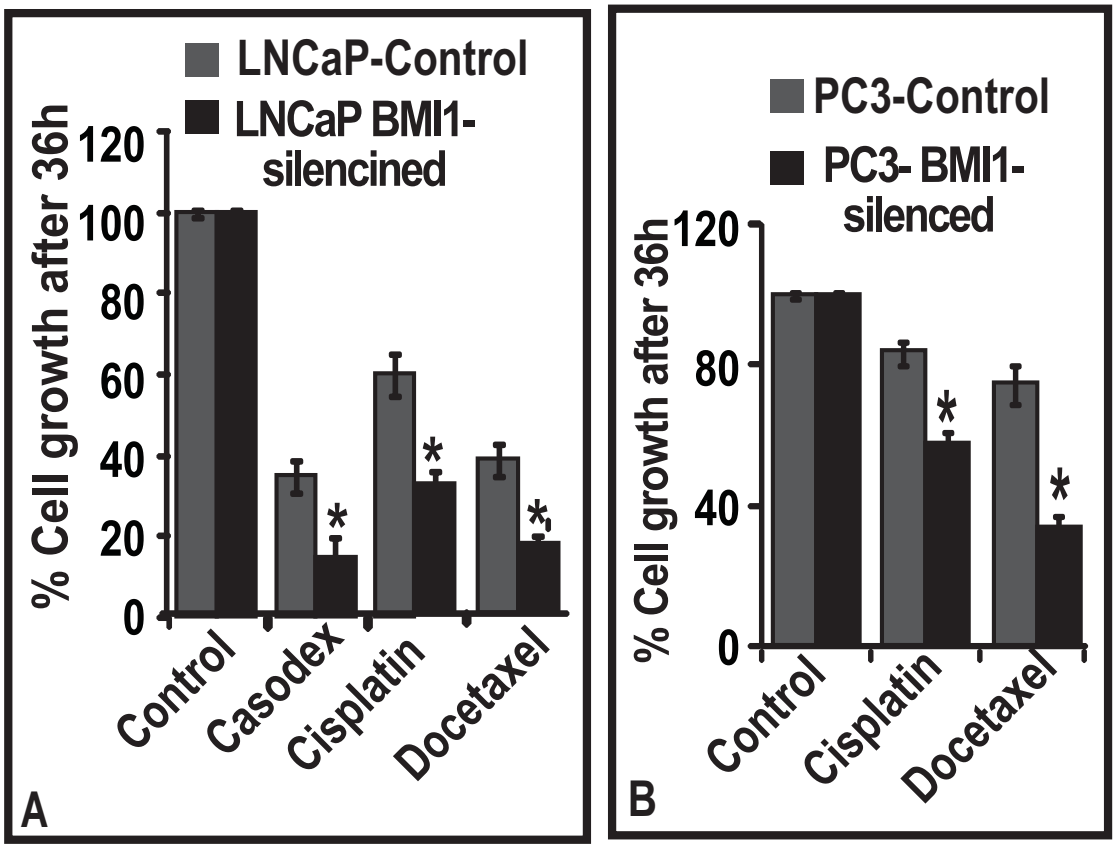

Figures 4A-B

STEM CELLS®

CANCER STEM CELLS

Concise Review: Role of BMI1, a Stem Cell Factor, in Cancer Recurrence and Chemoresistance: Preclinical and Clinical Evidences

HIFZUR RAHMAN SIDDIQUE, MOHAMMAD SALEEM

Department of Molecular Chemoprevention and Therapeutics, The Hormel Institute, University of Minnesota, Austin, Minnesota, USA

Key Words. BMI1 • Cancer stem cells • Cancer recurrence • Chemoresistance • Cancer

ABSTRACT

There is increasing evidence that a variety of cancers arise from transformation of normal stem cells to cancer stem cells (CSCs). CSCs are thought to sustain cancer progression, invasion, metastasis, and recurrence after therapy. Reports suggest that CSCs are highly resistant to conventional therapy. Emerging evidences show that the chemoresistance of CSCs are in part due to the activation of B cell-specific Moloney murine leukemia virus integration site 1 (BMI1), a stem cell factor, and a polycomb group family member. BMI1 is reported to regulate the proliferation activity of normal, stem, and progenitor cells. BMI1 plays a role in cell cycle, cell immortalization, and senescence. Numerous studies demonstrate that BMI1, which is upregulated in a variety of cancers, has a positive correlation with clinical grade/stage and poor prognosis. Although evidences are in support of the role of BMI1 as a factor in chemoresistance displayed by CSCs, its mechanism of action is not fully understood. In this review, we provide summary of evidences (with mechanism of action established) suggesting the significance of BMI1 in chemoresistance and recurrence of CSCs. STEM CELLS *2012; 30:372–378*

Disclosure of potential conflicts of interest is found at the end of this article.

INTRODUCTION

Traditional cancer therapies typically target the rapidly dividing tumor cells, however, some cells of the tumor are spared [1–3]. These spared tumor cells which are reported to be present within many tumor types exhibit the potential to regenerate and are called cancer stem cells (CSCs) [1–5]. This may explain the clinical scenario in which a tumor has an apparent volumetric reduction, however, is subsequently followed by local recurrence. While debate continues as to the precise identity and function of CSCs, there is general agreement that CSCs display increased chemoresistance and radioresistance [1-3, 6]. Therefore, understanding the biology of chemoresistance potential of CSCs may contribute to our understanding of tumor biology and would have far-reaching clinical implications. Although several molecules have been reported to confer chemoresistance to CSCs, much is not known whether stem cell factors play a role in chemoresistance of tumor cells including CSCs.

There is increasing evidence that polycomb group (PcG) proteins (discovered in *Drosophila* as epigenetic gene silencers) play a crucial role in cancer development and recurrence. PcG of proteins is composed of two multimeric protein complexes, that is, the polycomb repressive complex 1 (PRC1) and the polycomb repressive complex 2 (PRC2) [7]. The PRC1 complex includes B cell-specific Moloney murine leukemia virus integration site 1 (BMI1), Mel-18, Mph1/Rae28, M33, Scmh1, and Ring 2, while the PRC2 complex includes Eed, EzH, Suz12, and YY1 [7]. BMI1 is reported to play an important role in self-renewal of stem cells and is associated with a number of human malignancies [2, 5, 8-10]. Recent studies suggest that BMI1 is involved in the initiation of cancer, and targeting BMI1 by gene therapy abolishes chemoresistance in tumor cells [2, 3]. In this review, we summarized (a) the evidences supporting the role of BMI1 in cancer recurrence and chemoresistance, (b) the mechanisms underlying, and (c) the potential approaches that could be used to target BMI1 for cancer therapy.

GENE AND PROTEIN STRUCTURE OF BMI1

Human *BMI1* gene localizes on short arm of chromosome 10 (10p11.23), which comprises 10 exons and 9 introns. The gene encodes a cDNA of approximately 3.4 kb length and a 36.8 kDa protein consisting of 326 amino acids, whereas mouse *Bmi1* gene encodes a protein of 45–47 kDa [2, 5]. With respect to amino acid sequence, a high degree of homology is found between human BMI1 and murine Bmi1 that was the first member of the PcG gene family identified in mammals. BMI1 protein contains a conserved ring finger domain in its N terminal end and a central helix-turn-helix-turn-

Author contributions: H.R.S: data collection, literature collection, and manuscript writing; M.S.: manuscript evaluation and literature verification and writing.

Correspondence: Mohammad Saleem, Ph.D., The Hormel Institute, Department of Laboratory Medicine and Pathology, University of Minnesota-Twin Cities Campus, Minneapolis, Minnesota, USA. Telephone: 507-437-9662; Fax: 507-437-9606; e-mail: msbhat@umn.edu Received October 11, 2011; accepted for publication December 30, 2011; first published online in STEM CELLS *EXPRESS* January 17, 2012; available online without subscription through the open access option. 1066-5099/2012/$30.00/0 doi: 10.1002/stem.1035

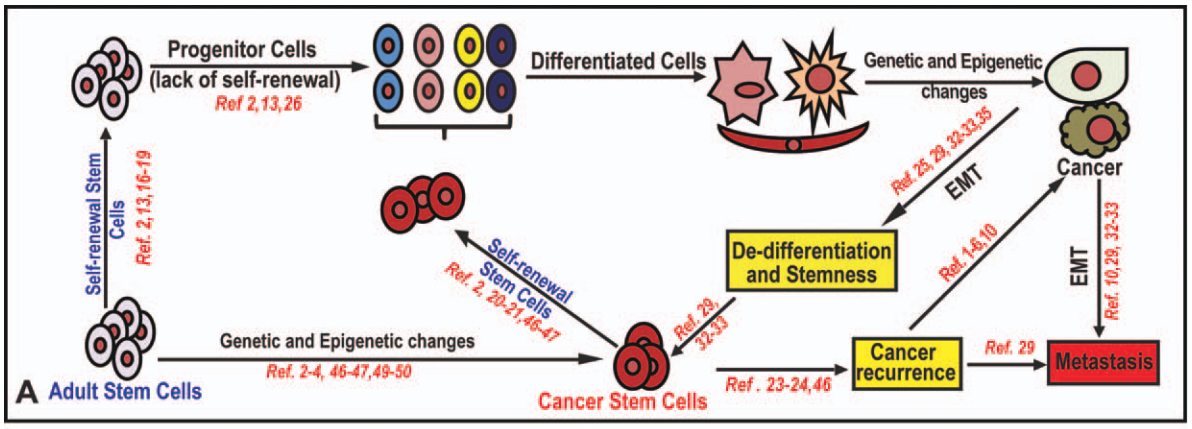

Table showing correlation of BMI1 expression with chemoresistance in different cancer types

Phenotype	Model	Model species	BMI1 status	Therapeutic agents	Function of the therapeutic agents	Chemoresistance	References
Prostate cancer	LNCaP & Du-145	Human	Overexpression	Docetaxel	Pro-apoptotic & anti-proliferative	Yes	3
Pancreatic cancer	Panc-1 (CD44+ cells)	Human	Overexpression	Gemcitabine	Pro-apoptotic & anti-proliferative	Yes	6
Squamous cell carcinoma	SCC-13	Human	Overexpression	EGCG	Pro-apoptotic & anti-proliferative	Yes	11
Normal cell	Keratinocytes	Human	Overexpression	Okadaic acid	Pro-apoptotic	Yes	12
Ovarian	Cancer Stem Cells	Human	Overexpression	Cisplatin and Paclitaxel	Pro-apoptotic & anti-proliferative	Yes	23
Ovarian cancer	A-2780, OCCAR-5 OV-202, OV-167, and CP-70	Human	Overexpression	Cisplatin	Pro-apoptotic & anti-proliferative	Yes	37
Glioma cells	U87MG, U251MG SNB19	Human	Overexpression	Doxorubicin & BCNU	Pro-apoptotic & anti-proliferative	Yes	38
Ovarian cancer	CP-20 mouse model	Mouse	Silenced	Cisplatin	Pro-apoptotic & anti-proliferative	No	37

B

Figure 1. Role of BMI1 in malignant transformation of stem cells into cancer stem cells and chemoresistance. **(A):** Pictorial diagram representing role of BMI1 during cellular events associated with the malignant transformation of stem or differentiated cells into cancer stem cells. The numerical number given on each arrow within the figure represents the reference number cited in the manuscript. **(B):** Table showing correlation of BMI1 expression with chemoresistance in different cancer types assessed in in vitro and in vivo models. Abbreviations: BCNU, Bis-chloroethylnitrosourea; BMI1, B-cell-specific Moloney murine leukemia virus integration site 1; EGCG, epigallocatechin-3-gallate; EMT, epithelial–mesenchymal transition.

helix-turn motif (H-T-H-T), which is essential for inducing telomerase activity [2, 5]. BMI1 contains two nuclear localization signals, KRRR and KRMK.

BMI1 has a ubiquitous pattern of expression in almost all tissues and its expression levels are observed to be high in the brain, esophagus, salivary gland, thymus, kidney, lungs, gonads, placenta, blood, and bone marrow [5]. Balasubramanian et al. [11] has reported the expression of BMI1 in basal and suprabasal keratinocytes. BMI1 is reported to be present in epidermal layers but not in dermis [12].

BMI1 in Normal Stem Cells

Stem cells are of two types (a) embryonic stem cells (ESCs) and (b) adult stem cells (ASCs). ESCs are pluripotent stem cells capable of developing into different cells, however, ASCs maintain and repair their resident tissues in adult organisms. Thus, self-renewal, differentiation, and prevention of senescence of ASCs are critical for tissue homeostasis. BMI1 plays crucial role for self-renewal and differentiation of leukemic stem and progenitor cells [13 and references therein]. BMI1 has also been reported to prevent senescence and immortalize cells through the activation of telomerase [8, 14]. It is reported that Bmi1 plays a crucial role during proliferation of normal stem and progenitor cells derived from fetal liver [13]. Hosen et al. [15] showed that the expression of BMI1 is high in primitive hematopoietic stem cells (HSCs) and is decreased when HSCs are differentiated into a particular lineage. The self-renewal and maintenance of HSCs and neural stem cells (NSCs) were reported to depend on the level of BMI1 protein [8, 16]. These studies suggest a strong correlation of BMI1 with the differentiation and growth of stem cells [15, 16]. BMI1 is reported to play a crucial role during the self-renewal and maintenance of prostate, intestinal, lung epithelial and bronchioalveolar stem cells [17–19].

BMI1 and CSCs

Over the past two decades, evidence has emerged to suggest that cancer could be considered as a stem cell disease and molecular mechanisms governing stem cell self-renewal are subverted during tumorigenesis to maintain cancerous growth (Fig. 1A, 1B) [2]. CSCs were first identified from the blood of patients with acute myeloid leukemia (AML) by Lapidot et al. in 1994 [4]. The CSC theory assumes that both primary and metastatic tumors develop from a small population of cancer cells possessing the characteristics of self-renewal and multipotency and are responsible for initiation and maintenance of tumors (Fig. 1A) [20, 21]. Additionally, CSCs can give rise to wide variety of differentiated cancer cells that comprise the

bulk of the tumor and provide the basis of tumor heterogeneity [20–22]. However, the stability of the CSC phenotype has not yet been completely understood [22]. Published reports suggest that CSCs are responsible for cancer recurrence after therapy and that this property of CSCs is attributed to the activation of different molecules including BMI1 [23–25].

BMI1 expression is frequently upregulated in various types of human cancers [1-2, 23-27]. There are reports that BMI1 acting as an epigenetic modifier protein is involved in the maintenance of CSCs [23, 25]. It is noteworthy that BMI1 is highly enriched in CSCs, however, all BMI1-expressing cells are not CSCs. BMI1 is coexpressed with other stem cell markers (CD133 and CD44) in CSCs [1, 6, 7, 23-26].

Aberrant BMI1 expression is reported in many CSC population. Bmi1 has been reported to be highly expressed in $CD133^+$ murine liver CSCs and play a role in maintenance of hepatic stem/progenitor cells [26]. Zhang et al. [23] observed that ovarian CSCs exhibit higher BMI1 levels than differentiated tumor cells. BMI1 has been shown to be involved in the regulation of CSCs from type-I neuroblastoma [9]. BMI1 was reported to regulate the self-renewal of CSCs by controlling their specific lineage commitment in an expression-dependent manner [9]. AML is a type of cancer in which the bone marrow makes abnormal myeloblasts, red blood cells, and platelets [13]. The proliferation of leukemic stem cells (LSCs) in a mouse model of AML was reported to be promoted by Bmi1 [13]. Bmi1-expressing LSCs were able to induce leukemia when transplanted into irradiated mice, whereas *Bmi1*-null LSCs exhibited limited proliferative potential and were unable to induce disease [13]. This study suggested the critical role of Bmi1 in proliferation of CSCs in leukemia [13]. Medulloblastoma is a type of brain tumor that originates from progenitor cells residing in the external cerebellum. Role of BMI1 in medulloblastoma can be ascertained from the fact that knockdown of *BMI1* in progenitor cells caused suppression in the proliferation and development of disease [27]. These studies suggest that the presence of BMI1 plays an important role in the proliferation of stem cells involved in tumorigenesis.

Different cell types that express BMI1 (such as endothelial cells, mesenchymal stem cells [MSCs], along with CSCs) reside within the tumor microenvironment [20, 28, 29]. The communication between CSCs and other cell types within tumor microenvironment plays an important role in invasion and therapeutic resistance [20, 28, 29]. Each established cell population within tumor exhibit a unique molecular marker that identifies and distinguishes it from other cell types [20-21, 28]. For example, MSCs express aldehyde dehydrogenase 1 (ALDH1) among breast CSCs population [20]. However, there is possibility that unique parental marker/trait still persists in cells that are in a stage of phenotypic transition such as mesenchymal transition [20, 28]. This also holds true with CSCs. A comprehensive discussion on this topic is beyond the scope of the theme of current manuscript.

BMI1, Self-Renewal and Cell Cycle

BMI1 controls self-renewal and cell cycle by regulating the tumor suppressor proteins p16INK4a and p14ARF in cells [8, 14]. BMI1 has been shown to activate the self-renewal ability of NSCs [16]. Recently, Dong et al. [30] demonstrated that loss of BMI1 in endometrial cancer cells reduces expression of stemness genes SOX-2 and KLF4 suggesting that BMI1 is required for regulation of stemness of this cell type.

The p16INK4a protein inhibits binding of Cyclin D to CDK4/6, resulting in the (a) suppression of retinoblastoma (RB) activity and (b) induction of cell cycle arrest [8, 31]. p19Arf (a homolog of human p14ARF) induces p53 and causes cell cycle arrest [8, 16, 31] (Fig. 2A, 2B). BMI1 promotes cell proliferation by suppressing p16INK4A/RB and/or p14ARF/MDM2/p53 tumor suppressor pathways [31]. The absence of BMI1 is reported to relieve the repression of the *INK4a* and resulting in the expression of p16INK4a and p14ARF. Data accumulated so far suggest that BMI1 abolishes cell cycle check points p16/p14 in various cell types (which exhibit different rates of growth/cell cycle kinetics) [7]. We speculate that this holds true for CSCs too. However, the possibility is that BMI1 could not be a sole factor deciding the fate of cells. Although BMI1 is present in CSCs, there is possibility that different subpopulation among CSCs (such as quiescent CSCs) exhibit different rate of growth. This could be possible due to the presence of factors other than BMI1 [18].

BMI1, Epithelial–Mesenchymal Transition and CSCs

The epithelial–mesenchymal transition (EMT) is a key developmental program that is often activated during cancer development [32, 33]. The occurrence of EMT in cancer cells may lead to the number of changes including loss of polarity and epithelial cell markers, loss of contact inhibition, reorganization of the actin cytoskeleton, remodeling of extracellular matrix components, gain of mesenchymal phenotypes along with genetic/epigenetic modifications of different genes, and persistent activation of different growth factors [32, 33]. Published reports suggest a direct link between the EMT and the gain of MSC-like properties [32, 33]. Raimondi et al. [33] reported that the induction of EMT program does not only allow cancer cells to disseminate from the primary tumor but also promotes their self-renewal capability. The sustained stimulation of growth factors may result in an upregulation of diverse gene products in CSCs and their differentiated progenies during the EMT process [32, 33]. Experimental evidence revealed that EMT is involved in anticancer drug resistance [32]. Thus, identification of molecular events that regulate EMT could lead to the development of a new therapeutic approach to suppress growth of CSCs. Song et al. [25] demonstrated that ectopic expression of BMI1 in normal nasopharyngeal epithelial cells is sufficient to cause EMT. Furthermore, this study showed that BMI1 induces EMT by targeting the tumor suppressor PTEN [25]. This in vitro observation was consistent with a cohort of human biopsy samples where an inverse correlation between BMI1 and PTEN was observed [25]. Recently, Yang et al. [29] showed that BMI1 is essential for EMT during tumor development in head and neck cancer patients. This study showed that increased levels of BMI1 were correlated with the worst prognosis in patients with head and neck cancer [29]. The molecules which are frequently altered in cancer cells during the EMT process are E-cadherin, N-cadherin, Vimentin, Tenascin C, NF-κB, SLUG, TWIST, SNAIL, β-Catenin, and CXCR4 [32, 33]. Collectively, these molecules are thought to contribute to the metastatic phenotypes of CSCs and enhance resistance to radiotherapy and chemotherapy [32, 33]. It has been reported that normal human mammary epithelial cells adopt a mesenchymal phenotype and exhibit stem cell-like properties upon expression of SNAIL and TWIST [32]. TWIST is reported to inhibit the senescence inducer proteins (p16 and p21) and co-operates with activated rat sarcoma (RAS) to trigger EMT [32]. Induction of SLUG is known to suppress E-cadherin, which results in the promotion of EMT [34]. Interestingly, $CD133^+$ breast

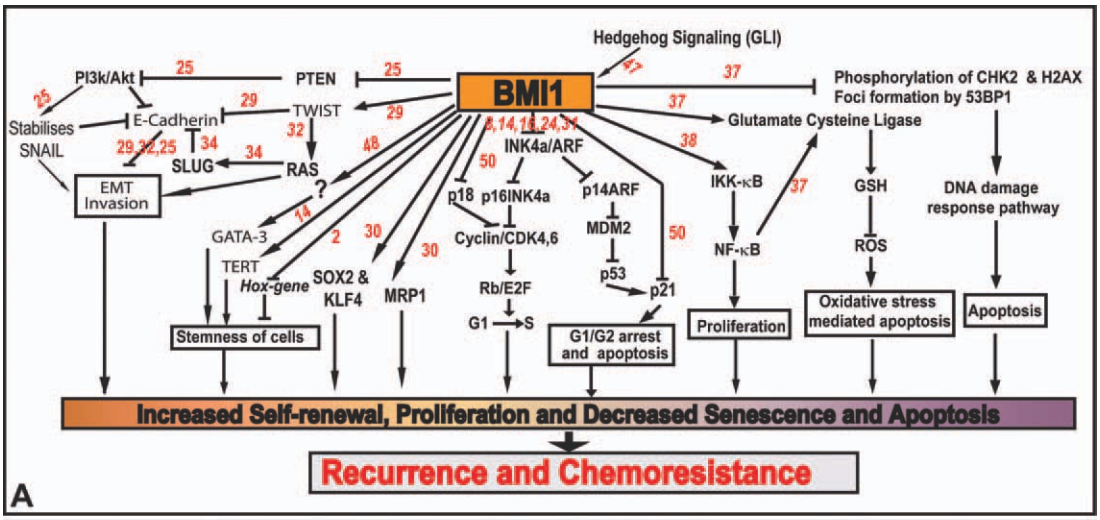

Table showing the published literature that formed the basis of model as represented in Fig. 2A

References	Reference number	References	Reference number
Cao et al., [2011]	2	Jacobs et al., [1999]	31
Park et al., [2004]	8	Thiery et al., [2009]	32
Dimiri et al., [2002]	14	Schmidt et al., [2005]	34
Molofsky et al., [2005]	16	Wang et al [2011]	37
Song et al., [2006]	24	Li et al., [2010]	38
Song et al., [2009]	25	Liu et al., [2006]	47
Yang et al., [2010]	29	Hosokawa et al., [2006]	48
Dong et al., [2011]	30	Facchino et al., [2011]	50

B

Figure 2. Role of BMI1 in cancer recurrence and chemoresistance. **(A):** Flowchart represents role of BMI1 and its interacting proteins during self-renewal, proliferation, and chemoresistance of cancer cells. **(B):** Table showing the published literature that formed the basis of model as represented in (A). The numerical number given on each arrow within the figure represents the reference number cited in the manuscript. ⊣ Represents inhibition and → represents activation. Abbreviations: BMI1, B-cell-specific Moloney murine leukemia virus integration site 1; EMT, epithelial–mesenchymal transition; GSH, reduced glutathione; IKK, IKB kinase; NF, nuclear factor; ROS, reactive oxygen species.

CSCs that express SLUG are also found to express high BMI1 [35]. BMI1 in co-operation with TWIST1 was reported to promote cancer dedifferentiation and metastasis [29]. Keeping in view that (a) EMT and stemness are interlinked processes, (b) EMT and stemness processes confer chemoresistance to tumor cells, and (c) BMI1 plays role in both EMT and stemness processes, the importance of BMI1 in chemoresistance as a major factor is further strengthened.

BMI1 and Chemoresistance: Preclinical Evidences

The inability of tumor cells to undergo apoptosis in response to chemotherapy poses a selective advantage for tumor progression, metastasis, and resistance to therapy. BMI1 has been reported to be associated with the protection of tumor cells from apoptosis (Fig. 1B). Cui et al. [9] showed that the ectopic expression of BMI1 rescues keratinocytes from stress-induced apoptosis. Bmi1 knockdown was observed to increase the apoptosis in lymphocytes in spleen and thymus in an animal model [36]. Zhang et al. [23] observed that ovarian CSCs exhibiting high BMI1 levels have increased resistance to Cisplatin and Paclitaxel. Crea et al. showed that BMI1 silencing significantly enhanced the antitumor efficiency of Docetaxel against prostate cancer cells. BMI1 (by modulating antioxidant machinery) was observed to allow prostate tumor cells to survive after chemotherapy [3]. Examination of clinical datasets revealed a positive correlation of BMI1 and antioxidant gene expression in patients exhibiting chemoresistance [3]. Recently, Wang et al. [37] reported that BMI1 is involved in chemoresistance of ovarian cancer cells, and targeting BMI1 by gene therapy sensitizes tumor cells to Cisplatin chemotherapy. Modulation of reduced glutathione (GSH) and CHK2 and H2AX molecules by BMI1 was reported as the underlying mechanism for chemoresistant behavior of ovarian tumor cells [37]. BMI1 silencing was found to reduce intracellular GSH levels and sensitize cancer cells to Cisplatin [37]. It is noteworthy that Cisplatin-induced apoptosis in such cell was found to be mediated by reactive oxygen species (ROS) generation [37]. Recent studies showed that overexpression of BMI1 rescues tumor cells from the apoptosis induced by Okadaic acid and Epigallocatechin-3-gallate, well-known apoptotic agents [11, 12]. Interestingly, artificial introduction of BMI1 in chemosensitive tumor cells was observed to confer chemoresistance in such cells [11]. Yin et al. [6] showed that $CD44^+/CD24^+$ pancreatic cancer cells expressing high levels of BMI1 exhibit chemoresistance to Gemcitabine treatment. Li et al. [38] reported that BMI1 by activating NF-κB significantly inhibits Doxorubicin-, BCNU-, and UV irradiation-induced apoptosis in glioma cells. Recently, we observed that the reduction of BMI1 protein levels by gene therapy abolishes chemoresistance in prostate carcinoma cells (Siddique et al., unpublished data). Taken together, these studies support the role BMI1 plays in conferring chemoresistance to tumor cells.

BMI1 and Chemoresistance: Clinical Evidences

The clinical significance of BMI1 in chemoresistance and its correlation with therapy failure in several cancer types has been established [5, 9, 10, 39–40]. BMI1 was found to be one of the key regulatory factors determining a cellular phenotype captured by the expression of a death-form-cancer signature in a broad spectrum of therapy-resistant cancers, including five epithelial (prostate, breast, lung, ovarian, and bladder cancers) and five nonepithelial (lymphoma, mesothelioma, medulloblastoma, glioma, and AML) malignancies [39]. Glinsky et al. [39] described a conserved BMI1-driven pathway of 11-gene signature which defines stemness of highly invasive tumors of multiple tissue origin and correlation with therapy failure. High level of BMI1 in tumors was reported to be positively correlated with poor prognosis in nasopharyngeal carcinoma patients [24]. BMI1 was identified as predictive factor for overall survival in patients with head and neck squamous cell carcinomas (HNSCC) [41]. BMI1 levels were observed to be increased in 79% of HNSCC patients, and a positive correlation was observed between BMI1 levels and lack of response to radiotherapy or chemotherapy [41]. Van Kemenade et al. [42] reported that poor outcome and aggressive tumor behavior were correlated with high BMI1 levels in patients with non-Hodgkin B-cell lymphomas and nasal pharyngeal carcinoma. Li et al. [38] showed that BMI1 was upregulated in 93.9% glioma specimens from 297 patients. This study showed that BMI1 expression was inversely correlated with survival time of glioma patients and positively correlated with the poor prognosis of the disease [38]. Mihic-Probst et al. [10] studying 329 melanoma patients reported that high expression of BMI1 in 64% of primary and 71% metastatic melanoma was associated with clinical progress of the disease. Recent reports show a correlation between BMI1 levels and recurrence cum survival of disease in tongue cancer, oropharyngeal squamous cell cancer, and non-small cell lung cancer (NSCLC) patients [5, 43, 44]. Disease-free survival for stage I and II of NSCLC patients who had received adjuvant therapy was reported to be better in BMI1-negative patients than BMI1-positive counterparts [44]. We observed a stage-dependent increase in human prostatic tumors and decreased chemoresistance in cells exhibiting reduced BMI1 levels (Siddique et al., unpublished data). Collectively these studies also suggest that BMI1 might be applicable as predictive markers of therapy during the follow-up of patients undergoing chemotherapy.

Molecular Mechanisms of BMI1-Induced Chemoresistance

Chemoresistance has been reported to be caused by the aberration of several molecular pathways in tumor cells. CSCs have been shown to display chemoresistance through (a) modulation of DNA repair machinery, (b) ATP-binding cassette (ABC) multidrug resistance, (c) quiescence, and (d) upregulation of antiapoptotic genes [45]. Emerging evidences support the notion that BMI1 is an important molecule in the process of chemoresistance. However, the precise mechanism of BMI1 on the regulation of chemoresistance in tumor cells is not completely understood. As presented in Figure 2, BMI1 is reported to modulate several molecular pathways within the cells. BMI1 has been shown to induce its effect at epigenetic as well as genetic level [7, 13, 46]. It is believed that chromatin modifications induced by PcG proteins (including BMI1) create an obstacle to transcription factors and RNA polymerase binding [46]. BMI1 has been shown to modulate chromatin by (a) forming a complex with methylated Lys_{27} of H3 and (b) catalyzing the ubiquitinylation of histone H2A [7, 46]. The co-operation between the Eed complex (that modifies chromatin by recruiting histone deacetylases) and BMI1 complex leads to the silencing of target gene expression [7, 46]. BMI1 induces immortalization of cells by downregulating the p16INK4a and p14ARF [8, 16]. Huber et al. [5] reported a correlation between low expression of p16 and high expression of BMI1 in human cancer patients. It is reported that the cooperation of BMI1 with c-MYC results in induction of telomerase activity and downregulation of *INK4a*/ARF [36].

Sonic Hedgehog (SHH) pathway is reported to play a role in the self-renewal of breast stem/progenitor cells [47]. SHH-activated mammosphere formation is reported to be mediated by BMI1 [47]. BMI1 is reported to regulate intracellular GSH levels by modulating glutamate cystine ligase, which is also positively regulated by Nrf-1 and nuclear factor κB (NF-κB) [37]. It is noteworthy that BMI1 expression was reported to be positively associated with activity of Nrf-1 and NF-κB in glioma cells [38]. BMI1 is reported to occupy the *PTEN* locus and downregulates *PTEN* expression [25]. Occupancy of BMI1 on *PTEN* locus results in the activation of Phosphatidylinositol 3-kinases/protein kinase B (PI3K/AKT) pathway, stabilization of SNAIL, and downregulation of E-cadherin. BMI1 directly occupies the promoters of CDH1 (which encodes E-cadherin) and *INK4a* [25]. Lee et al. [12] showed that BMI1 influences cell proliferation by increasing the expression levels of cyclin-dependent Kinase 2, 4 (CDK2, CDK4), and Cylin D1. BMI1 is reported to regulate stability of GATA binding protein 3 (GATA3), a transcription factor that is involved in Th2 cell development and differentiation [48]. Recently, Dong et al. [30] demonstrated that loss of BMI1 in endometrial cancer cells reduces expression of drug resistance gene MRP1, suggesting that BMI1 is required for the drug resistance. Quiescent nature of CSCs represents an inherent mechanism that at least partially explains chemotherapy resistance and recurrence in post-therapy in cancer patients [18, 20, 30]. Recent study by Tian et al. [18] suggest that Bmi1 plays an important role in the maintenance and growth of quiescent cells. Bmi1-expressing quiescent cells were shown to contribute to the generation of epithelial cells of intestine [18]. It is noteworthy that this effect of BMI1 was observed under conditions when proliferative cells were not sufficient and BMI1 expressing-quiescent cells were found to grow into tissue [18].

BMI1: A Potential Target for Cancer Therapy

CSCs may be eliminated by selectively targeted therapies against BMI1 [49, 50] (Siddique et al., unpublished data). However, it would be much complex to selectively target CSCs without any harmful effects to normal stem cells because normal stem cells and CSCs share the same pathways to maintain their self-renewal capability. It appears that CSCs are more likely to be more dependent on certain putative pathways. In this context, Liu et al. showed that human BMI1 is critical for the short-term survival of cancer cells, and inhibition of BMI1 has minimal effect on the survival of normal cells. These findings provide a foundation for developing a cancer-specific therapy targeting BMI1 [49]. Recently, Facchino et al. showed that glioblastoma multiforme (GBM) stem cells acquire an oncogenic trait by BMI1 overexpression thus distinguishing CSCs from normal stem cells. This situation was observed to render GBM stem cells

more sensitive to BMI1 inhibition than normal stem cells [50]. Based on compelling evidences (which suggest the critical role of BMI1 in growth and proliferation), using BMI1 as a target for anticancer therapy seems an ideal option. Wang et al. successfully tested 1,2-dioleoyl-sn-glycero-3-phosphatidylcholine nanoparticles carrying small inhibitory RNA (siRNA) to target BMI1 and reported an inhibition in the growth of chemoresistant ovarian tumors implanted in a xenograft mouse model [37]. This study showed that gene therapy-induced BMI1 silencing along with Cisplatin completely abrogated ovarian tumor growth [37].

We recently showed that targeted inhibition of BMI1 by adopting gene therapy approach resulted in the reduction in the invasive potential and tumorigenic potential of prostate cancer cells (Siddique et al., unpublished data). We have embarked upon a broad program aimed to evaluate the potential and usefulness of BMI1 as a molecular target for human cancers. We have developed specific BMI1 small molecule inhibitors (Siddique et al., unpublished data), which were observed to inhibit the proliferative potential of prostate, pancreatic and skin cancer cells (Siddique et al., unpublished data).

Conclusions

BMI1 has been reported to be associated with the progression, recurrence, and chemoresistance to the various types of cancer cells. Hence, it is of great clinical value to further understand the molecular mechanism underlying the regulation of BMI1 in CSCs and chemoresistance. This will not only help in understanding the role of BMI1 in the growth of CSCs and chemoresistance but will also provide insights for the establishment of new strategies and effective clinical therapies for the treatment of chemoresistant cancers. Taken together, these studies show that BMI1 has the potential to be developed as a target for therapeutic agents and small molecules efficiently targeting BMI1 offer an option as future anticancer drugs.

Acknowledgments

The data from our laboratory cited in this manuscript was funded in part by a New Investigator grant from CDMRP-Department of Defense (W81XWH-08-1-0605) to the corresponding author.

Disclosure of Potential Conflicts of Interest

The authors indicate no potential conflict of interest.

References

1 Bertolini G, Roz L, Perego P et al. Highly tumorigenic lung cancer CD133$^+$ cells display stem-like features and are spared by cisplatin treatment. Proc Natl Acad Sci USA 2009;106:16281–16286.
2 Cao L, Bombard J, Cintron K et al. BMI1 as a novel target for drug discovery in cancer. J Cell Biochem 2011;112:2729–2741.
3 Crea F, Serrat MAD, Hurt EM et al. BMI1 silencing enhances docetaxel activity and impairs antioxidant response in prostate cancer. Int J Cancer 2011;128:1946–1954.
4 Lapidot T, Sirard C, Vormoor J et al. A cell initiating human acute myeloid leukaemia after transplantation into SCID mice. Nature 1994; 367:645–648.
5 Huber GF, Albinger-Hegyi A, Soltermann A et al. Expression patterns of BMI1 and p16 significantly correlate with overall, disease-specific, and recurrence-free survival in oropharyngeal squamous cell carcinoma. Cancer 2011 [Epub ahead of print].
6 Yin T, Wei H, Gou S et al. Cancer stem-like cells enriched in panc-1 spheres possess increased migration ability and resistance to gemcitabine. Int J Mol Sci 2011;12:1595–1604.
7 Raaphorst FM. Deregulated expression of Polycomb-group oncogenes in human malignant lymphomas and epithelial tumors. Hum Mol Genet 2005;1:R93–R100.
8 Park IK, Morrison SJ, Clarke MF. Bmi1, stem cells, and senescence regulation. J Clin Invest 2004;113:175–179.
9 Cui H, Hu B, Li T et al. BMI1 is essential for the tumorigenicity of neuroblastoma cells. Am J Pathol 2007;170:1370–1378.
10 Mihic-Probst D, Kuster A, Kilgus S et al. Consistent expression of the stem cell renewal factor BMI1 in primary and metastatic melanoma. Int J Cancer 2007;121:1764–1770.
11 Balasubramanian S, Lee K, Adhikary G et al. The BMI1 polycomb group gene in skin cancer: Regulation of function by (-)-epigallocatechin-3-gallate. Nutr Rev 2008;66(suppl 1):S65–S68.
12 Lee K, Adhikary G, Balasubramanian S et al. Expression of BMI1 in epidermis enhances cell survival by altering cell cycle regulatory protein expression and inhibiting apoptosis. J Invest Dermatol 2008;128: 9–17.
13 Lessard J, Sauvageau G. Bmi-1 determines the proliferative capacity of normal and leukaemic stem cells. Nature 2003;423:255–260.
14 Dimri GP, Martinez JL, Jacobs JJ et al. The BMI1 oncogene induces telomerase activity and immortalizes human mammary epithelial cells. Cancer Res 2002;62:4736–4745.
15 Hosen N, Yamane T, Muijtjens M et al. BMI1-green fluorescent protein-knock-in mice reveal the dynamic regulation of BMI1 expression in normal and leukemic hematopoietic cells. Stem Cells 2007;25: 1635–1644.
16 Molofsky AV, He S, Bydon M et al. BMI1 promotes neural stem cell self-renewal and neural development but not mouse growth and survival by repressing the p16Ink4a and p19Arf senescence pathways. Genes Dev 2005;19:1432–1437.
17 Lukacs RU, Memarzadeh S, Wu H et al. Bmi-1 is a crucial regulator of prostate stem cell self-renewal and malignant transformation. Cell Stem Cell 2010;7:682–693.
18 Tian H, Biehs B, Warming S et al. A reserve stem cell population in small intestine renders Lgr5-positive cells dispensable. Nature 2011; 478:255–260.
19 Zacharek SJ, Fillmore CM, Lau AN et al. Lung stem cell self-renewal relies on BMI1-dependent control of expression at imprinted loci. Cell Stem Cell 2011;9:272–281.
20 Korkaya H, Liu S, Wicha MS. Breast cancer stem cells, cytokines networks, and the tumor microenvironment. J Clin Invest 2011;121: 3804–3809.
21 Dudley AC, Khan ZA, Shih SC et al. Calcification of multipotent prostate tumor endothelium. Cancer Cell 2008;14:201–211.
22 Clevers H. The cancer stem cell: Premises, promises and challenges. Nature Med 2011;17:313–319.
23 Zhang S, Balch C, Chan MW et al. Identification and characterization of ovarian cancer-initiating cells from primary human tumors. Cancer Res 2008;68:4311–4320.
24 Song LB, Zeng MS, Liao WT et al. BMI1 is a novel molecular marker of nasopharyngeal carcinoma progression and immortalizes primary human nasopharyngeal epithelial cells. Cancer Res 2006;66: 6225–6232.
25 Song LB, Li J, Liao WT et al. The polycomb group protein BMI1 represses the tumor suppressor PTEN and induces epithelial–mesenchymal transition in human nasopharyngeal epithelial cells. J Clin Invest 2009;119:3626–3636.
26 Oishi N, Wang XW. Novel therapeutic strategies for targeting liver cancer stem cells. Int J Biol Sci 2011;7:517–535.
27 Wiederschain D, Chen L, Johnson B et al. Contribution of polycomb homologues BMI1 and Mel-18 to medulloblastoma pathogenesis. Mol Cell Biol 2007;27:4968–4979.
28 Sangiorgi E, Capecchi MR. BMI1 lineage tracing identifies a self-renewing pancreatic acinar cell subpopulation capable of maintaining pancreatic organ homeostasis. Proc Natl Acad Sci USA 2009;106: 7101–7106.
29 Yang MH, Hsu DS, Wang HW et al. Bmi1 is essential in Twist1-induced epithelial–mesenchymal transition. Nat Cell Biol 2010;12: 982–992.

30 Dong P, Kaneuchi M, Watari H et al. MicroRNA-194 inhibits epithelial to mesenchymal transition of endometrial cancer cells by targeting oncogene BMI-1. Mol Cancer 2011;10:99.
31 Jacobs JJ, Kieboom K, Marino S et al. The oncogene and Polycombgroup gene bmi-1regulates cell proliferation and senescence through the ink4a locus. Nature 1999;397:164–168.
32 Thiery JP, Acloque H, Huang RYJ et al. Epithelial–mesenchymal transitions in development and disease. Cell 2009;139:871–890.
33 Raimondi C, Gianni W, Cortesi E et al. Cancer stem cells and epithelial–mesenchymal transition: Revisiting minimal residual disease. Curr Cancer Drug Targets 2010;10:496–508.
34 Schmidt CR, Gi YJ, Patel TA et al. E-cadherin is regulated by the transcriptional repressor SLUG during Ras-mediated transformation of intestinal epithelial cells. Surgery 2005;138:306–312.
35 Storci G, Sansone P, Trere D et al. The basal-like breast carcinoma phenotype is regulated by SLUG gene expression. J Pathol 2008;214:25–37.
36 Jacobs JJ, Scheijen B, Voncken JW et al. BMI1 collaborates with c-Myc in tumorigenesis by inhibiting c-Myc-induced apoptosis via INK4a/ARF. Genes Dev 1999;13:2678–2690.
37 Wang E, Bhattacharyya S, Szabolcs A et al. Enhancing chemotherapy response with BMI1 silencing in ovarian cancer. PLoS One 2011;6:e17918.
38 Li J, Gong LY, Song LB et al. Oncoprotein BMI1 renders apoptotic resistance to glioma cells through activation of the IKK-nuclear factor-kappaB Pathway. Am J Pathol 2010;176:699–709.
39 Glinsky GV, Berezovska O, Glinskii AB. Microarray analysis identifies a death-from-cancer signature predicting therapy failure in patients with multiple types of cancer. J Clin Invest 2005;115:1503–1521.
40 Hayry V, Tynninen O, Haapasalo HK et al. Stem cell protein BMI1 is an independent marker for poor prognosis in oligodendroglial tumours. Neuropathol Appl Neurobiol 2008;34:555–563.
41 Vormittag L, Thurnher D, Geleff S et al. Co-expression of BMI1 and podoplanin predicts overall survival in patients with squamous cell carcinoma of the head and neck treated with radio(chemo)therapy. Int J Radiat Oncol Biol Phys 2009;73:913–918.
42 van Kemenade FJ, Raaphorst FM, Blokzijl T et al. Coexpression of BMI1 and EZH2 polycomb-group proteins is associated with cycling cells and degree of malignancy in B-cell non-Hodgkin lymphoma. Blood 2001;97:3896–3901.
43 Hayry V, Makinen LK, Atula T et al. BMI1 expression predicts prognosis in squamous cell carcinoma of the tongue. Br J Cancer 2010; 102:892–897.
44 Vrzalikova K, Skarda J, Ehrmann J et al. Prognostic value of BMI1 oncoprotein expression in NSCLC patients: A tissue microarray study. J Cancer Res Clin Oncol 2008;134:1037–1042.
45 Friedman GK, Gillespie GY. Cancer stem cells and pediatric solid tumors. Cancers 2011;3:298–318.
46 Crea F, Danesi R, Farrar WL. Cancer stem cell epigenetic and chemoresistance. Epigenome 2009;1:63–79.
47 Liu S, Dontu G, Mantle ID et al. Hedgehog signaling and BMI1 regulate self-renewal of normal and malignant human mammary stem cells. Cancer Res 2006;66:6063–6071.
48 Hosokawa H, Kimura MY, Shinnakasu R et al. Regulation of Th2 cell development by Polycomb group gene BMI1 through the stabilization of Gata-3. J Immunol 2006;177:7656–7664.
49 Liu L, Andrews LG, Tollefsbol TO. Loss of the human polycomb group protein BMI1 promotes cancer-specific cell death. Oncogene 2006;25:4370–4375.
50 Facchino S, Abdouh M, Bernier G. Brain cancer stem cells: Current status on glioblastoma multiforme. Cancers 2011;3:1777–1797.

OPEN ACCESS Freely available online

PLOS ONE

BMI1 Polycomb Group Protein Acts as a Master Switch for Growth and Death of Tumor Cells: Regulates TCF4-Transcriptional Factor-Induced BCL2 Signaling

Hifzur Rahman Siddique[1], Aijaz Parray[1], Rohinton S. Tarapore[2], Lei Wang[3], Hasan Mukhtar[2], R. Jeffery Karnes[4], Yibin Deng[3], Badrinath R. Konety[5], Mohammad Saleem[1,5,6]*

1 Department of Molecular Chemoprevention and Therapeutics, The Hormel Institute, University of Minnesota, Austin, Minnesota, United States of America, **2** Department of Dermatology, University of Wisconsin, Madison, Wisconsin, United States of America, **3** Department of Cell Death and Cancer Genetics, The Hormel Institute, University of Minnesota, Austin, Minnesota, United States of America, **4** Department of Urology, Mayo Medical School and Mayo Clinic, Rochester, Minnesota, United States of America, **5** Department of Urology, University of Minnesota, Minneapolis, Minnesota, United States of America, **6** Department of Laboratory Medicine Pathology, University of Minnesota, Minneapolis, Minnesota, United States of America

Abstract

For advanced prostate cancer (CaP), the progression of tumors to the state of chemoresistance and paucity of knowledge about the mechanism of chemoresistance are major stumbling blocks in the management of this disease. Here, we provide compelling evidence that BMI1 polycomb group protein and a stem cell factor plays a crucial role in determining the fate of tumors vis-à-vis chemotherapy. We show that progressive increase in the levels of BMI1 occurs during the progression of CaP disease in humans. We show that BMI1-rich tumor cells are non-responsive to chemotherapy whereas BMI1-silenced tumor cells are responsive to therapy. By employing microarray, ChIP, immunoblot and Luciferase reporter assays, we identified a unique mechanism through which BMI1 rescues tumor cells from chemotherapy. We found that BMI1 regulates (i) activity of TCF4 transcriptional factor and (ii) binding of TCF4 to the promoter region of anti-apoptotic *BCL2* gene. Notably, an increased TCF4 occupancy on *BCL2* gene was observed in prostatic tissues exhibiting high BMI1 levels. Using tumor cells other than CaP, we also showed that regulation of TCF4-mediated BCL2 by BMI1 is universal. It is noteworthy that forced expression of BMI1 was observed to drive normal cells to hyperproliferative mode. We show that targeting BMI1 improves the outcome of docetaxel therapy in animal models bearing chemoresistant prostatic tumors. We suggest that BMI1 could be exploited as a potential molecular target for therapeutics to treat chemoresistant tumors.

Citation: Siddique HR, Parray A, Tarapore RS, Wang L, Mukhtar H, et al. (2013) BMI1 Polycomb Group Protein Acts as a Master Switch for Growth and Death of Tumor Cells: Regulates TCF4-Transcriptional Factor-Induced BCL2 Signaling. PLoS ONE 8(5): e60664. doi:10.1371/journal.pone.0060664

Editor: Natasha Kyprianou, University of Kentucky College of Medicine, United States of America

Received December 28, 2012; **Accepted** March 1, 2013; **Published** May 6, 2013

Funding: This work was supported by the Department of Defense CDMRP grant W81XWH-08-1-0605 to MS. The funder had no role in study design, data collection and analysis, decision to publish, or preparation of the manuscript.

Competing Interests: The authors have declared that no competing interests exist.

* E-mail: msbhat@umn.edu

Introduction

According to American Cancer Society, an estimated 241,740 new cases of prostate cancer (CaP) were diagnosed and 28,170 CaP patients were projected to die in the year 2012 in USA alone [1]. CaP is the second most frequently diagnosed cancer in men in the western world [2–3]. CaP patients (30–50%) exhibit a local or distant recurrence of disease after surgery or therapy [4–6]. Although castration is a common treatment option for metastatic CaP, it does not significantly prolong the survival of patients and majority of these patients progress to castration-resistant prostate cancer (CRPC). A treatment option for CRPC is cytotoxic chemotherapy; however, chemotherapy improves overall survival in such patients by only a median of 2.9 months [6–7]. Despite chemotherapy, CRPC patients typically show rapid progression and develop chemoresistant disease [8–10]. Therefore emergence of chemoresistance is considered a major hurdle in the management of CaP. The dismal outcome of the management of chemoresistant CRPC disease could also be associated to the lack of knowledge about the molecular mechanism involved in the development of chemoresistant disease.

There is increasing evidence that polycomb group (PcG) proteins, first discovered in *Drosophila* as epigenetic gene silencers of homoeotic genes, play a crucial role in cancer development and recurrence [11]. BMI1, a member of PcG family of proteins, is a marker used in stem cell biology [11–12]. There is an enormous body of evidence suggesting that increased expression of BMI1 could facilitate chemoresistance [11–12]. Recent studies show that BMI1 is positively correlated with poor prognosis in cancer patients [13–16]. We recently reviewed the significance of BMI1 in the emergence of chemoresistance in various types of cancers [11]. Glinsky et al. identified BMI1 as one the signature molecules in a broad spectrum of therapy-resistant cancers including CaP [17]. Except a few regulatory functions of BMI1 in cell cycle (suppressing p16INK4a and p14ARF), not much is known about it mechanism of action. In this study, we determined the relevance of BMI1 in chemoresistance of CaP and delineate its mechanism of action both *in vitro* and *in vivo*. In addition, we establish the utility of

BMI1 as a molecular target for therapeutic agents to overcome chemoresistance.

Materials and Methods

Cell Lines and plasmids

Normal primary prostate epithelial cell (PrEC) was procured from Cambrex BioScience (Walkersville, MD, USA). Normal and transformed prostate epithelial cell line (RWPE1), CaP cell lines (LNCaP, 22Rv1, C42b, PC3 and Du145), prostatic stromal myofibroblasts (WPMY1), and colon cancer cell lines HT29 were obtained from ATCC (Manassas, VA, USA). LAPC4 cells were gifted by Dr. Robert Reiter (UCLA, Los Angeles, CA, USA) who generated these cells [18]. The pbabe-BMI1 plasmid was a kind gift from Dr. Chi V. Dang (The John Hopkins University, Baltimore, MD, USA). pGeneClip, pbabe plasmids and pGeneClip-BMI1-shRNA were procured from SA-Biosciences Corporation (Fredrick, MD, USA). pTK-TCF-Luc (TopFlash and FopFlash) was procured from Upstate Laboratories (Lake Placid, NY, USA). Cells were cultured in appropriate media and were kept in 5% CO_2 in an incubator at 37°C.

Tumor tissues

Frozen surgical prostatic tissues and tissues in paraffin blocks were procured from NCI-sponsored Cooperative Human Tissue Network (CHTN, Mid-West Division, University of Ohio, Columbus, USA). The quality of the frozen tissue was excellent as per the data sheet provided by the supplier (CHTN). The frozen tissues were kept at −80°C and paraffin blocked tissues stored at room temperature.

Chemicals and reagents

Docetaxel, casodex, cyclopamine and cisplatin were purchased from LKT Laboratories (St. Paul, MN, USA). Puoromycin, G418 and BrdU labeling reagent were purchased from Invitrogen (Carlsbad, CA, USA). The anti-BMI1 antibody, ChIP-grade anti-TCF1 and anti-TCF4 antibody was obtained from Millipore (Bedford, MA, USA). Anti-BCL2 and anti-BrdU antibodies were purchased from Cell Signaling (Danvers, MA, USA).

Transfections

Transfections were performed using Lipofectamine in CaP lines (LNCaP, PC3, Du145) and colon cancer cell line (HT29) (Invitrogen, Carlsbad, CA, USA) as per Vendor's protocols and as described earlier [19–20]. The effectiveness of transient transfections varied (65–85%) from cell line to cell line with the least (65%) in LNCaP and maximum (85%) in PC3 cells.

Cell growth assay

Cell growth was determined by MTT (3-[4, 5-dimethylthiazol-2-yl]-2, 5-diphenyl tetrazoliumbromide; Sigma, Saint Louise, MO) assay as described earlier [19–20]. Briefly, transfected cells were grown in complete medium. Each condition was repeated in 10 wells. After incubation for specified time at 37°C in a humidified incubator, MTT (5 mg/ml in phosphate buffered saline, PBS) was added to each well. After 2 h of incubation with MTT, the plates were centrifuged at 500 *g* for 5 min. After careful removal of the solution, 0.1 ml of DMSO was added to each well and plates were shaken. The absorbance was recorded on a microplate reader at the wavelength of 540 nm. The cell growth was assessed as percent cell growth where vehicle-treated cells were taken as 100% viable.

3[H]-thymidine incorporation assay

3[H]-thymidine incorporation assay was performed as described earlier [19]. Briefly, Cells grown in 24-well plates in the presence of 3[H]thymidine (0.5 μCi/ml). Cells were then washed twice with cold PBS and then were incubated with trichloroacetic acid solution on ice for 30 min. Next, acid-insoluble fraction was dissolved in 1 ml of NaOH (1 M). Incorporated 3[H]thymidine were quantified using a scintillation counter.

Colony formation assay

A total of 0.5% agar was prepared in appropriate culture media containing 20% fetal calf serum (bottom layer). Cells (1×10^5 cell/100 mm plate) in 20% fetal calf serum and 0.7% agarose (top layer) were plated and incubated at 37°C. The medium was removed and replaced with fresh medium in every 2 days. After 14 days of incubation, the cells were stained with 0.05% crystal violet/methanol for 2 h and colonies were counted in two colony grids using a microscope.

Immunohistochemistry

Immunostaining was performed as described earlier [20–21]. Briefly, paraffin embedded sections (to be evaluated for BMI1, BrdU and BCL2) were treated with Retrievagen A solution (pH 6) for antigen retrieval (BD Biosciences, San Diego, CA). Sections were incubated with primary antibody for overnight at 4°C. Slides were then washed and incubated for 2 h at room temperature with appropriate HRP-conjugated secondary antibody. Finally, slides were developed in 3, 3′-diaminobenzidene (DAB kit, Invitrogen) and counter stained with hematoxylin. The stained slides were dehydrated and mounted in permount solution.

Western blot Analysis

Western blot analysis was performed as described earlier [19–21]. Briefly, cell lysates were prepared by incubation of cells for 30 min in ice-cold lysis buffer [(0.05 mmol/L Tris-HCl, 0.15 mmol/L NaCl, 1 mole/L EGTA, 1 mol/L EDTA, 20 mmol/L NaF, 100 mmol/L Na_3VO4, 0.5% NP-40, 1% Triton X-100, 1 mol/L phenyl methylsulfonyl flouride (pH 7.4)] with protease inhibitor cocktail (Roche, Indianapolis, IN). The lysate was collected; insoluble materials were removed by centrifugation at 4°C for 15 minutes at 15,000 g, and stored at −80°C. BCA protein estimation kit was used to estimate the protein concentration in the lysates (Pierce, Rockford, IL), as per the vendor's protocol. Next, 40 μg protein was resolved in 10% SDS-PAGE gels, transferred onto PVDF membranes (Millipore) and incubated in blocking buffer (5% nonfat dry milk/1% Tween 20; in 20 mmol/L TBS, pH 7.6) for 2 h. The blots were incubated with appropriate primary antibody, washed and incubated with HRP-conjugated secondary antibody (Sigma). The blots were detected with chemiluminescence (ECL kit, Amersham Biosciences, Piscataway, NJ). Equal loading of protein was confirmed by stripping the blots and re-probing with ß-actin (Sigma).

Luciferase reporter activity

In these studies, cells were co-transfected with the pTK-TCF, (200 ng/well) and pGeneClip-BMI1-shRNA or pbabe-BMI1. *Renilla* luciferase (pRL-TK) was used as an internal control and reporter activity was measured as described earlier [19–20]. For controls, the similar amount of empty vectors (pGL3, pbabe and pGeneClip) was transfected in cells.

Quantification of apoptosis

Apoptosis was evaluated using the Annexin V-FITC Apoptosis detection kit from MBL International Corporation (Watertown, MA). Briefly, docetaxel resistant and BMI1-silenced docetaxel resistant cells were harvested with 0.025% trypsin + 5 mM EDTA in PBS (containing 2.5% FBS). Then the cells were washed with PBS and incubated for 5 min at room temperature with Annexin V-FITC plus propidium iodide (PI) as per vendor's protocol. Cells were analyzed on a Becton Dickinson FACS Calibur flow cytometer (BD Biosciences), placing the FITC signal in FL1 and the PI signal in FL2. Intact cells were gated in the FSC/SSC plot to exclude small debris. Cells in the lower right quadrant of the FL1/FL2 dot plot (labeled with Annexin V-FITC only) are considered to be in early apoptosis, and cells in the upper right quadrant (labeled with Annexin V-FITC and PI) are in late apoptosis/necrosis.

Generation of stable cell lines

To generate BMI1-overexpressing and BMI1-silenced stable cells, PC3 cells were transfected with either pbabe-BMI1 or pGeneClip-BMI1-shRNA using Lipofectamine. BMI1 overexpressing cells were selected in presence of puromycin (1 μg/ml) and BMI1-silenced were selected in presence of G418 (400 μg/ml) starting at 48 h after transfection. The selection of cells under antibiotics was continued for 4-weeks and clones were tested for BMI1 expression. The stable BMI1-overexpressing and BMI1-slinencing clones were maintained in RPMI containing 10% FBS and respective antibiotics (0.5 μg/ml puromycin for overexpressing clones, and 300 μg/ml G418 for silenced clones). During stable cell selection, we obtained several clones which expressed BMI1 for different durations of time. We selected clones for our studies which exhibited the expression or suppression of BMI1 upto 4 months.

Generation of chemoresistant cells

Chemoresistant cells were generated as per the method described by O'Neill et al. [22] (with modifications). Briefly, one million cells were seeded in 100 mm tissue culture dish with advanced-RPMI (Invitrogen) media containing 5% FBS and 1% penicillin/streptomycin for 24 h. At 24 h, the cells were exposed to 10 nM docetaxel for 48 h. The selection of concentration was based on the IC_{50} value. The drug containing medium was replaced after two days and the surviving (adherent) cells were cultured in a fresh drug-free complete medium. The cycle was repeated total 10 times. Following each treatment, cells were allowed to fully recover before next treatment. Next, the adherent cells were collected and exposed to higher doses of docetaxel (15, 20, to 25 nM) for 6 weeks (two weeks for each concentration). Finally, the surviving cells were maintained in RPMI/5% FBS containing 10 nM docetaxel. Untreated PC3 cells aged along side the treated cells (to avoid aging effect) were considered as control.

RNA isolation and cDNA synthesis

Total RNA was isolated from cells in culture plates using Trizol reagent as per the vendors protocol (Invitrogen). 1 μg RNA was used to synthesize cDNA as described earlier [19].

CaP-specific membrane hybridization and quantitative RT-PCR array

The membrane (printed with probes for CaP-specific genes) was hybridized with cRNA (synthesized from RNA of cells) and detected by chemiluminescence as per vendor's protocol (SA-Biosciences Super Array). Further, RNA from cells was used for qRT-PCR-array of CaP specific genes. The data analysis was performed by using array analyzer software (SA-Biosciences Super Array). The array data have been deposited to Gene bank database (accession number-GSE44049).

Senescence-associated ß-Galactosidase analysis

ß-galactosidase activity was performed by using X-gal (5-bromo-4-chloro-3-indolyl-ß-d-galactopyranoside) kit (Cell Signaling) as per vendor's protocol.

Chemosensitivity assay

Transfected cells at 12 h post-transfection were treated with casodex (10 μM), docetaxel (10 nM) and cisplatin (10 μM) for additional 24 h. Cells growth and proliferation were determined by 3[H]thymidine incorporation and colorimetric MTT-assay as described previously [19–20].

Quantitative Chromatin Immunoprecipitation (ChIP) assay

ChIP analysis for TCF1 and TCF4 occupancy on promoter region of *BCL2* gene was performed as described [19]. Briefly, samples were cross-linked with 1% formaldehyde. Anti-AR antibodies were used with protein A-Sepharose (Sigma) to adsorb immune-specific complexes. Preimmune serum was used as a control. Purified DNA was analyzed by real-time PCR (ABI Prism 7500) using appropriate primers. Product was measured by SYBR green fluorescence and the amount of product was calculated by determining relative expression to a standard curve generated from a titration of input chromatin. Following primers were used to amplify segments that overlap with the appropriate regions: BCL2 (−3.91 Kb), Forward, *5′CTGTGGGAGCAAAGGAAGAC3′*; Reverse, *5′AGAAGGAAACGGATCCCCTA3′*: BCL2 (P2-promoter, TATA site), Forward, *5′CAAGTGTTCCGCG'TGATTG3′;* Reverse *5′CCCGGTTA TCGTACCCTGTT3′:* BCL2 (−0.8 Kb), Forward, *5′GTCCAAGAATGCAAAGCACA3′;* Reverse- *5′CCCCCAGAGAAA-GAAG AGGA3′;* SP5 (promoter) - Forward 5′-*GGGTCTCCAGGCGGC AAG-3′***;** Reverse, *5′-AGCGAAAG-CAAATCC TTTGAA-3′*.

Tumor studies in animals

Athymic (nu/nu) male nude mice (6-weeks old) were implanted with stably transfected-PC3 cells (1×10^6 in 50 μl RPMI +50 μl Matrigel) subcutaneously. The study comprised of two protocols. Animals under each protocol were further divided into four groups described as following:

Overexpression protocol. Group-1 (n = 10) implanted with empty-vector (pbabe) transfected cells and treated with vehicle served as control. Group-II (n = 10) implanted with vector transfected cells was treated docetaxel (10 mg/kg in 100 μl of saline; thrice/week) through intraperitoneal (*i.p.*) administration. Group-III (n = 10) implanted with BMI1-overexpressing cells received *i.p.* administration of saline (100 μl). Group-IV (n = 10) mice bearing BMI1-overexpressing tumors received docetaxel (thrice/week).

Silencing protocol. Group-1 (n = 10) implanted with empty-vector (pGenClip) transfected cells and treated with vehicle served as control. Group-II (n = 10) implanted with vector transfected cells was treated with docetaxel (10 mg/kg). Group-III (n = 10) implanted with BMI1-silenced cells received *i.p.* administration of saline. Group-IV (n = 10) implanted with BMI1-silenced cells received docetaxel.

Tumor measurement. Body weights and tumor growth were recorded weekly as described [19–20]. Tumors from three

animals from each group/protocol were excised at the 35th day post- administration when 100% of control animals reached the preset end-point tumor volume of 1000 mm^3. Rest of the animals remained under protocol for a maximum time of 10 weeks. Before 2 h of sacrifice, each animal received an *i.p.* administration of BrdU (10 ml/kg) to label proliferating cells within tumors [20]. Animal were euthanized by a CO_2 inhalation method. All procedures were approved by University of Minnesota Institutional Animal Care and Use Committee (IACUC). The approved IACUC protocol number from University of Minnesota is 1003A79141. All procedures were conducted in accordance with the IACUC guidelines.

Statistical analyses

Student's *t test* for independent analysis was applied to evaluate differences between the treated and untreated cells. A Kaplan-Meier survival analysis with the corresponding Log-Rank and Linear Regression analysis was used to measure the rate of mean tumor volume growth as a function of time. Statistical analyses were carried out by using S-PLUS (Insightful, Seattle, WA). A p-value of <0.05 was considered to be statistically significant.

Results

BMI1 protein levels in human prostatic tissues increase with progressive stages of CaP

As an attempt towards identifying the expression status of BMI1 in during progressive stages of CaP, we measured its levels by performing immunoblot analysis of human prostatic tissues from normal, dysplasia and CaP patients. Expression levels of BMI1 protein were higher in malignant than normal prostatic tissues (Figure 1A). We next determined the expression of BMI1 in human specimens of normal and CaP by employing immunohistochemical analysis. Immunostains showed granular cytoplasmic staining in both non-neoplastic and neoplastic epithelium. In general, the staining was stronger in neoplastic epithelial cells than in non-neoplastic epithelial cells (Figure 1B). A progressive increase of BMI1 in epithelial cells was observed as the disease progressed from low-grade to high-grade (Figure 1B). Recently, we observed that the staining pattern is stronger in neoplastic stroma than in non-neoplastic stroma of tissues from CaP patients [23]. Taken together, these data show that expression of BMI1 increases with increasing stage of CaP.

BMI1 expression is independent of androgen

We investigated if the observed increase in BMI1 expression during the progression of CaP has a correlation with presence or absence of androgen. Androgen (R1881; 1 nM)-treated cells (LNCaP, LAPC4, 22Rv1 and C42b) did not show significant change in the levels of BMI1 protein (Figure 1C) suggesting that BMI1 expression is independent of influence of androgen.

BMI1 regulates the proliferation of CaP cells

We investigated whether BMI1 regulates the growth of CaP cells. We employed a two-way approach where BMI1 was (i) either silenced by transfecting a vector-based pGenCLIP-BMI1-shRNA or (ii) overexpressed by transfecting pbabe-BMI1 plasmid in cells (LNCaP, Du145 and PC3) (Figure S1). As measured by MTT viability assay, LNCaP cells duplicate within 48–72 h while as Du145 and PC3 cells duplication takes 24 h *in vitro*. It is noteworthy that BMI1-silenced cells did grow only 50–65% even at 72 h post-transfection (Figure 1Di). However BMI1-overexpressing cells achieved 65–90% confluence only at 36 h post-transfection suggesting that presence of BMI1 has the significance in the growth of CaP cells (Figure 1Dii).

We next asked if the pro-growth role of BMI1 is due to its effect on the proliferative potential of tumor cells. The rate of 3[H]thymidine uptake by CaP cells showed that knockdown of BMI1 decreased the proliferation (Figure 1Ei). Conversely, overexpression of BMI1 significantly increased the rate of proliferation in cells (Figure 1Eii). Taking advantage of the use of vector-based shRNA that enabled us to investigate the effect of BMI1-silencing over a long period, we determined clonogenic proliferation of CaP cells. Suppression of BMI1 significantly reduced number of colonies formed in soft-agar. Conversely, BMI1-overexpressing CaP cells formed increased number of colonies suggesting that BMI1 confers proliferative attributes to tumor cells (Figure 1Fi–Fii).

BMI1 increases the replicative life of normal cells

Proliferation promoting properties of BMI1 compelled us to ask this protein drives the proliferation. For this purpose, we used primary prostate epithelial cells (PrEC). PrEC grow slowly and enter into senescence after 4–5 passages under culture conditions. Notably, forced expression of BMI1 caused an increase in the replicative cycles of normal PrEC (Figure 2A). Due to transient nature of transfection, the effect of overexpression lasted up to 8th passage. Further, to validate senescence in PrEC, we measured senescence-associated β-galactosidase (SA-ß-gal) activity (marker of senescence). Normal cells exhibited positive staining for SA-ß-gal at the 4th passage. However BMI1-overexpressing PrEC did not show positive staining for SA-ß-gal at the 4th passage, continued growing and exhibited SA-ß-gal activity at the 7th passage (Figure 2B). These data show that BMI1 has the potential to drive normal as well tumor cells towards proliferation.

Molecular mechanism of action of BMI1 in tumor cells

To investigate the mechanism through which BMI1 controls the proliferation, we performed CaP-focused membrane and qPCR-based array analysis (of genes involved in the proliferation). Since LNCaP cells exhibit the expression of majority of the human genes, we performed the primary analysis in these cells. A cut-out point of 2-fold was selected for analysis. After observing the effect of BMI1-silencing in LNCaP cells, the data was further validated in Du145 and PC3 cells (data not shown). BMI1-silenced LNCaP cells exhibited a significant change in the expression of several proliferation-associated genes (Figure 2C and Table S1). These included Cyclin-D1, BCL2, IL and NFκB (Figure 2C and Table S1). An increased expression of p16, p15 and TIMP3 in BMI1-silenced tumor cells was observed (Figure 2C and Table S1). The array data was validated by performing immunoblot analysis of selected gene products in CaP cells. BMI1-silenced cells exhibited decreased Cyclin-D1 and BCL2 and increased p16 protein levels (Figure 2D). These data were further validated by conducting RT-PCR based microarray study and immunoblotting of BMI1-overexpressing cells, which exhibited increased BCL2 and Cyclin-D1 levels (Figure 2E; Figure S2A). The data suggested a possible association between the BMI1, BCL2 and Cyclin-D1 in tumor cells.

BMI1 in survival, growth and chemoresistance of tumor cells

Since BMI1 was observed to regulate the expression of proliferation-associated genes, we sought to determine if this phenomenon is responsible for chemoresistance. We determined the growth potential of BMI1-overexpressing and BMI1-silencing

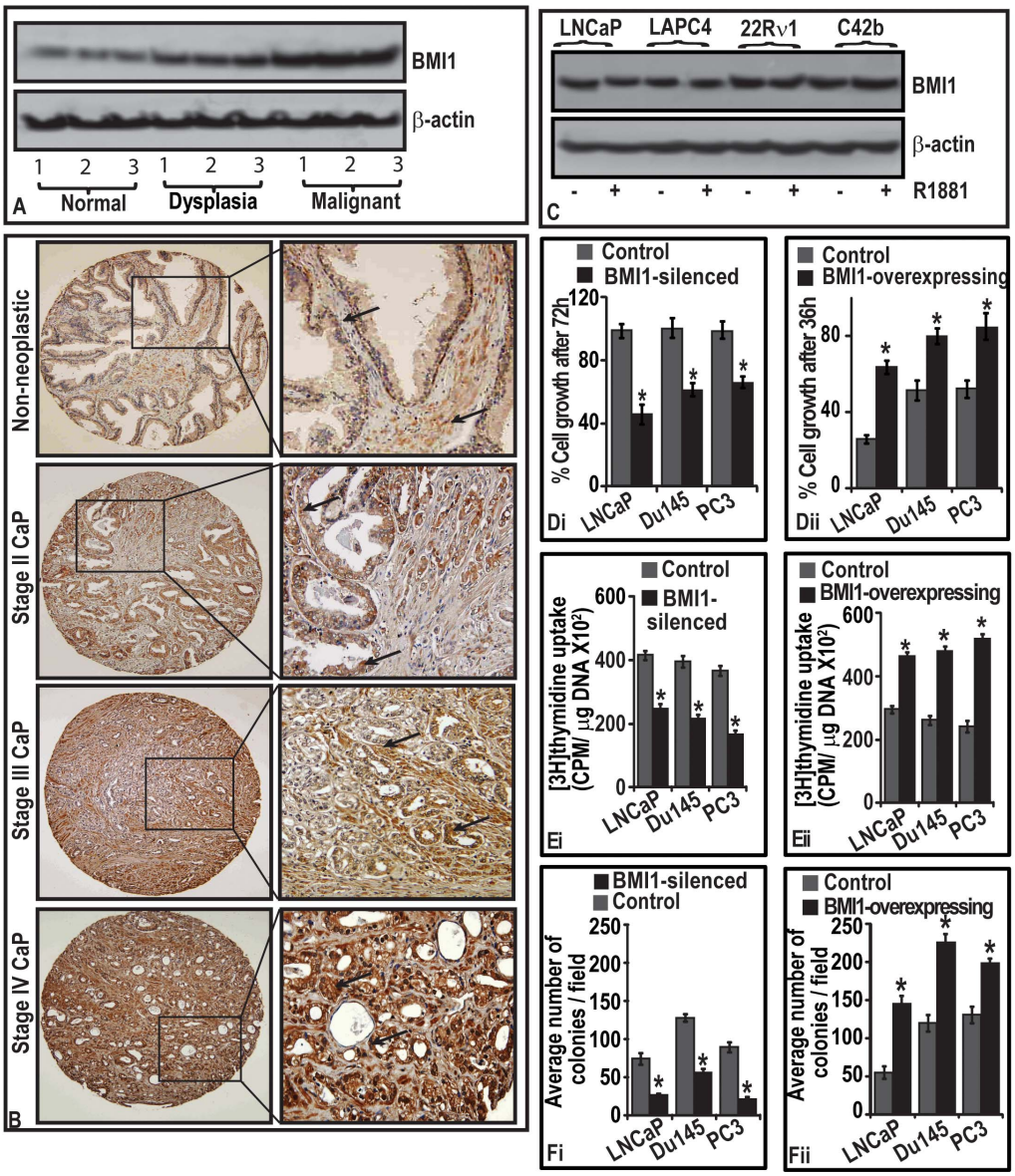

Figure 1. BMI1 protein levels are increased during the progression of CaP disease in human patients and BMI1 induces CaP cell proliferation. (A) Immunoblot represents BMI1 protein levels in normal, dysplasia and tumor prostatic tissues as assessed by immunoblotting **(B)** → in representative photomicrographs point to BMI1-positive immunostaining in neoplastic and non-neoplastic regions of prostatic specimens. Magnification 40X. **(C)** Immunoblot represents the effect of androgen on BMI1 expression in cells assessed by immunoblotting. (Di–Dii; Ei–Eii and Fi–Fii) Histograms represent the growth, rate of proliferation and clonogenic proliferation of BMI1-silenced and -overexpressed CaP cells measured by MTT, 3[H]thymidine uptake and soft-agar colony formation assays. Each histogram represents mean ± S.E. of three independent experiments, * indicates $p<0.05$. Equal loading of protein for immunoblotting was confirmed by ß-actin.
doi:10.1371/journal.pone.0060664.g001

CaP cells treated with clinically used chemotherapeutic agents (bicalutamide/casodex, docetaxel and cisplatin). The selection of dose of chemotherapeutic agents was based on their growth-inhibitory potential against LNCaP cells in a time and dose-dependent study (Figure S2C–D). The 3[H]thymidine incorporation analyses showed that BMI1-overexpressing CaP cells proliferate at high rate and are non-responsive to drugs (Figure 3B and D). However, BMI1-silenced cells were responsive to drugs and exhibited reduced rate of proliferation (Figure 3A and C). The observed differences between the BMI-overexpressing and -silenced tumor cells in responsiveness towards chemotherapy were also reflected in cell viability (Figures S3 and S4). These data suggest that presence of BMI1 in tumor cells plays a critical role in deciding the therapeutic outcome and could be clinically relevant.

BMI1 is critical for regrowth of tumors post-chemotherapy

We conducted a proof of principle study with chemoresistant PC3 cells. We showed that chemoresistant PC3 cells exhibited increased growth and expression of BMI1, BCL2 and Cyclin-D1 (Figure 3Ei–ii). We asked if targeting BMI1 could render the chemoresistant cells amenable to therapy and guide these to apoptosis. As evident from 3[H]thymidine uptake and FACS-analysis data, knocking-down of BMI1 inhibited the proliferation

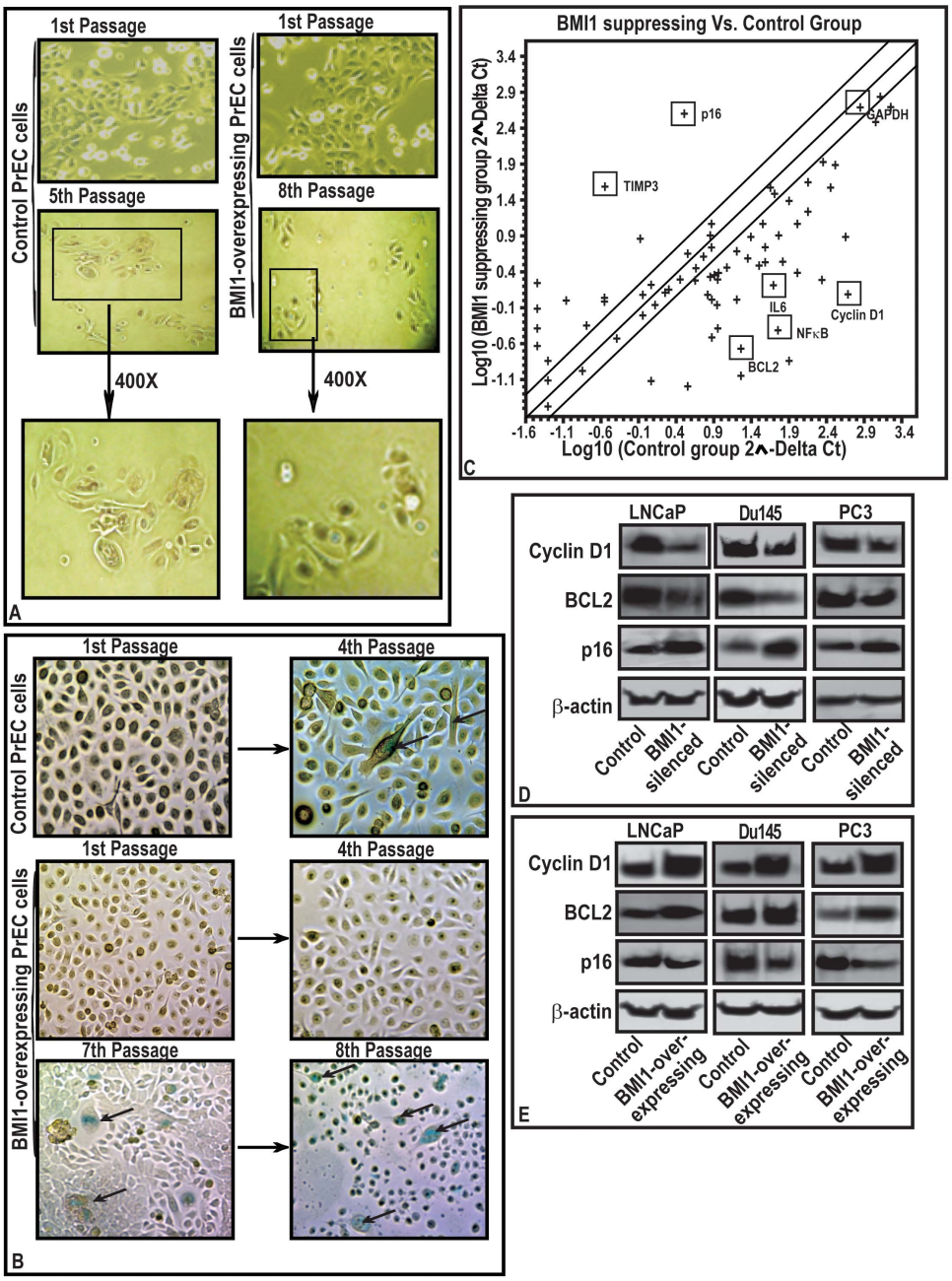

Figure 2. BMI1 induces growth of normal primary prostate cells (PrEC) by abolishing senescence and regulates the expression of proliferation-associated genes in CaP cells.. (A–B) While PrEC replicated for 5 passages and entered into senescence, BMI1-rich counterparts replicated and avoided senescence upto 8th passages. (A) **Inset** 400X of magnified areas show senescent morphology features i.e. globular shape and (B) → indicate staining for ß-galactosidase. **(C)** Scattered Plot for qPCR array. The dots indicate gene expression on a log-scale representing the change in BMI1 silenced-LNCaP cells. Fold change (2^- Delta Ct) is the normalized expression (2^-Delta Ct) in the BMI-silenced cells divided by the normalized expression of Control. **(D and E)** Immunoblots represents the effect of BMI1-silencing and BMI1-overexpression on the expression of Cyclin-D1, BCL2 and p16 proteins in cells. The equal loading of protein was confirmed by ß-actin.
doi:10.1371/journal.pone.0060664.g002

and increased apoptosis of chemoresistant cells concomitant to a decrease in BCL2/Cyclin-D1 levels (Figure 3F–H). These data establish role of BMI1 in the recurrence of tumor cells post-chemotherapy.

Molecular mechanism through which BMI1 regulates BCL2 in cells

Cyclin-D1 and BCL2 are down-stream targets of Wnt and Sonic hedgehog (Shh) signaling [24–25]. Therefore, we asked if BMI1 (i) has any association with Wnt and Shh-signaling in proliferating cells, and (ii) regulates BCL2 under Wnt or Shh guidance. We first determined the status of Wnt-signaling in BMI1-silenced and BMI1-overexpressing cells. By utilizing the

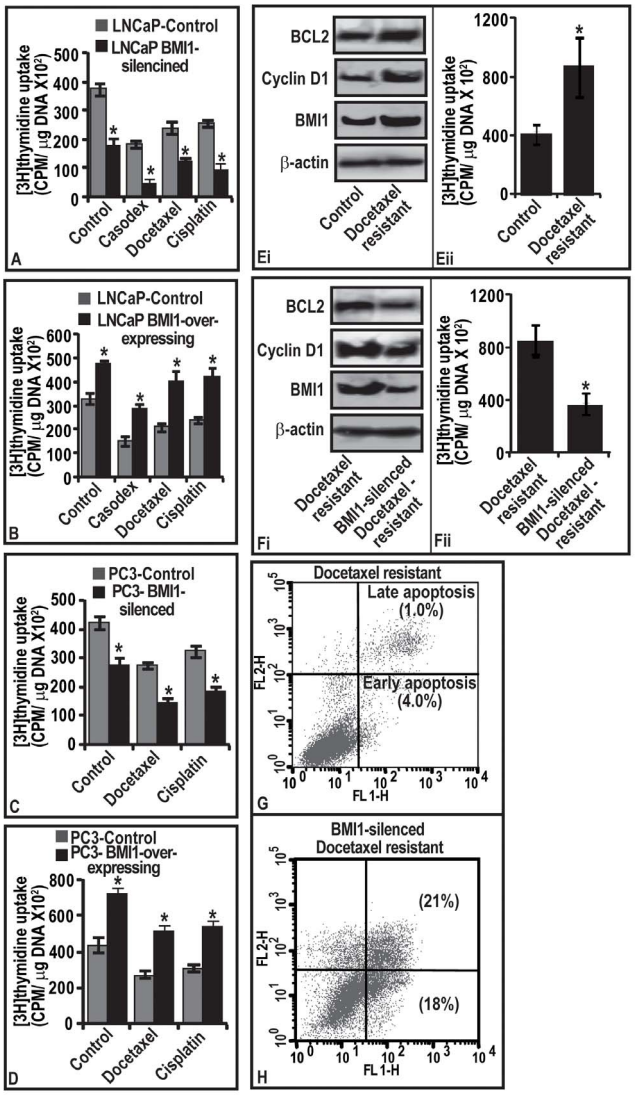

Figure 3. BMI1 confers chemoresistance to tumor cells. Rate of proliferation and apoptosis in cells were determined by 3[H]thymidine uptake and flow cytometery respectively. **(A–D)** Histograms represents the rate of proliferation in **(A–B)** LNCaP and **(C–D)** PC3 cells harboring varied BMI1 levels and treated with chemotherapeutic agents. Vehicle treated cells served as control. **(Ei and Fi)** immunoblots represent the levels of BMI1, Cyclin-D1 and BCL2 proteins in docetaxel-resistant, and BMI1-silenced docetaxel-resistant cells. (Eii and Fii) Histograms showing the rate of proliferation in docetaxel-resistant, and BMI1-silenced docetaxel-resistant cells. For immunoblot analyses (Figure Ei and Fi), equal loading of proteins was confirmed by ß-actin. (A–D, Eii and Fii) Each bar represents mean ± SE of three independent experiments, * represents $P<0.05$. **(G–H)** represents quantitative estimation of apoptosis in BMI1-silencing chemoresistant cells. The lower right quadrant of the FL1/FL2 plot (Annexin V-FITC) represent early apoptosis and the upper right quadrant (labeled with AnnexinV-FITC and PI) represent late apoptosis.

doi:10.1371/journal.pone.0060664.g003

reporter activity of *TCF-responsive element* (biomarker for Wnt activation), we observed that BMI1-overexpressed cells harbor increased TCF-transcriptional activity concomitant with the increased BCL2 and Cyclin-D1 (Figure 4A). Notably, BMI1-silenced cells exhibited decreased TCF-transcriptional activation (Figure 4B). Since our data showing a regulatory role of BMI1 on TCF-transcriptional activity in tumor cells is novel, we asked if this phenomenon is limited to CaP cells. To validate, we selected colon-cancer cell-line HT29 (exhibits increased Wnt signaling) and expresses BMI1 [26]. Interestingly, either BMI1-silencing or BMI1-overexpression caused significant modulations of TCF-transcriptional activity concomitant with changes in BCL2 and Cyclin-D1 in HT29 cells. These data establish the regulatory role of BMI1 on TCF-transcriptional activity in other cell types (Figure 4C–E).

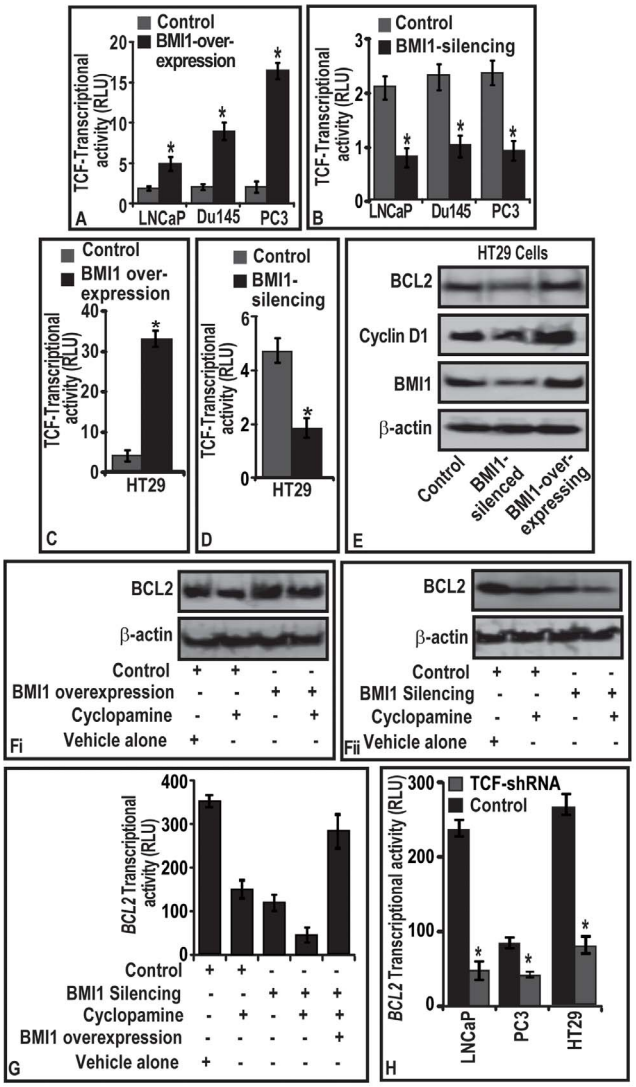

Figure 4. BMI1 regulates BCL2 expression through activation of TCF-transcriptional activity in tumor cells. (A–B; C–D) Histograms represent the effect of BMI1-overexpression and BM1-silencing on the transcriptional activation of *TCF-responsive element* in CaP and HT29 cells cells as assessed by luciferase-reporter assays. **(E–F)** representative immunoblots showing the effect of BMI1-silencing and -overexpression on the levels of BCL2 and Cyclin-D1 proteins in **(E)** HT29 cells, and (Fi–Fii) CaP cells treated with Cyclopamine (Shh inhibitor) for 12 h. Control cells were treated with DMSO. (G–H) Histogram represents the effect of **(G)** cyclopamine treatment and (H) TCF silencing on the transcriptional activity of BCL2 promoter in LNCaP, PC3 and HT29 cells. (A–D; G–H), relative luciferase activities were calculated with the values from vector group, and each bar represents mean ± SE of three independent experiments, *represents $p<0.05$. **(E–F)** Equal loading of proteins was confirmed by testing immunoblots for ß-actin.

doi:10.1371/journal.pone.0060664.g004

BCL2 is a well-established downstream target of Shh signaling [27]. We asked if BMI1 (i) partially regulates BCL2, or (ii) is regulation of BCL2 solely under the control of Shh? For this reason, cyclopamine (5 μM), an inhibitor of Shh-signaling was used. As expected cyclopamine treatment caused a reduction in BCL2 in control cells, however failed to modulate BCL2 levels in BMI1-overexpressing cells (Figure 4Fi). Notably, targeted-knock-down of BMI1 caused cyclopamine-resistant BMI1-rich cells to respond well to cyclopamine and reduced BCL2 (Figure 4Fii). To further validate the Shh-independent role of BMI1 in regulating BCL2 expression, we next reintroduced BMI1 in (a) cyclopamine treated, and (b) BMI1-silenced cells. Reintroduction of BMI1 in cyclopamine treated and BMI1-silenced cells caused a gain in BCL2 promoter-activity (Figure 4G). Taken together these data (Figure 4F–G) suggest that BCL2 expression is regulated in part by BMI1 and partially by Shh-signaling.

Since both TCF and BCL2 were observed to be under the guidance of BMI1, we next investigated whether there is a direct association of TCF and BCL2 gene in tumor cells. CaP and HT29 cells were co-transfected with TCF-shRNA and BCL2-luc reporter and were analyzed for BCL2-promoter activity. TCF-silenced CaP and HT29 cells exhibited decreased BCL2-promoter-activity (Figure 4H). This report suggests that BCL2 acts as a downstream target of TCF-signaling.

TCF4-transcriptional factor binds to promoter region of BCL2 gene in tumor cells

To further identify the underlying mechanism, we investigated whether BCL2 gene has possible TCF binding sites on its promoter. By employing TESS analysis, we observed that BCL2-promoter region exhibits multiple sites where TCF possess the affinity to bind (data not shown) [28]. We next sought the validation of TESS data (which is a mathematical data) by biochemical analysis. We tested TCF1 and TCF4 occupancy on multiple sites on the promoter region of BCL2 gene by employing ChIP assay. The TCF unresponsive SP5-promoter was used as a negative control (data not shown). TCF1 was observed to have insignificant occupancy on the examined sites of BCL2-promoter in both CaP and colon cells (data not shown). Among the three region analyzed, TCF4 was observed to occupy only TATA region of BCL2-promoter (P2-promoter). We found very little or no occupancy by TCF4 on −3.41 Kb and −8.41 kb of BCL2 promoter (data not shown). Notably, BMI1-overexpression was observed to increase the TCF4 occupancy on the TATA region of BCL2-promoter in the PC3 and HT29 cells (Figure 5A–B). An opposite result was observed with that of BMI1-silenced CaP and HT29 cells (Figure 5A–B).

TCF4 binds to promoter region of BCL2 gene in human prostatic tissues

We next investigated if the *in vitro* observation of TCF4-occupancy on BCL2-promoter binding has translational relevance. From the outcome of immunoblot analysis data (Figure 5C), we selected human normal and malignant prostatic tissues (which exhibited increased BMI1) and determined TCF4-occupancy on *BCL2*-promoter. As compared to the normal prostatic tissues, TCF4 exhibited increased occupancy at TATA region of *BCL2* in human CaP tissues (Figure 5D).

BMI1 confers chemoresistance to human prostatic tumors in xenograft mouse models

Since BMI1 was observed to be involved in the chemoresistance of CaP cells to various antitumor agents under *in vitro* conditions, we next determined whether these observations could be translated under *in vivo*. For this purpose, we measured the differential growth rate of tumors-derived from BMI1-overexpressing and –silencing PC3-stable cells under two protocols.

BMI1-overexpression protocol. At one week post-implantation, the average volume of control and BMI1-overexpressing tumors in mice increased as a function of time (Figure 5E). BMI1-overexpressing tumors were observed to grow at faster rate and larger in size than control tumors (Figure 5E). Mice implanted with control-tumors reached a preset end-point tumor volume of 1000 mm3 at 49th day of post-implantation (Figure 5E). However, mice implanted with BMI1-overexpressing tumors reached the preset end-point tumor volume at 35th day of post-implantation (Figure 5E). At 49th and 35th days, mice implanted with control and BMI1-overexpressing tumors exhibited average tumor volumes of 1076 and 1023 mm3, respectively (Figure 5E).

Docetaxel treatment decreased the growth of tumors in control mice (Group-II). Interestingly, docetaxel treatment failed (for 10-weeks) to produce an effect on the growth of tumors expressing high BMI1 protein. At 49^{th} day, the average tumor volume in control mice (Group-II) treated with docetaxel was 850 mm^3 (Figure 5E). However, BMI1-overexpressing tumors though treated with docetaxel reached an average tumor volume of 997 mm^3 at 35^{th} day (Figure 5E). Next, we evaluated whether treatment of docetaxel to animals caused a delay in the growth of tumors harboring increased BMI1 levels. As evident from the number of mice reaching the preset end-point tumor volume (1000 mm^3), the observed differences between the control and BMI1-overexpresed group of animals for the outcome of docetaxel therapy was statistically significant (Figure 5F).

BMI1-silenced protocol. BMI1-silenced cell-derived tumors were observed to grow at slower rate than control (Figure 5G). This was evident from the significant difference in the rate of growth and tumor volumes between control and BMI1-silenced groups (Figure 5G). Control group reached a preset end-point average tumor volume of 1000 mm^3 at 49^{th} day post-implantation (Figure 5G). Notably BMI1-silenced group did not reach the end-point even at 70^{th} day post-implantation (Figure 5G). At 49^{th} day, animals treated with docetaxel exhibited an average tumor volume of 850 mm^3. However at this point, BMI1-silenced group treated with docetaxel exhibited only an average tumor volume of 230 mm^3 suggesting that knocking down of BMI1 sensitized tumor cells to therapy (Figure 5G). Further docetaxel caused a delay in the growth of BMI1-silenced tumors. The observed differences between control and BMI-silenced group were significant (Figure 5H).

Discussion

Recent studies showed that dysregulation of BMI1 play a crucial role in epithelial mesenchymal transition, cell proliferation, senescence and self-renewability of several human cancers [11,16,29]. However, the role of BMI1 in CaP progression and chemoresistance is not well studied [30]. It is speculated that inability of tumor cells to undergo apoptosis in response to chemotherapy results in a selective advantage for such cells to become more aggressive compared to chemoresponsive cells [11]. Although several studies demonstrate that BMI1 rescues tumor cells from apoptosis, the concrete mechanism of action is yet to be known [13–15]. CRPC is hard-to-treat disease and identifying a critical molecule that confers the chemoresistant characteristic to such tumors would be an important advancement in this field. In the current study, we provide mechanism-based evidence that BMI1 plays a deciding role in the fate of tumor cells undergoing

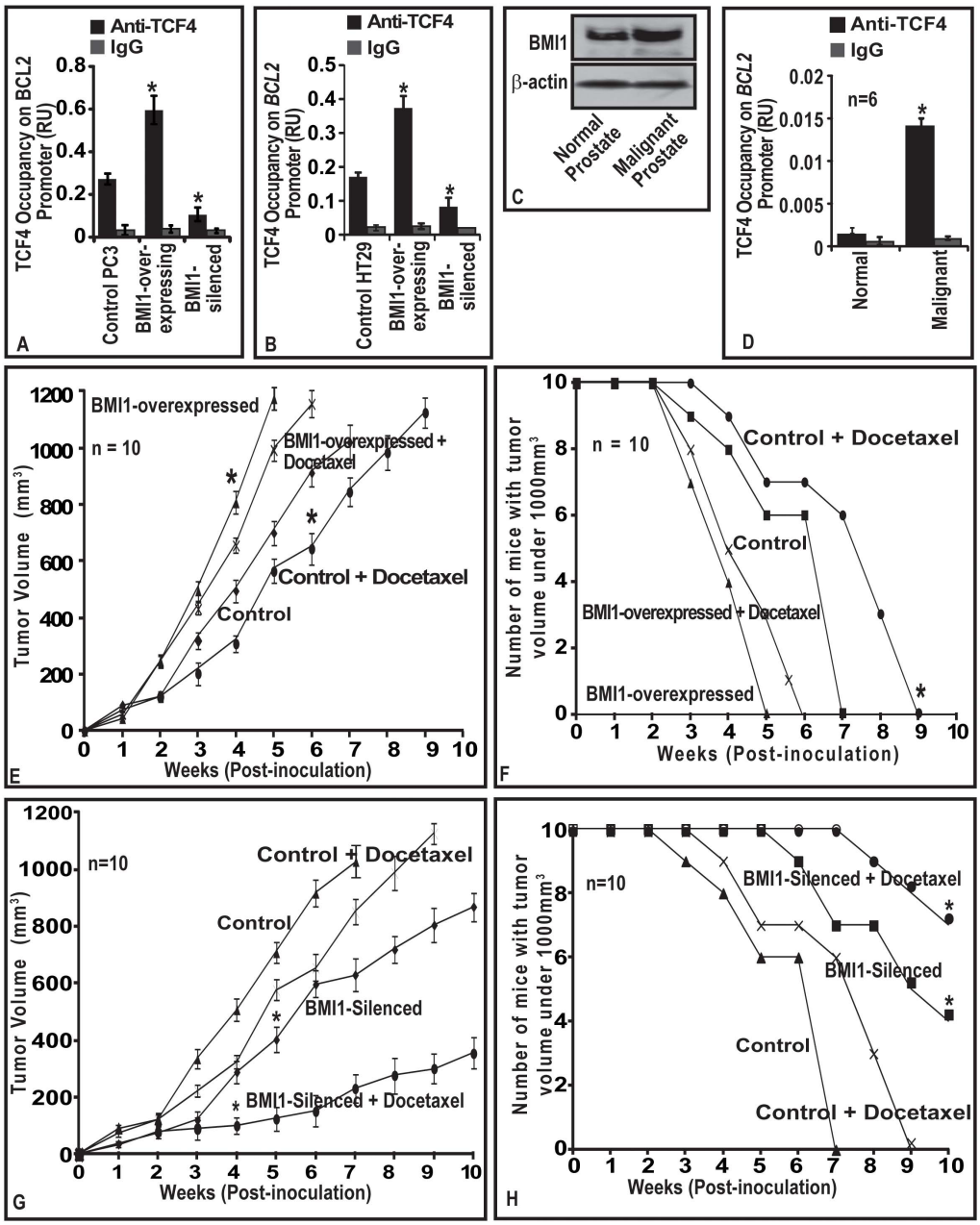

Figure 5. (A–B) BMI1 induces TCF4 binding to promoter region of *BCL2* gene. (C) TCF4 occupancy on *BCL2* is elevated in malignant prostatic tissues. (D) BMI1 confers chemoresistance to tumors in a mouse model. (A–B) Histogram represents effect of BMI1 expression on TCF4-occupancy on promoter regions of *BCL2* in PC-3 and HT29 cells as assessed by ChIP assay. **(C–D)** immunoblot and histogram represents the BMI1 protein expression, and TCF4-occupancy on *BCl2 gene* in normal and malignant human prostate tissues as assessed by immunoblotting and ChIP assays. Equal loading of proteins was confirmed by ß-actin for immunoblotting. (A–B, D). Each bar represents mean ± SE of three independent experiments. **(E–F)** The line graph represents average volume of BMI1-overexpressing and BMI1-suppressed tumors as a function of time vis-à-vis docetaxel therapy on in nude mice. **(G–H)** The line graph shows the number of mice with tumor volumes <1000 mm^3 for indicated weeks. Data is represented as mean$\pm$SE; * indicates $p<0.05$.

doi:10.1371/journal.pone.0060664.g005

chemotherapy. This study is significant because we demonstrated that BMI1 equally confers chemoresistance to hormone-sensitive CaP and CRPC cells. CRPC tumors in men are reported to proliferate under low androgen conditions [7,31]. An important clinically relevant information from this study is that BMI1 expression does not get influenced by androgen suggesting a possibility for BMI1 playing a role in driving indolent disease to aggressive androgen-independent phenotype. Based on our data we suggest that targeting BMI1 should be a part of therapeutic strategy to combat chemoresistant cancer.

Expression of BCL2 and Cyclin-D1 is reported to be high in chemoresistant tumors [24,32–34]. Notably, BCL2 and Cyclin-D1 have a commonality to be also the functional members of Wnt and Shh pathways. Recent studies suggest that targeting BCL2 directly (anti-BCL2 immunotherapy) or blocking the pathways (such as Shh) regulating it, could be a possible therapeutic strategy to

overcome chemoresistance [30,35–36]. Shh inhibitors (which downregulate BCL2) are currently being investigated as therapeutic agents for basal cell carcinoma, medulloblastoma and glioblastoma [37]. Despite treated with anti-BCL2 therapies, the tumors resurge for unknown reasons. Our study is significant because we provide evidence that BCL2 is not completely lost in chemoresistant tumor cells post-chemotherapy, and alternate pathways regulate BCL2. This is based on data that (i) BMI1 regulates BCL2 independent of Shh-signaling and (ii) elevated levels of BMI1 and BCL2 are found in cells those escape chemotherapy. We suggest that this mechanism could be an explanation for the survival of chemoresistant cells post-chemotherapy. Although the previous report showed that BMI1 itself is a target of Shh-signaling, our data show that BMI1 acts independent of Shh [38]. It is possible that chemoresistant cells expressing BMI1 are a highly selected sub-population that remains hard to treat and play an important role in indolence of disease in CaP patients.

BMI1 activity is manifested in the form of repression of target genes and the mode of action could be through epigenetic silencing [11]. However, in this study we observed that BMI1-upregulates BCL2. Keeping in view the repressive nature of BMI1, there was a need to understand the mode of action through which BMI1 induces BCL2 activity. We provided evidence that BCL2 activation in chemoresistant cells under the guidance of BMI1 is mediated by TCF4. This was validated in prostate and colon cancer cells; and in human prostatic tissues. Although the complete information about the regulation of TCF4 by BMI1 is not completely understood, current data suggest that TCF4 indeed is in part under the control of BMI1. The significance of our data is that it (***i***) identifies BMI1-induced TCF4 as a molecular module that drives Wnt-signaling within chemoresistant cells, and (***ii***) BCl2 as a target of BMI1/TCF4 molecular module. Based on our data, we speculate that molecular module could be operational during emergence of chemoresistance and also responsible for proliferation of chemoresistant CaP cells after therapy.

Docetaxel has been tested under several clinical trials alone and in combination with other agents to treat CaP. Docetaxel therapy was observed to result in a PSA drop of more than 50% in CaP patients, an observation made in several trials such as the SWOG trial [31]. However, docetaxel alone, and in combination do not completely abrogate the tumor or bring down PSA levels to the normal in human CaP patients [39]. Although effective in CaP patients to an extent, some CaP conditions do not respond to docetaxel therapy [40]. Resistance to docetaxel is explained in part, by over-expression of deferent multidrug resistance proteins at both genetic and epigenetic levels [41–42]. In this context, this study is significant as we show that targeting BMI1 in chemoresistant cells sensitizes cells to therapy. This study identified BMI1 as an ideal molecule to be targeted to overcome the chemoresistance of CaP cells and corroborates to earlier report showing the utility of BMI1 as a target to overcome chemoresistance in ovarian cancer cells [15]. Under *in vivo* conditions, the significance between BMI1-positive, BMI-silenced and BMI1-overexpressed tumor cells vis-à-vis docetaxel therapy was significant. The success of docetaxel therapy against prostatic tumors in a xenograft mouse model was observed to be highly dependent on the level of BMI1. We suggest that preventing the development of chemoresistance in CaP patients will be beneficial for a large group of patients and interventions directed against BMI1 may provide opportunities to enhance the efficacy of chemotherapy. In this direction we have opened another front by identifying small molecule inhibitors (SMIs) of BMI1. We suggest that these should be explored against chemoresistant tumors. The advanced work with SMIs of BMI1 against chemoresistant tumors is underway in our laboratory.

Supporting Information

Figure S1 Representative immunoblot shows the effect of BMI1-silencing and -overexpression on the level of BMI1 protein in CaP cells. Equal loading was confirmed by reprobing immunoblots for ß-actin.
(TIF)

Figure S2 BMI1 modulates number of proliferation related genes in CaP cells and time-course and dose titration curves for the chemotherapeutic drugs. (A) Figure represents clustrogram of gene expression as assessed by PCR array in control and BMI1-silenced LNCaP cells. **(B–D)** Time-course and dose titration curves for the chemotherapeutic agents Casodex **(B)**, Cisplatin **(C)** and Docetaxel **(D)** as assessed by MTT assay. Vehicle treated cells were considered as control. Data represents mean ± SE of three independent experiments.
(TIF)

Figure S3 BMI1 regulates the growth of CaP cells. BMI1-rich CaP cells exhibit increased growth and chemoresistant against chemotherapeutic drugs. (A–B) The histogram represents the rate of proliferation of cells as measured by MTT assay in BMI1 overexpressing **(A)** LNCaP and **(B)** PC3 cells treated with different chemotherapeutic agents. Vehicle treated cells were considered as control. Each bar in the histogram, represents mean ± SE of three independent experiments, * represents $P<0.05$.
(TIF)

Figure S4 BMI1 regulates the growth of CaP cells. BMI1-deficient CaP cells exhibit decreased growth and chemo-sensitivity against chemotherapeutic drugs. (A–B) The histogram represents the rate of proliferation of cells as measured by MTT assay in BMI1-silenced **(A)** LNCaP and **(B)** PC3 cells treated with different chemotherapeutic agents. Vehicle treated cells were considered as control. Each bar in the histogram, represents mean ± SE of three independent experiments, * represents $P<0.05$.
(TIF)

Table S1 List of selected genes modulated by BMI1-supression in CaP cells.
(DOC)

Acknowledgments

We thank Dr. Chi V. Dang (The Johns Hopkins University, USA) and Dr. Robert Reiter (UCLA, CA, USA) for providing pbabe-BMI1 plasmid and LAPC4 cells respectively. We highly thank Ms. Ellen Krock (supervisor of Animal facility, The Hormel Institute, UMN, MN, USA) for providing help in animal studies. We acknowledge the technical support provided by Ms. Neelofar Jan (Junior Technician) in animal studies.

Author Contributions

Conceived and designed the experiments: MS HRS. Performed the experiments: HRS AP RST. Analyzed the data: MS HRS AP RJK BK LW. Contributed reagents/materials/analysis tools: MS HM YD. Wrote the paper: HRS.

References

1. Siegel R, Naishadham D, Jemal A (2012) Cancer Statistics. CA Cancer J Clin 62:10–29.
2. Jemal A, Siegel R, Hao Y, Xu J, Thun MJ (2010) Cancer statistics CA Cancer J Clin 60: 277–300.
3. Jemal A, Bray F, Center MM, Ferlay J, Ward E, et al. (2011) Global cancer statistics. CA Cancer J Clin 61:69–90.
4. Mahon KL, Henshall SM, Sutherland RL, Horvath LG (2011) Pathways of chemotherapy resistance in castration-resistant prostate cancer. Endocr Relat Cancer 18: R103–123.
5. Zhang L, Jiao M, Li L, Wu D, Wu K, et al. (2012) Tumorspheres derived from prostate cancer cells possess chemoresistant and cancer stem cell properties. J Cancer Res Clin Oncol 138: 675–686.
6. Kotb AF, Elabbady AA (2011) Prognostic factors for the development of biochemical recurrence after radical prostatectomy. Prostate Cancer 2011: 485189.
7. Parray A, Siddique HR, Nanda S, Konety BR, Saleem M (2012) Castration-resistant prostate cancer: potential targets and therapies. Biologics 6: 267–276.
8. Catalona WJ, Smith DS (1998) Cancer recurrence and survival rates after anatomic radical retropubic prostatectomy for prostate cancer: intermediate-term results. J Urol 160: 2428.
9. Pound CR, Partin AW, Eisenberger MA, Chan DW, Pearson JD, et al. (1999) Natural history of progression after PSA elevation following radical prostatectomy. JAMA 281:1591–1597.
10. Han M, Partin AW, Zahurak M, Piantadosa S, Epstein JI, et al. (2003) Biochemical (Prostate Specific Antigen) recurrence probability following radical prostatectomy for clinically localized prostate cancer. J Urol 169: 517–523.
11. Siddique HR, Saleem M (2012) Role of BMI1, a Stem Cell Factor in Cancer Recurrence and Chemoresistance: Preclinical and Clinical Evidences. Stem Cells 30: 372–378.
12. Kang MK, Kim RH, Kim SJ, Yip FK, Shin KH, et al. (2007) Elevated BMI1 expression is associated with dysplastic cell transformation during oral carcinogenesis and is required for cancer cell replication and survival. Br J Cancer 96: 126–133.
13. Jacobs JJ, Scheijen B, Voncken JW, Kieboom K, Berns A, et al. (1999) BMI1 collaborates with c-Myc in tumorigenesis by inhibiting c-Myc-induced apoptosis via INK4a/ARF. Genes Dev 13: 2678–2690.
14. Cui H, Hu B, Li T, Ma J, Alam G, et al. (2007) BMI1 is essential for the tumorigenicity of neuroblastoma cells. Am J Pathol 170: 1370–1378.
15. Wang E, Bhattacharyya S, Szabolcs A, Rodriguez-Aguayo C, Jennings NB, et al. (2011) Enhancing chemotherapy response with BMI1 silencing in ovarian cancer. PLoS One 6: e17918.
16. Huber GF, Albinger-Hegyi A, Soltermann A, Roessle M, Graf N, et al. (2011) Expression patterns of BMI1 and p16 significantly correlate with overall, disease-specific, and recurrence-free survival in oropharyngeal squamous cell carcinoma. Cancer 117: 4659–4670.
17. Glinsky GV, Berezovska O, Glinskii AB (2005) Microarray analysis identifies a death-from-cancer signature predicting therapy failure in patients with multiple types of cancer. J Clin Invest 115: 1503–1521.
18. Klein KA, Reiter RE, Redula J, Moradi H, Zhu XL, et al. (1997) Progression of metastatic human prostate cancer to androgen independence in immunodeficient SCID mice. Nat Med 3: 402–408.
19. Siddique HR, Mishra SK, Karnes RJ, Saleem M (2011) Lupeol, a novel androgen receptor inhibitor: implications in prostate cancer therapy. Clin Cancer Res 17: 5379–5391.
20. Siddique HR, Liao DJ, Mishra SK, Schuster T, Wang L, et al. (2012) Epicatechin-rich cocoa polyphenol inhibits kras-activated pancreatic ductal carcinoma cell growth in vitro and in a mouse model. Int J Cancer 131: 1720–1731
21. Saleem M, Adhami VM, Zhong W, Longley BJ, Lin CY, et al. (2006) A novel biomarker for staging human prostate adenocarcinoma: overexpression of matriptase with concomitant loss of its inhibitor, hepatocyte growth factor activator inhibitor-1. Cancer Epidemiol Biomarkers Prev 15: 217–227.
22. O'Neill AJ, Prencipe M, Dowling C, Fan Y, Mulrane L, et al. (2011) Characterisation and manipulation of docetaxel resistant prostate cancer cell lines. Mol Cancer 10:126.
23. Siddique HR, Parray A, Zhong W, Karnes JR, Bergstralh EJ, et al. (2013) BMI1, Stem Cell Factor Acting as Novel Serum-biomarker for Caucasian and African-American Prostate Cancer. PLOS ONE 8: e52993
24. Hegde GV, Munger CM, Emanuel K, Joshi AD, Greiner TC, et al. (2008) Targeting of sonic hedgehog-GLI signaling: a potential strategy to improve therapy for mantle cell lymphoma. Mol Cancer Ther 7:1450–1460.
25. Rohrs S, Kutzner N, Vlad A, Grunwald T, Ziegler S, et al. (2009) Chronological expression of Wnt target genes Ccnd1, Myc, Cdkn1a, Tfrc, Plf1 and Ramp3. Cell Biol Int 33: 501–508.
26. Kanwar SS, Yu Y, Nautiyal J, Patel BB, Majumdar AP (2010) The Wnt/beta-catenin pathway regulates growth and maintenance of colonospheres. Mol Cancer 9:212.
27. Bigelow RL, Chari NS, Unden AB, Spurgers KB, Lee S, et al. (2004) Transcriptional regulation of BCL2 mediated by the sonic hedgehog signaling pathway through Gli-1. J Biol Chem 279: 1197–1205.
28. Schug J (2008) Using TESS to predict transcription factor binding sites in DNA sequence. Curr Protoc Bioinformatics. Chapter 2: Unit 2.6. doi: 10.1002/0471250953.bi0206s21.
29. Song LB, Li J, Liao WT, Feng Y, Yu CP, et al. (2009) The polycomb group protein BMI1 represses the tumor suppressor PTEN and induces epithelial-mesenchymal transition in human nasopharyngeal epithelial cells. J Clin Invest 119: 3626–3636.
30. Crea F, Duhagon Serrat MA, Hurt EM, Thomas SB, Danesi R, et al. (2011) BMI1 silencing enhances docetaxel activity and impairs antioxidant response in prostate cancer. Int J Cancer 128: 1946–1954.
31. Siddique HR, Nanda S, Parray A, Saleem M (2012) Androgen receptor in human health: a potential therapeutic target. Curr Drug Targets 13: 1907–16.
32. Casimiro M, Rodriguez O, Pootrakul L, Aventian M, Lushina N, et al. (2007) ErbB-2 induces the cyclin D1 gene in prostate epithelial cells in vitro and in vivo. Cancer Res 67: 4364–4372.
33. Kang MH, Reynolds CP (2009) BCL2 inhibitors: targeting mitochondrial apoptotic pathways in cancer therapy. Clin Cancer Res 15: 1126–1132.
34. Brunelle JK, Letai A (2009) Control of mitochondrial apoptosis by the BCL2 family. J Cell Sci 122(Pt 4): 437–441.
35. Mackler NJ, Pienta KJ (2005) Drug insight: use of docetaxel in prostate and urothelial cancers. Nat Clin Pract Urol 2: 92–100.
36. Straten P, Andersen MH (2010) The anti-apoptotic members of the Bcl-2 family are attractive tumor-associated antigens. Oncotarget 1: 239–245.
37. Mahindroo N, Punchihewa C, Fujii N (2009) Hedgehog-Gli signaling pathway inhibitors as anticancer agents. J Med Chem 52: 3829–3845.
38. Liu S, Dontu G, Mantle ID, Patel S, Ahn NS, et al. (2006) Hedgehog signaling and BMI1 regulate self-renewal of normal and malignant human mammary stem cells. Cancer Res 66: 6063–6071.
39. Petrylak DP (2007) New paradigms for advanced prostate cancer. Rev Urol 9 Suppl 2: S3–S12.
40. Ross RW, Beer TM, Jacobus S, Bubley GJ, Taplin ME, et al. (2008) Prostate Cancer Clinical Trials Consortium. A phase 2 study of carboplatin plus docetaxel in men with metastatic hormone-refractory prostate cancer who are refractory to docetaxel. Cancer 112: 521–6.
41. Sánchez C, Mercado A, Contreras HR, Mendoza P, Cabezas J, et al. (2011) Chemotherapy sensitivity recovery of prostate cancer cells by functional inhibition and knock down of multidrug resistance proteins. Prostate 71: 1810–7.
42. Chen KG, Sikic BI (2012) Molecular pathways: regulation and therapeutic implications of multidrug resistance. Clin Cancer Res 18: 1863–9.

APPENDIX II

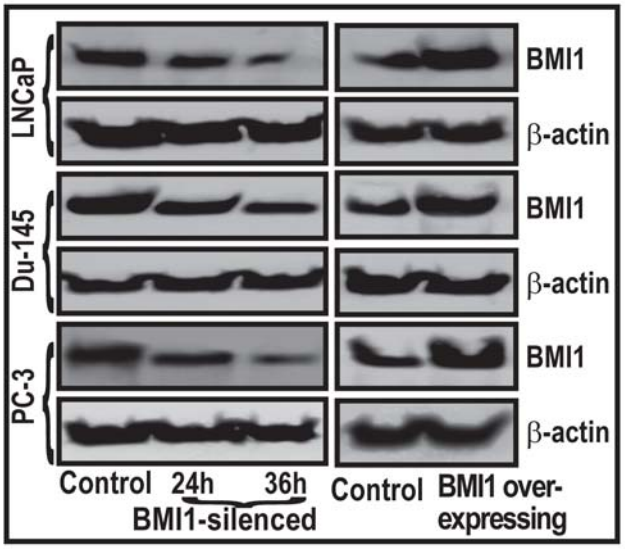

Figure S1

APPENDIX II

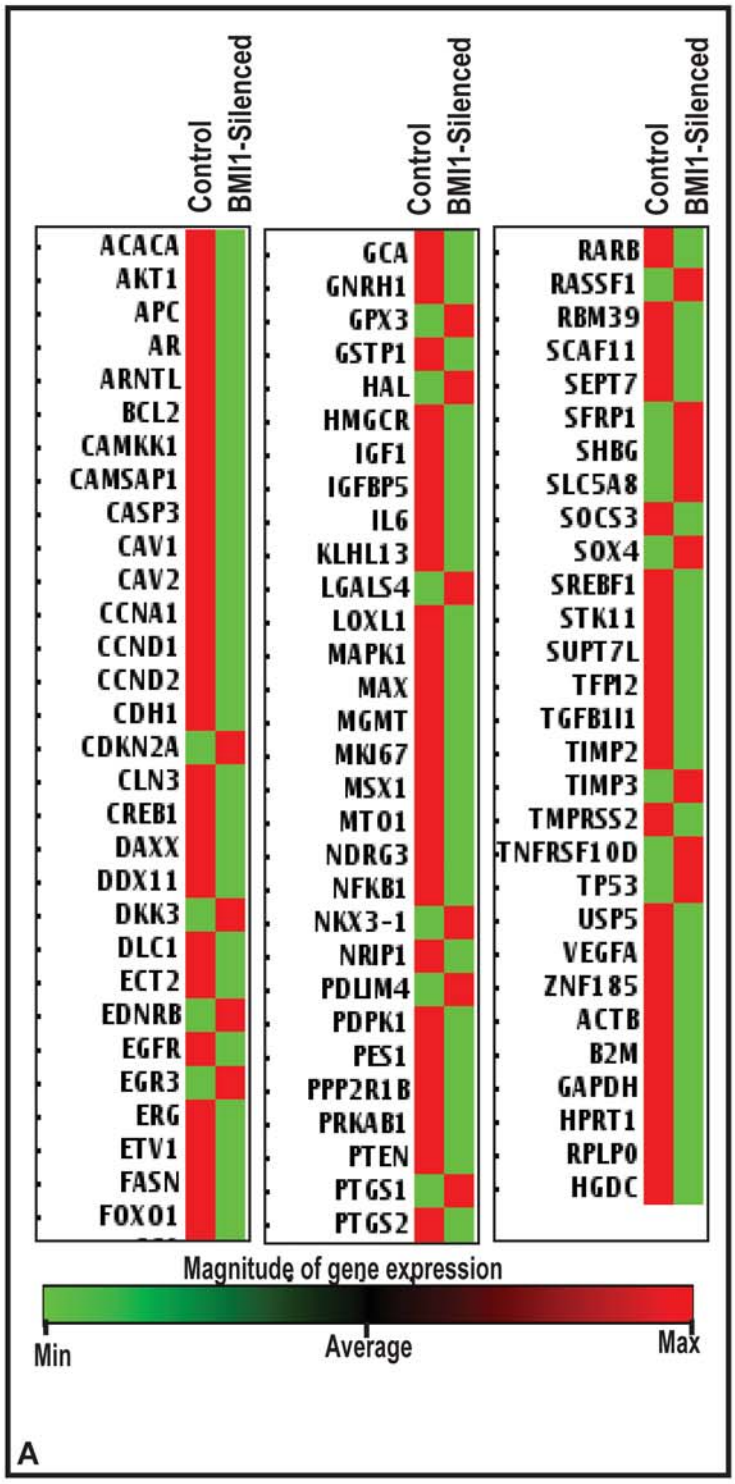

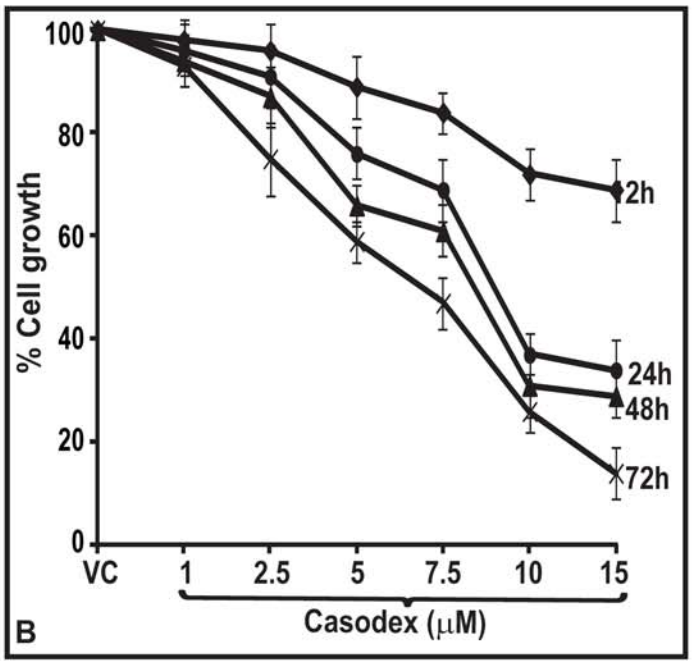

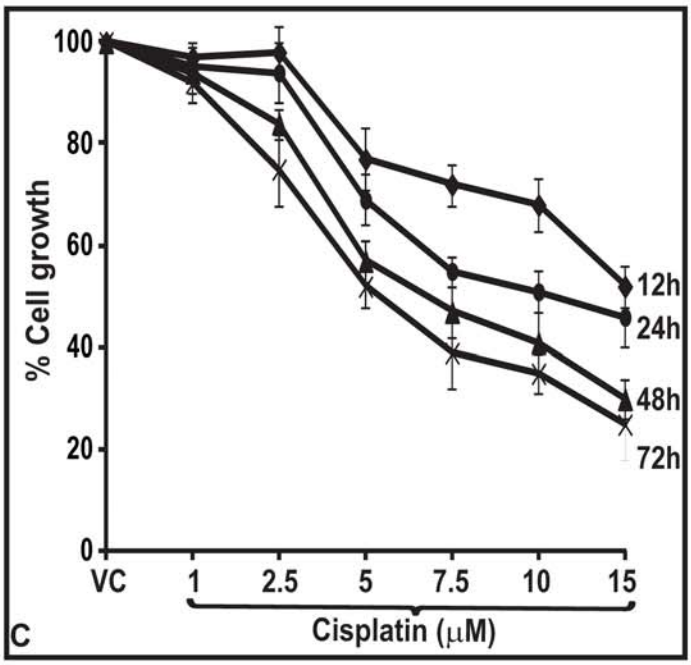

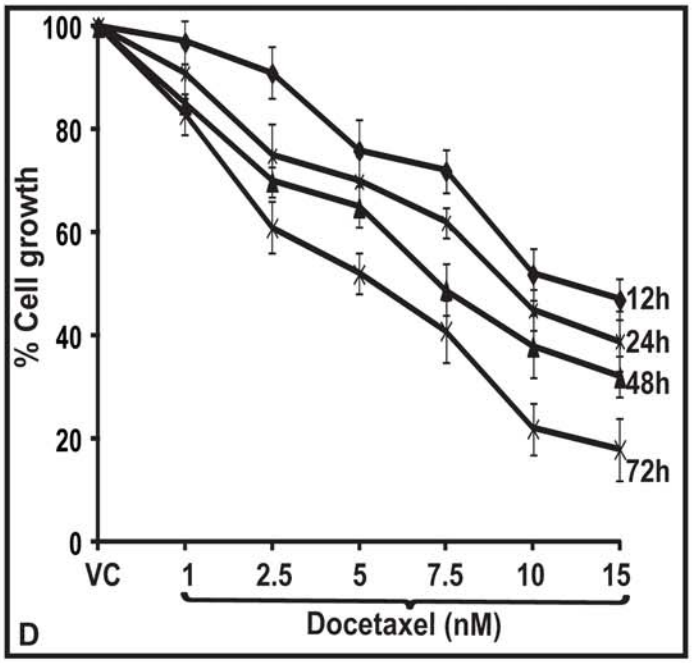

Figure S2(A-D)

APPENDIX II

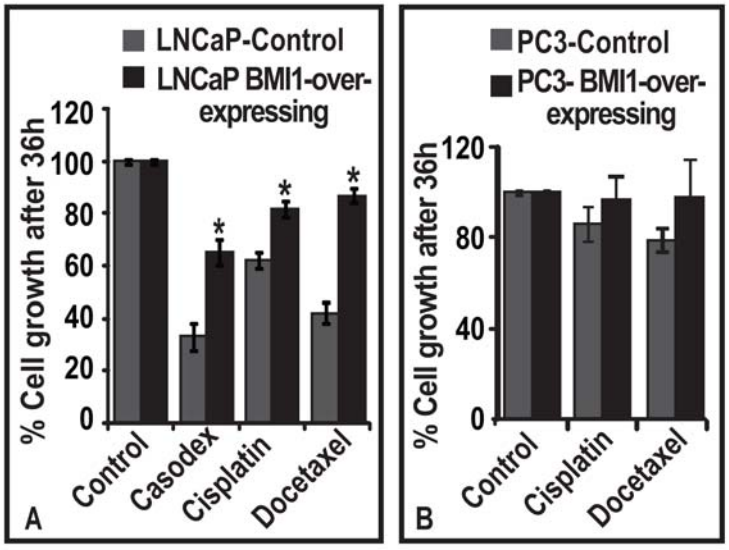

Figure S3(A-B)

APPENDIX II

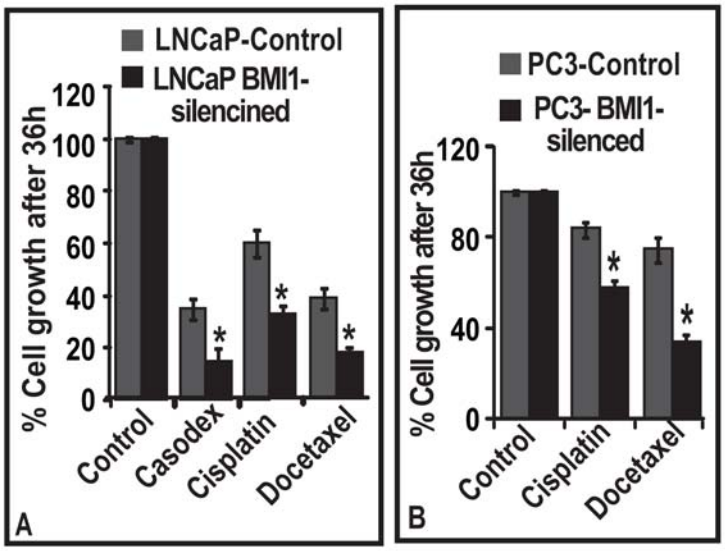

Figure S4(A-B)

APPENDIX II

Table S1. List of Selected Genes Modulated by BMI1-supression in CaP Cells.

Gene Symbol	Fold Changes	Function	Potential implication in CaP pathogenesis
Downregulated			
Cyclin D1	26.0	Cell cycle, cell growth and/or maintenance	Cell proliferation
Cdk4	7.5	Regulation of cell cycle; protein Kinase activity	Cell Proliferation
Bcl-2	20.0	Mitochondrial protein that blocks the apoptotic death	Cell proliferation and chemoresistance
Akt-1	3.5	Survival factors; suppress apoptosis	Cell proliferation and chemoresistance
PI3K	3.0	Pro-survival factor	Cell Proliferation
u-PA	6.5	Involved in degradation of the extracellular matrix	Cell migration and proliferation
Erbb2	7.0	Kinase activity, phosphorylation, receptor activity	Cell proliferation and tumorigenesis
Src	2.5	Regulation of cell growth and development	Cancer progression
c-Myc	8.5	Transcription factor	Cell proliferation and tumorigenesis
c-Jun	2.5	Transcription factor	Cell survival and tumorigenesis
H-Ras	2.0	Signal transduction	Tumorigenesis
VEGF	6.5	Growth factor	Promoting cell migration, and inhibiting apoptosis
MMP-9	11.0	Endopeptidases degrades extracellular matrix	Metastasis
NFκB1	4.0	Signal transduction, transcription factor	Survival, invasion and chemoresistance
HIF-1	3.0	Transcription factor	Tumor angiogenesis
IGF1	8.0	Growth factor receptor binds insulin-like growth factors	Cell survival and tumorigenesis
IGF2	9.0	Growth factor receptor binds insulin-like growth factors	Tumorigenesis
IL-2	10.0	Inflammation response, cell proliferation	Inflammation, cell growth
GGT2	3.5	Glutathione homeostasis	Tumorigenesis
PKC δ	2.5	Cell signaling, phosphorylation	Cell growth
PKCε	2.0	Cell Signaling	Cell growth, tumorigenesis
Upregulated			
p16/Ink4	22.0	Tumor suppressor, cell-cycle arrest in G1 & G2 phase	Proliferation inhibition
p15	9.0	Cell growth regulator, controls cell cycle	Growth inhibition
p57	10.0	Stem cell localization to the bone marrow	Proliferation inhibition
CD164	3.0	Negatively regulating cell proliferation	Negative regulator of cell proliferation
Cadherin-9	4.0	Calcium-dependent cell-cell adhesion	Invasion and metastasis inhibition
TIMP-3	2.5	Metalloendopeptidase inhibitor activity	Induces apoptosis, inhibits invasion
PIas2	2.0	Sumoylation	Cytokine inhibitors, Inflammation inhibitors